

NASA Contractor Report 185151

BEAM RIDER MODULE for an ARTICULATED ROBOT MANIPULATOR (ARM)

Accurate Positioning of Long Flexible Manipulators

M. J. Malachowski, Ph.D.* *Principal Investigator

CCE - Robotics/Electronic Photography
P. O. Box 9315
Berkeley, California 94709

April 1990

Prepared for
Lewis Research Center
Under Grant NAS 3 - 25917

NASA

National Aeronautics and
Space Administration

(NASA-CR-185151) (NASA REPORT) AN
ARTICULATED ROBOT MANIPULATOR (ARM) ACCURATE
POSITIONING OF LONG FLEXIBLE MANIPULATORS
Final Report (Cellulose Conversion
enterprises) 190 p

CSCL 098 63/63

185151

Unclass
0294715

6

7

10
11
12
13
14
15
16
17
18
19
20
21
22
23
24
25
26
27
28
29
30
31
32
33
34
35
36
37
38
39
40
41
42
43
44
45
46
47
48
49
50
51
52
53
54
55
56
57
58
59
60
61
62
63
64
65
66
67
68
69
70
71
72
73
74
75
76
77
78
79
80
81
82
83
84
85
86
87
88
89
90
91
92
93
94
95
96
97
98
99
100

TABLE OF CONTENTS

| | |
|---|-----|
| TABLE OF CONTENTS | iii |
| LIST OF FIGURES | v |
| LIST OF TABLES | v |
| | |
| SUMMARY | 1 |
| INTRODUCTION | 2 |
| TRACK I OVERVIEW | 5 |
| Positioning Detectors | 5 |
| Beam Rider Module | 6 |
| Active System | 6 |
| Actuators | 7 |
| Linear Voice Coil Motor | 7 |
| Simplified Alternatives | 8 |
| Mirror Mover | 8 |
| Passive Beam Rider Module | 10 |
| Beam Positioning Module | 11 |
| Mirror Mover | 11 |
| Motors and Controllers | 12 |
| Encoders | 12 |
| Distance Measuring Equipment | 13 |
| Light Pulse Collision | 13 |
| Time of Flight | 13 |
| Interferometer | 13 |
| Single Beam Configuration | 14 |
| Lateral Displacement Prism | 14 |
| Reciprocity | 15 |
| Fiber Optics Beam Delivery | 15 |
| Rotational Measurement Equipment | 16 |
| TRACK II - THE PHYSICAL ARM | 18 |
| Elbow | 19 |
| Shoulder Elevation Articulation | 20 |
| Shoulder Azimuthal Articulation | 21 |
| ARM III | 21 |
| TRACK III - CONTROL | 23 |
| Hardware | 24 |
| Hardware parameters definition, design and specification | 25 |
| 1. High level control | 25 |
| 2. Control processing unit | 26 |
| 3. I/O Processing unit | 27 |
| 4. System memory subsystem | 27 |
| 5. Backplane, enclosure, and power supply | 27 |
| 6. Peripherals | 28 |
| Software | 28 |
| Programs | 30 |
| 1. Device specification packages | 31 |
| 2. Device driver packages | 31 |
| 3. Action level packages | 31 |
| 4. Task level code | 32 |
| 5. Event level code | 32 |
| 6. Mission level code | 32 |
| Target Dependent Programming | 33 |

| | |
|--|-----|
| Control | 35 |
| Adaptive Control | 35 |
| Control Considerations | 36 |
| Modeled System Behavior | 38 |
| Stiffness | 39 |
| RESULTS | 42 |
| BR | 42 |
| BP | 42 |
| DME | 42 |
| RME | 43 |
| Elbow | 43 |
| Shoulder | 43 |
| Segments | 44 |
| Hardware | 44 |
| Software | 45 |
| Adaptive Control | 46 |
| Safety | 47 |
| DISCUSSION | 48 |
| Track I - Positioning System | 48 |
| BR | 49 |
| BP | 50 |
| DME | 50 |
| RME | 51 |
| Track II - Physical ARM | 52 |
| Elbow | 53 |
| Shoulder | 53 |
| Segments | 54 |
| Track III - Control System | 54 |
| Hardware | 55 |
| Software | 55 |
| Adaptive Control | 57 |
| CONCLUSIONS | 59 |
| CONCLUDING REMARKS | 61 |
| APPENDIX A Segment Modeling/Simulation Software | 62 |
| APPENDIX B Hardware and Software Evaluated | 66 |
| APPENDIX C ARM Model | 75 |
| APPENDIX D Motor and Gear Model | 87 |
| APPENDIX E Safety Assessment | 98 |
| REFERENCES | 103 |
| BIBLIOGRAPHY | 104 |
| TABLES | 108 |
| FIGURES | 114 |

LIST OF FIGURES

| | Page in Text |
|--------------------|--|
| Figure 1 | End tip displacement 2 |
| Figure 2 | ARM configuration 3 |
| Figure 3 | Sensor configurations 5 |
| Figure 4 | Detector circuitry output 7 |
| Figure 5 | Original beam rider configuration 7 |
| Figure 6 | Linear voice coil motor 8 |
| Figure 7 | Beam splitter beam rider configuration 9 |
| Figure 8 | Mirror positioner 9 |
| Figure 9 | BEI Fast steering mirror assembly 9 |
| Figure 10 | Original DME plane mirror configuration 14 |
| Figure 11 | Laser reference system 14 |
| Figure 12 | Original RME scheme 16 |
| Figure 13 | Preliminary ARM model configuration 19 |
| Figure 14 | Mode contribution graph 1 19 |
| Figure 15 | Mode contribution graph 2 19 |
| Figure 16A | Base and Shoulder Assembly photographs 22 |
| Figure 16B | Base and Azimuthal Motor Assembly 22 |
| Figure 16C | Shoulder Elevation Articulation 22 |
| Figure 17 | Software control system scheme 30 |
| Figure 18 | Task scheduling scheme 32 |
| Figure 19 | Robust control 37 |
| Figure 20 | Adaptive control 37 |
| Figure 21 | Identification/control 37 |
| Figure 22 | Indirect adaptive control 38 |
| Figure 23 | ARM III System configuration 45 |
| Figure 24a and 24b | MOTGER model configuration 47 |
| Figure 25 | ARM behavior with DC input 47 |
| Figure 26 | ARM behavior with exponentially decay DC 47 |
| Figure 27 | ARM behavior with ramp up DC input 47 |
| Figure 28 | ARM behavior with ramp up DC and decay AC 47 |
| Figure 29 | SIM1AC display for ramp up inputs 47 |
| Figure 30 | Six degrees of freedom 48 |

LIST OF TABLES

| | Page in Text |
|---------|---|
| Table 1 | Resonant modes for payloads 4 to 400 lb. 21, 39, 54 |
| Table 2 | Segment model configuration 39 |
| Table 3 | Modal frequency calculations 39 |
| Table 4 | Stiff and flexible segment calculations 41 |
| Table 5 | ARM MODEL data file 47 |

SUMMARY

The preliminary design of a positioning system for a flexible Articulated Robot Manipulator (ARM) was developed, prototyped, and tested. The positioning system consisted of a laser Beam Positioning (BP) module and a Beam Rider (BR) module. The laser BP module was incorporated into the proximal articulation while the BR module was incorporated into the distal articulation. The two articulations were connected by a long hollow flexible segment. The concept required only a single laser reference beam. The system was designed for millimetric positioning precision for each of six degrees of freedom over a ten meter range.

Several physical ARMs were prototyped as testbeds for the laser positioning system. The physical ARM was designed with a no-degree-of-freedom, wrist, a one-degree-of-freedom, elbow, and a two-degree-of-freedom, shoulder, articulations; a flexible segment was used to connect articulations. Space rated or applicable technology was used; these systems were tested and evaluated under earth gravity and environmental conditions.

An Intel 80386 based computer system was used for overall command and control of the ARM. The system was designed to operate under an ADA real-time operating system kernel. The software was of a hierarchical design; this programming structure was selected to provide a degree of artificial intelligence to the system. The software was designed for implementation on a dedicated VME bus based parallel processing multi-tasking computer system.

A controller design was developed to position the ARM. The technique of Indirect Adaptive Control (IAC) was selected as the preferred controller mode of operation. Nominally, the laser reference beam was collinear with the segment. Forces acting on the physical ARM induced a mismatch between the position of the laser reference beam and the physical ARM's distal end-tip. The input to the controller was this end-tip mismatch under static and dynamic conditions. The output of the controller was the appropriate signals to control the torque of the motor moving and positioning the ARM.

Initially, a mathematical model of the system was developed. Subsequently, a computer simulation model was constructed to predict the behavior of the system. The model served a dual purpose. First, the model was used to test and validate the mathematical assumptions made and the behavior of the physical ARM. Second, the model was to serve as the basis of the IAC.

The model was designed to derive the contributions of the first three modes of vibration to the end-tip behavior. The model input variable was the motor driving torque as modified by the gearbox. Given the parameters of the system the model provided the behavior of the end tip response for specific inputs. By varying the input torque it was demonstrated that it was possible to minimize end-tip oscillations and, thereby, smoothly position the end-tip.

More development is necessary to integrate these systems into a functioning robotic manipulator. All of the concepts necessary for implementation have been demonstrated. The feasibility of the approach has been validated. It is possible to significantly improve the utility of articulated robot manipulators through the use of long flexible segments.

INTRODUCTION

There are numerous uses for articulated robotic manipulators (ARM's) with long reaches and large load carrying capacities. The problem is that any material beam with a length L will bend when a perpendicular force is applied at the end. This will displace the end tip by an amount d from its expected position, Figure 1.

When designing an ARM, there are two ways of dealing with this problem. The first is to make the segment, or beam, between articulations so stiff that, for the forces involved, the value of d is less than the positioning accuracy required. Therefore, d can be ignored. The corollary to this approach is that a massive segment is required to obtain this rigidity. The second approach is to calculate the value of d for any particular displacement force. These calculations are non-trivial at best and may not have a solutions at worst. In the latter case the equations of motion must be truncated and a best estimate made. The accuracy of the estimates must be more precise than the required positioning precision for this approach to work.

Thus, the accurate positioning of long flexible manipulators is difficult. Because of the compliance and number of degrees of freedom inherent to these systems it is a formidable task to calculate the end tip position with precision. These calculations are possible for a static situation when the base position and all of the system variables and characteristics are known and well defined. For dynamic situations requiring real time control, calculations must be performed rapidly on changing variables. Therefore, for all but the most simple systems, the complexity of the calculations quickly exceeds processing power and the task of control becomes impossible.

Several years ago we were funded by the Department of Energy to evaluate the feasibility of a laser tree trimmer (LTT). To function the LTT required millimetric positioning precision at distances of 10 to 20 meters. The beam was to be delivered through hollow segments, which would join the articulations, or joints. We developed a concept that used the laser beam both for cutting and positioning the beam delivery system. Basically, the laser beam was treated as an infinitely rigid structure and used to define the position of the end tip of the delivery system. Thus, the cutting beam became its own absolute reference system.

To be meaningful the position of the end tip must be defined in six degrees of freedom. The impetus of this Beam Rider project was to develop a positioning beam rider module/system which would provide the position of a segment end tip with millimetric accuracy in six degrees of freedom.

The specific NASA application of this positioning system was for an Articulated Robot Manipulator (ARM). The ARM would be suitable for use in loading and unloading experimental modules from the microgravity free flyer platform located in proximity of the Space Station Freedom. The goal of the project was, therefore, to develop the design of an ARM suitable for this function.

To reach this goal a three tracked effort was undertaken. These tracks

were first, the positioning system; second, the physical ARM; and third, the control system. To be successful each track required novel developments and the use of emerging technology. The effort, as was envisioned, was unique. The successful development of this positioning concept opens a new area of robotic control and manipulation. This is significant because it is no longer necessary to restrict ARMs to short rigid, and heavy, segments just to gain micrometric positioning accuracy.

The purpose of this project was to investigate the feasibility of the design of an inertia-less two segmented ARM. The ARM would have a ten meter reach and be capable of position a 100 kilogram payload under microgravimetric conditions with millimetric precision. Eventually, the ARM would be suitable for use in the space environment conditions of the free flyer of the space station.

We proposed to develop a ground based prototype ARM suitable for testing and evaluating the concepts being developed for the space based ARM, Figure 2. The information, data and experience gained from the construction and operation of the ground based ARM was to be used to develop a preliminary design for a space rated ARM suitable for testing under microgravimetric conditions.

The effort was divided into ten systems or research areas. These were:

Track I - Positioning System

1. Positioning Beam Rider Module - The system that sits on a segment's distal end tip and tracks and monitors the beam position.
2. Beam Positioning Module - The system that sits in the segment's proximal end and directs the beam at the distal end tip.
3. Distance Measuring Equipment - The system that measures the length, or changes in length, of the segment.
4. Rotational Measuring Equipment - The system that measures the rotation of the segment, end to end.

Track II - Physical ARM

5. Elbow - The single degree of freedom mid-joint or articulation of a two segment manipulator.
6. Shoulder - The base joint or articulation with two mutually orthogonal axes of rotation.
7. Segments - The physical connection between two articulations.

Track III - Control System

8. Hardware - Computer system and associated circuitry required to interface with the positioning system, the physical ARM, the operator, and to run the control programs.
9. Software - Instructions to the computer that let it recognize

current events and direct the motion of the ARM.

10. Adaptive control - The program which senses the behavior of the ARM and modifies its behavior to perform the requisite tasks.

In order to function the ARM requires the integration of these systems. Our approach was to develop each system separately but compliant to and cognizant of the requirements, parameters and characteristics of each system. Each system had to be modified to function under the constraints imposed by the other systems. The end result was a compromise between systems to provide the best overall performance.

TRACK I OVERVIEW

The purpose of this project was to develop a Beam Rider Module (BR) suitable for incorporation into an Articulate Robot Manipulator (ARM). The concept under investigation utilized a pair of systems. The first was the positioning system and the second was the physical ARM.

The initial portion of the positioning system was referenced at the shoulder base of the ARM and at the elbow articulation. Between these two points the system was nominally collinear but separate from the physical ARM. The positioning system served as an absolute point of reference while the position of the physical ARM was relative to this reference frame. The physical ARM could, therefore, be flexible between these two points.

The elbow articulation was a rigid assembly. It connected the proximal and distal segments and positioning systems. Thus, the elbow must be stiff or rigid. The Elbow and wrist were connected by a flexible segment. Concentric to this was the positioning system; which served as the rigid frame of reference.

Positioning Detectors

Central to the positioning of a laser beam was the detector. The detector was a sensor sensitive to the wavelength of light produced by the laser. Five different sensor configurations were evaluated, Figure 3. These were:

1. Rectangular Matrix - A matrix of sensing elements arranged in an x-y format.
2. Annular Matrix - A matrix of sensing elements arranged in a polar coordinate system.
3. Quadrant - A 2 x 2 rectangular matrix
4. Quadrant with orifice - A 2 x 2 matrix with a central orifice or hole.
5. Lateral Effects diode - A nominally square sensor with connections at the edges; the output at each edge is proportional to the position of the beam on the detector.

The rectangular matrix detector was the first to be evaluated. We used a charged coupled device with raster scanning. The output was digitized and stored as pixels in computer memory. In general, the beam would stimulate a number of pixels. Two tasks were required to determine the position of the beam. The first was to locate the stimulated pixels. The second was to determine the centroid of the beam spot. The problem factors to one of image recognition. The computational power require to solve this problem was considerable. Because of the large computational requirement this approach was determined to be unfeasible.

The annular matrix suffered from the same basic problems as the rectangular matrix. However, because of the polar coordinate system, the output was more directly applicable and, therefore, required one less

transformation. Unfortunately, this configuration was not a standard commercial item and the cost of custom fabrication was excessive.

The quadrant detectors worked well, were of quick response, and were, generally, inexpensive. The drawback of these detectors was they basically provide only the direction of movement and not much information on the magnitude of the movement. As long as the beam spot was smaller than any single sensor element, position displacement equal to the diameter of the beam can be extracted from the decoder circuitry.

The quadrant detector with a central orifice worked well, were of fairly quick response, and were, generally, inexpensive. They suffered from the same lack of position offset information as did the quadrant detectors. Additionally, because of the large central orifice, their output was less linear, and they tended to have more dead space. In general, the size of the elements were larger than other quadrant detectors and, thus, their capacitance was larger and they had a concomitant loss in response speed.

The lateral effects diodes had the best of all characteristics. They had a high spatial resolution, typically 2000 x 2000. They had a quick response time. They were insensitive to spot size and shape; their operation automatically integrates stimulus information to provide a single x-y position value. The major drawback was cost. A two centimeter square unit with a central one centimeter highly accurate linear region cost several thousand dollars. A second drawback was stray light. Because of the nature of its operation, any stray light striking the detector was integrated with the light from the beam. Subsequently, the apparent position of the beam at the output was shifted.

We evaluated several lateral effects diodes from different manufacturers. We determined that the unit produced by Hamamatsu functioned well with HeNe laser light. Resolution was within that specified by the manufacturer. The unit maintained its accuracy for reasonable beam spot sizes and shapes, i.e., centroid shapes much smaller than the total detector size.

Beam Rider Module

Two sets of design schemes for the BRM were evaluated. One set was active systems that required actuator movement of an assembly that tracked the laser beam. The second set were passive systems that relied on optics and detectors to track and monitor the laser beam. Initially, to compare and evaluate these two types of scheme we planned to place the active system in the proximal portion and the passive system in the distal portion of the ARM.

Active Systems

The first active system concept evaluated used a quadrant detector with a central orifice. When the beam was aligned, it passed through the hole. The penumbra of the beam uniformly illuminated all four quadrants and produced signals of equal intensity from all four quadrants. When the beam shifts, the quadrants were mismatched in signal intensity. This mismatch information was converted to provide the x or y offset values.

The second system evaluated used a quadrant detector. A beam splitter was used to split a portion of the reference beam out to this detector. Its operation is similar to the previously described detector.

We have prototyped electronic circuitry for these detectors. The circuitry was analog and, therefore, fast. Its performance, in general, exceeded the response times required to monitor third order modes of vibrations induced into the segments under consideration. The major problems were associated with the high frequency ability of the circuitry. There was a tendency for high frequency oscillations to develop and degrade the performance of the circuitry. The filtering capacitors required to bypass these oscillations tended to degrade the performance of the circuitry. The result was a balance between the need to prevent unwanted oscillations while maintaining the required frequency response. Thus, the final design was a compromise between these two factors.

The outputs of the detector circuitry were a x value, a y value, and a signal intensity value, Figure 4. In operation, the x and y values were sent to the actuators which move the assembly which serves to position the laser beam. They were also routed to the computer to provide information about the position of the laser beam. The signal intensity value used by the Rotational measurement (RME) system.

A number of designs were evaluated for the BR assembly. The initial requirements for this system were an x,y travel over a 5 cm diameter circle at a speed faster that generated at the distal end tip by the principal modes of vibration of the system. Additional constraints were subsequently imposed by the operation of the DME and RME subsystems.

Actuators

We have evaluated several actuator designs. Concepts evaluated were either electromagnetic or piezoelectric in nature. The electromagnetic actuators included rotational and linear motors, solenoids, and voice coils. A significant problem was the linkage between the actuator, the assembly, and the the ARM. Assembly linkage was either direct or through a mechanical actuator.

The initial configuration consisted of two detectors, each with a pair of actuators, and a mirror. The reference beam entered the assembly, activated the detectors, bounced off of the mirror and return upon itself. Figure 5.

The difficulty with implementing this design was to develop a scheme which would allow positioning in four independent degrees of freedom, x1y1 and x2y2. We evaluated, trade studied, and ranked the possible actuator/linkage combinations. The preferred actuator design was a variation of a linear motor/voice coil; a linear multi-element voice coil.

Linear Voice Coil Motor

In operation a cylindrical magnet slid through a hollow central core. A stiff flexible wire connected the magnet to the BR assembly. Individually driven coils of wire were wrapped around the core. Each coil was driven separately, the magnitude and polarity of the current could be varied, as

required, to position the assembly. Coils could operate in tandem or opposed, as required, to generate the necessary positioning forces.

We prototyped a hollow core 20 coil 10 turn unit which was 1.5 cm in length, Figure 6. Each coil had a bipolar drive circuit with a +/- 5 amp current capability. Each coil's current driver was regulated by electronic circuitry which functioned as the controller. In operation the controller created a "waveform". (The waveform can be represented as a map of current in each coil as a function of distance along the axis of the motor.) The waveform could be tailored to provide the optimum driving and holding force. (Example are sinusoid, triangular, or square waves.) The waveform was stored in memory and was reconfigurable. In operation, the waveform was transposed along the axis of the motor to move the magnetic slug and, thus, the assembly.

As mentioned above the controller had two functions. The first was to create the required waveform and the second was to transpose the waveform. This transposition was used to move the magnet along the axis of the coil and thus position the beam rider. We designed a pulse width modulated driver capable of performing these tasks. Twenty integrated circuit chips were required on the interface board and the control required the dedicated use of an 8088 based computer system with appropriate I/O lines and interfacing. Position sensing was a separate set of circuitry.

At this point an assessment was made as to the feasibility of continuing with this approach. While the design functioned well, the complexity and hardware requirements were deemed to be beyond the capacity of the project. Therefore, this approach was dropped.

Simplified Alternative

We have subsequently developed an alternative ARM III beam rider configurations. Because of the constraints involved, i.e., the mechanical linkages between articulations, it appeared possible to simplify the detector assemblies. Because of the attachment of the segment to the articulation at the proximal end, the angular offset at the distal end was a function of lateral displacement. Thus, a feedback loop involving a mirror on the distal end of a segment and a quadrant detector on the proximal end of a segment could provide information about the location of the distal end tip.

Therefore, we should be able to measure mirror position relative to the articulation to define two angles to specify two degrees of freedom. Thus, for microgravity environments we could use a single quadrant detector at the base and an active mirror in the beam rider module. The current driving the mirror's positioning coils provided a method of measuring the deflection force. Unfortunately, on earth the gravitational force on the beam rider varied with position. Thus, driver current was ARM orientation dependent and a second detector was required.

Mirror Mover

To simplify the BR assembly we developed configurations in which the detectors were fixed and only the mirror would be required to move. The beam would be split by a beam splitter and the different portions of the

beam used for different purposes, Figure 7. Several mirror mover configurations, Figure 8, were evaluated, trade studied, and ranked. These were motor driven, electromagnetic, and piezoelectric.

The highly ranked commercially available units were evaluated. Several units were found to be too expensive for this project. One possible solution was a Fast Steering Mirror (FSM) mover of the type built by the Ball Aerospace Company. They indicated that the requisite parameters can be met by their units. These units appeared somewhat expensive. For \$100 to \$200k they could deliver a unit in 9 to 12 months. For \$500k they could provide a unit more quickly.

Micro Pulse Systems has developed a two axis piezoelectric mirror positioner which appears to be feasible for use in the BR. They are in the \$3-5000.00 range. Unfortunately, they will not be ready to ship until after the end of this project. Therefore, this was not a viable alternative.

Two units were purchased and evaluated in house. The first was the TU - 216 two axis served 4 inch mirror assembly built by General Electric. This unit has a roll excursion of +/- 20 degrees and a Pitch of +/- 7 degrees. It was evaluated for use in both the BR and the BP. For the BR there were several problems. First, its size and mass limited its response to the first and, possibly, the second modes of vibration of the physical ARM. Second, its geartrain had backlash which limited its high speed performance fine positioning utility. For the BP it had too limited a range of motion.

The second was the LA08-05 A linear actuator built by BEI Motion Systems Company. Significant effort was required to make this unit operational. There were three needs; power supply/driver circuitry, positioner mounting assembly, and flexible pivot.

The BEI unit consisted of two pieces. The base consisted of an assembly holding four magnets arranged in a quadrant. Four holes were spaced around the periphery. Two of these holes were tapped and were used to mount the base. The other two holes were used for guide pins during system assembly. A central orifice allowed the passage of the flexible pivot, Figure 9.

The second part was the voice coil assembly. It contained four voice coils which slipped over the four magnets mounted on the base portion. A central orifice was used to mount the flex pivot. A mirror was mounted on the front surface of this assembly.

Two +/- 0.5 amp current supplies were required to drive the positioner in two axes. A pair of regulated +/- 15 volt supplies were used to supply each driver circuit. A voltage controlled current amplifier was used to drive each pair of coils which position in one axis. Absolute linearity was required to ensure absolute positioning. Frequency response was greater than one kilohertz to allow control of third order modes of ARM vibration.

The assembly holder performed two functions. First, it held the base portion of the positioner. Second, it held the flex pivot. A pair of holes through the holder allow passage of a pair of 2-56 screws which screwed into the base. A tapped (2-56) central orifice in the holder was used to hold

the base of the flex pivot assembly.

The flex pivot consisted of three pieces soldered together. The base portion consisted of a threaded tube which screwed into the assembly holder. The voice coil end consisted of a 1/8 in tube. The top of the tube necked down to 7/64 in to pass through the central orifice of the voice coil assembly. The top of the necked down area was threaded and a nut was used to affix the voice coil assembly to this tube. The center portion of the flex pivot consisted of seamless BeCu tubing obtained from Uniform Tubes INC. The maximum angular travel ranges from +/- 20 to +/- 50 milliradians, depending on the location of the joint between the flex pivot base and the BeCu tube. The maximum obtainable deviation was also dependent upon the stiffness of the tube.

Assembly required the base portion of the pivot to be screwed into the assembly holder. The BeCu tube was then soldered to this. The base was then mounted to the assembly holder. A sixty thousandths inch spacer was placed between the base and voice coil assembly. The voice coil end of the pivot was mounted to the voice coiled assembly and slipped over the protruding BeCu tube. The two alignment pins were placed in the base to align the voice coil assembly. The BeCu tube was then soldered at the voice coil assembly end. The assembly holder was removed, the unit was disassembled and the spacers and pins were removed. The unit was reassembled and subsequently ready for use.

For testing purposes the unit was controlled with a two axes joy-stick. A laser beam was reflected from the mirror onto a sheet of graph paper. The x and y drive currents were monitored on an oscilloscope. The beam position was then plotted as a function of input.

In operation the unit was interfaced to the output of a quadrant diode. As the beam was displaced from the center position, a feedback loop was used to drive the mirror positioning unit to center the beam. In practice this was used to keep the reflected beam collinear with the incident beam.

Initially, the system was unstable. This was traced to several sets of problems. One set involved instabilities and oscillations in the electronics. Several generations and revisions of the electronics were necessary to stabilize and compensate the circuitry. The second set was with the mirror mover.

Some of the problems with the mirror mover were linked to the flex pivot. We evaluated many schemes for mounting and holding the pivot at either end and different solid and tube materials for the pivot. We were able to obtain a gradient of sizes of precision flexible tube which allowed the development of an adequate flex pivot.

Because we still had problems with linearity and hysteresis, we disassembled and returned the mirror mover to BEI for evaluation. They cleaned and recalibrated the unit. The unit was returned in early July of 1989 and was found to have improved performance.

Passive Beam Rider Module

The passive BR used a lateral effects diode to provide the x and y

coordinate position of the laser beam. The electronics were similar to that used for the quadrant detectors and produced the same signals. The specifications for a REVISION 2 design of the electronics for the lateral effects detector were finished. Parts have been selected which increase the circuit's performance and simplify the circuit calibration tasks. A printed circuit board layout/tape-up was made which can be used to produce printed circuit boards in the future.

To evaluate the linearity of the lateral effects diode we constructed a test jig. The jig consisted of a precision x-y table. The table was moved by stepper motors under computer control. The position of the drive shafts were sensed by medium resolution encoders. The resolution of the encoders was five times the resolution of the motors. The five micron accuracy of the system allowed us to map the linearity of the diodes to the values specified by the manufacturer.

We conducted tests to determine the sensitivity of the diode and circuitry to laser beam spot size, uniformity, and intensity. We found that the positioning ability were in conformity with the manufacture's specifications. The unit nicely integrated various size and shaped beam spots to provide a single position for the centroid of the beam.

We prototyped and evaluated the optics for the passive BR. The design of the optical components required for the lateral effects diodes was minimal. The difficulty was incorporation of elements for the DME and RME systems.

We evaluated several optical configurations for the beam rider. We prototyped a simple beam rider for use on the distal segment tests. A pair of zoom lenses were configured to demagnify the beam over a 5 to 10 cm working aperture. The demagnified beam was incident upon the lateral effects diode.

We have developed a more simple optical design suitable for use as a simple telescope. A pair of aspheric lenses can be used to demagnify the input aperture to a dimension compatible with the parameters of the mirror and detector. (These factors are a function of the deflection of the segment when it is in operation.) Spherical optics required a greater number of lenses and, therefore, more reflective surfaces, with a concomitant lose of signal.

However, because the current DME signal is very weak, no focusing optical elements can be inserted in the beam path. ARM IV will require antireflection coatings and a dielectric mirror to improve beam transmission and reduce beam loses.

Beam Positioning Module

Based on the proposed positioning accuracy we determined the resolution required of the Beam Positioning (BP) module. For millimetric accuracy at 10 meters this was found to be on the order of 5 arcseconds. We, therefore, specified resolution and repeatability of the components to be in the 1 to 5 arcsecond range.

Mirror Mover

We identified several mirror movers which met our required specifications. These were evaluated, ranked, and trade studied. The top ranked units were produced by BEI motion control and Aerotech. BEI has produced a space rated unit for the space telescope project. BEI has a downgraded a comparable unit for earth based applications; it was too expensive to purchase for Phase II, but would integrate well with Phase III. Aerotech produced a two axis positioner which was quite close to the desired specifications.

The Aerotech unit had several drawbacks in terms of configuration and resolution. We negotiated with them for some modifications to the stock unit and for their selection of components from a production run which exceeded the nominal resolution and repeatability specifications. Subsequently, we purchased this unit.

This two axis positioning unit was evaluated for two modes of operation. The first was to project a laser beam through a central orifice onto a mirror which would reflect the beam down the center of the segment. The second was to mount the interferometer launch optics directly on the positioner. Based on development of the Distance Measuring Equipment (DME) the second mode of operation was selected.

Motors and Controllers

Included with the Aerotech positioning unit were stepper motors and a reducing gear train. A pair of American Precision Industries CMD-310 microstepper drivers were purchased to drive the stepper motors. Because of backlash in the gear train, a closed loop control system was determined to be required.

Interface circuitry for the motor controllers was designed, prototyped, and tested. The electronic were set to respond to computer input or to be controlled by panel switches for step and direction.

Encoders

We identified half a dozen encoders which provided arc second resolution. These were evaluated, trade studied, and ranked. The top ranked unit was the Canon R-2A laser rotary encoder. It provided a 64k incremental and a 256 gray scale output. The incremental output was run through an interpolation board to provide 1 arcsecond resolution. The gray scale output was available to provide 2 degree resolution in the event of power failure and during startup.

A pair of the Canon encoders were purchased. These were mounted on the Aerotech positioner and coupled to the positioner positioning shafts. The unit was tested and evaluated. It was found to be within the system specifications.

Interface circuitry for the encoders was designed, prototyped, and tested. The output can be routed to the computer or to front panel display lights. The lights represent the bit count from the interpolation board; they provide a visual presentation of the beam position. This display in conjunction with the stepper motor control switches allow manual operation

of the BP.

Distance Measuring Equipment

Several concepts for measuring the length of the segments were evaluated. Because of the ultimate objective of space operation only systems which could function in a vacuum were evaluated. Three conceptual designs were produced.

Light Pulse Collision

The first design was the light pulse collision system. In operation a laser light pulse would be produced and split into two packets. One would be launched down the center of the segment and the other into a fiber optic routed to the distal end of the segment. At the distal end of the segment would be a rectangular block of a non-linear crystal, e.g., LiNbO₃.

The light pulse traveling up the segment would enter from one end while the light pulse traveling along the fiber optic would enter the other. The path lengths would be adjusted such that the pulses would meet within the block. Upon collision the pulses would generate a harmonic light pulse which would exit the block transversely to the stimulus pulses. Detectors mounted along the side of the rectangle would sense the position of the pulse. This distance would correspond to segment length changes.

The light pulse collision concept had several advantages. It would be an absolute measurement system with relatively few parts. Unfortunately, as the segment flexed, the alignment would be lost. Thus, aligning the beams to overlap became a major problem. Additionally, we were not able to locate anyone who had actually demonstrated this system. Work was terminated on this approach to concentrate on the other approaches.

Time Of Flight

The second design was the time of flight concept. Like LIDAR, a pulse of photons would be launched along the segment. They would be reflected at the distal end by a mirror, or concentrated into a fiber optic for return, and sensed by a detector. The time between the input and output pulse would be processed to provide an indication of the flight time and, thus, the distance. There were numerous advantage to this scheme and it should be seriously considered for future generations of the ARM.

Unfortunately, for our purposes there were several major drawbacks. To provide the required measuring resolution would require a timing resolution on the order of 3 - 5 picoseconds. Commercially available components and systems would have cost \$50,000 - \$100,000; this exceeded the project budget. Recently, progress in GaAs devices and solid state lasers has reduced the estimated system price considerably.

Interferometer

The third system design utilized laser interferometry. A laser light beam is split in two. One beam travels along a movable path length, is reflected back to its source, and interacts with the other reference beam. As the path length changes, the phase between the two beam changes, which

causes fringes of light and dark. By counting these fringes it is possible to accurately, nanometers to microns, determine distance traveled. A system available through Coherent Radiation Laboratories was priced within the project's budget.

A major problem was the need for the incident and return beam to parallel and separated by 1 cm.. Under normal operation, distance was measured to a retroreflector. The retroreflector reflects the beam parallel to the incident beam. To function the beam must be reflected and displaced by one cm from the incident beam. Lateral movement of the retroreflector changed this spacing and the system stopped functioning.

Because there was significant lateral movement of the beam rider we needed to modify the retroreflector configuration. We evaluated several schemes for accomplishing this.

Single Beam Configuration

The most simple used a plane mirror to reflect the incident beam to a point close to the interferometer at the proper spacing, Figure 10. The difficulty was that this beam was not parallel to the incident beam. To correct for this angular error the beam was passed through a pair of rotatable wedges so that the exit beam was parallel to the incident beam. We determined that the required parallelism was less than 5 arcseconds of deviation. Within this deviant cone we found marginal operation.

The second scheme used a piece of calcite to laterally displace the return beam from the incident beam. This scheme was polarization sensitive. The beam was rotated by a 1/4 wave plate before and after striking the mirror for a total of 90 degrees rotation. In principal this scheme would work and we were able to demonstrate it for small displacements. For a 1 cm. beam displacement we required a 10 cm length of optical quality calcite. In actuality the high price and total unavailability of optical quality calcite of sufficient length made it impractical.

Lateral Displacement Prism

The third scheme used a pair of polarization sensitive beam splitting prisms. This system was similar in operation to the calcite system. We have called this concept the lateral displacement prism. The reflected beam was collinear with the incident beam and subsequently displaced as required in front of the interferometer, Figure 11.

There were two methods of construction for the lateral displacement prism. One was to cement two polarization beam splitting cubes together. The second was to use a parallelogram with two triangular prisms cemented to each end to form the rectangular lateral displacement prism. We solicited quotations for each configurations and determined that the first method, which used stock items, was the most cost effective.

Although the use of the lateral displacement prism produced the requisite parallel displaced beams, the system would not function. We constructed a fiber optic break out box for the interferometer's outputs. The light beams from the red and green coded fiber optic leads must be 90 degrees out of phase and of equal amplitude for the system to function. The

extra centimeter path in glass of one leg of the measurement beam was sufficient to alter the phase relationship of the beam. We found that this could be corrected by placing an additional 1 cm. beam splitting cube in the return light path.

Reciprocity

The phase change phenomena illustrates the principal of reciprocity in the DME system. As long as any transforming element effects both beams equally, the system functions. Transformation to either beam alone shifts the phase and must be compensated. An illustration of this principal in operation was our attempts to collimate the return beam. One purpose of collimating the beam was an attempt to pass the return beam through the center orifice of the quadrant detector. Our attempts to accomplish this were unsuccessful because this operation was performed on only one beam. On the other hand our attempts to demagnify the beam at the distal end tip before striking the mirror (this approach allows the use of a smaller mirror and spatial detector) were successful because we were transforming both beams, incident and return, equally.

Fiber Optics Beam Delivery

Our first interferometer used a standard configuration of a laser producing a beam which propagated out to a retroreflector and was subsequently reflected back towards the laser. The interferometer head was mounted in the beam path perpendicular to the beam. The perpendicularity requirement made the alignment of the interferometer difficult. The need to fold the beam with a mirror at the shoulder articulation compounded the difficulty both in interferometer alignment and operation and in the configuration of the BP module.

We decided that a preferred beam delivery system would use a fiber optic to transport the beam from the laser to the interferometer head. A more advanced design would use a fiber optic to return the beam from the distal segment end to the interferometer. The former concept should work without much difficulty because it does not violate reciprocity.

We specified a 5 meter polarization maintaining fiber for use with our system. It contained integrated receive and launch optics at the ends and was armored. Basically, the cable functioned. Unfortunately, with physical movement of the cable, there was some transfer between polarization modes. Therefore, although the beam entered linearly polarized, it exited with two components, the magnitudes of which depended upon cable orientation. This problem was solved by placing a polarizer in front of the interferometer. However, the magnitude of the intensity of the incident beam was then dependent upon the orientation of the beam delivery cable. Therefore, the output was not constant and could not be considered so for the rotation measurement equipment (RME).

The addition of the fiber optic delivery system significantly attenuates the beam intensity. We were able to operate the system with the lateral displacement prism over a 10 meter range. However, a 10% attenuation of the beam caused a loss of function. This restricts both the use of additional optics in the beam path and the maximum range of rotation.

Rotational Measurement Equipment

Several schemes for this system have been evaluated. JPL is developing a high resolution angular gyroscope which uses interferometric and fiber optic methods to measure small angular variations. We have inspected their prototype and discussed the incorporation of their design into the ARM. Currently, this unit is still under development. We are tracking progress, although it appears as if several more years will be required before the unit is completely operational.

The other schemes relied upon beam polarization. The technique was relatively straight forward. Basically, an analyzer was used to examine the polarization planes of the beam. Any rotation of the BR manifested itself as a change in intensity of the analyzed polarized beams, Figure 12.

The incident beam from the interferometer was polarized. A double pass through a waveplate shifted this polarization. One analyzer was mounted in front of the interferometer. Any rotation of the BR shifted the plane of polarization, which was split by the analyzer and measured by our detector. These output signals were used to provide a measure of the rotation. For calibration the mirror mover was coupled to our rotational encoder which is capable of 2×10^{21} bits (one arc second) of resolution. The difficulty was integrating this system with the rest of the BR, the DME, and the data link. The final configuration of the DME system required a reconfiguration of the RME.

Based upon the final design of the DME system a RME configuration was developed. The single beam passing down the segment twice through a quarter wave plate. This operation was required to rotate the beam polarization by 90 degrees and cause the double reflection in the lateral displacement prism and the resultant 1 cm. beam displacement. The operation of the quarter wave plate was orientation dependent. Any rotation of the waveplate caused an incomplete shift (less than 90 degrees) in beam polarization. Such an incomplete rotation resulted in a portion of the beam passed straight through the lateral displacement prism while the rest underwent the double reflection and displacement. Therefore, the intensity of the return beam to the interferometer was dependent upon the orientation of the distal quarter wave plate.

When the distal wave plate was mounted on the distal portion of the segment, e.g., at the elbow, any rotation of the segment also rotated the distal wave plate. This rotation resulted in a change in intensity of the return beam to the interferometer. Fortunately, the effect around maximum was flat, i.e., rotation ± 2 degrees about the maximum resulted in a very small change in intensity. For example, a rotation of 2 degrees resulted in a change in 2 mV from the sum amplifier of the quadrant detector. A rotation of 10 degrees resulted in a change of 100 mV. Unfortunately, this change was not linear.

Therefore, while we had a means of measuring rotations, there were two problems. First, the intensity of the output or incident beam was of variable intensity due to movement of the fiber optic cable. Second, the change of beam intensity due to rotation of the distal wave plate was non linear.

To solve the first problem we resorted to the same integrated circuit divider solution that was used in the quadrant detector decoding circuitry. A detector was mounted to intercept the light beam reflected at right angle from the lateral displacement prism as the incident passed through the prism. This beam served as the reference beam and provided an indication of the intensity of the incident beam. The sum signal from the quadrant detector (picked off of the compensating polarizing beam splitter placed in the return beam path) served to indicate the intensity of the return beam. Theoretically, for any given orientation of the distal quarter wave plate, the ratio between these two beams was constant even if the intensity of the input beam varied.

In practice several other problems surfaced. First, the linearity of the two detector systems was not the same, i.e., the detectors were not matched in their response. Therefore, for a change in incident output beam intensity, the ratio did not remain constant. Solutions to this problem include matching the detector responses and adding compensation circuitry, or both. Second, the electronics were not optimized and the circuitry tended to be unstable. Solutions to this problem include redesign of the circuitry and adding compensation, or both.

Once the ratio output is stabilized for variation of beam intensity, changes in the ratio value will represent rotation of the distal quarter wave plate. These values must then be mapped to angular displacement. This can be done in a computer lookup table.

A further problem was the dynamic range of the detectors. Given the values of intensity variation with rotation around maximum, sensors with dynamic ranges of 7 or 8 orders of magnitude are required for arcsecond resolution. The best we have been able to obtain were in the 6 orders of magnitude range. However, with biasing, it may be possible to change the operating points efficiently to obtain the required dynamic range.

TRACK II - THE PHYSICAL ARM

Our work started with the preliminary calculation of system parameters and physical attributes of the two segment, 3 degree of freedom ARM III. Next we constructed a single degree of freedom ARM, which was a modification of the testbed previously referred to as ARM II. Ultimately this structure served as the model for the elbow and distal segment.

A model (SIMI, Appendix A) was created to determine rough estimates of the segment sizes for ARM III. Calculations were made which provided approximate estimates of the first three modal frequencies of a flexible segment 7 meters long and carrying a 100 kg. payload. These were the basic assumptions which we made on the segment sizing and the payload capacity of the segments of the proposed space station arm.

The diameter of the segment was selected to meet several of the criteria and parameters of operation. We made a number of assumptions about payload, ARM mass, and acceleration. The basic criteria was that the segment would not bend more than one diameter at maximum acceleration. We based our calculations on a cylindrical model. We determined that the smaller the diameter of the segment, the thicker the wall of the segment needed to be. The thicker the wall, the greater the mass of the tube. As the diameter of the tube increases, so does the total mass. A diameter of 10 - 15 cm was determined to be the optimal range. Wall thickness and material were selected to carry the requisite loads.

In addition to possessing favorable dynamic characteristics, the material used in the construction of the arm segments must be able to withstand the harsh environment of space. (For example, since large temperature extremes are common in space, the appropriate material should be somewhat immune to large changes in its dynamic character due to these temperature variations.) We prepared a candidate list of materials. We requested information on the above materials from manufacturers to evaluate the usability and availability of tubes of these dimensions.

A tube which is 7 meters (23 ft.) long and 12.5 cm. (~5 in.) in diameter was not standard but could be manufactured by an extrusion process. Rough estimates of the prices of such tubes were about \$250 for aluminum, \$1250 for titanium and roughly \$100,000 for beryllium. Another candidate with favorable properties are resin composite tubes, e.g., graphite composite. The advantage of the composite types of materials lay in their construction. Lay-up could be orientated such that both longitudinal and rotational stiffness were controlled. All of these materials were commonly used in space.

Using SIMI, calculations were made assuming the use of these different types of materials -- both common and exotic. Results of these calculations were that it was reasonable to expect the first three modes of vibration to fall in a range of 4 to 130 Hz. Based on these results, the segments were scaled to different lengths with different payloads while maintaining the same fundamental mode of vibration. In general, as length and mass were decreased, keeping the fundamental mode constant, the frequency of the second and third modes increased.

In addition to determining the above mentioned modal frequencies,

further calculations were made to determine the first three mode shapes and compare their overall contribution to the ARM's motion, Figure 13. Results of these calculations were plotted as two graphs, Figures 14 and 15. Each graph was a plot of the first three modes of an aluminum segment whose size and physical attributes were previously described. (Note that figure 14 illustrates the relative sizing of the mode shapes which would result from a torque impulse of magnitude 1 applied at the base of the arm.) From this graph it was evident that the first mode of vibration contributions significantly dominated the behavior.

Rough estimates on system size were provided by the above mentioned calculations. From these we developed the preliminary specifications for ARM III and gained a feeling for the magnitude of the driver requirements. For example, a 100 kg payload at 10 meters at 1 g is 1000 nt-m or 6000 ft-lb. of torque. Given the mass of the rest of the physical ARM and counterweights (counterweights are for ground based gravity operation) the torque requirements rapidly escalate to values 5 to 10 times this.

Because of the ultimate space applications, the only motion drive sources suitable were electrically powered. Because of the required response times, we were limited to direct or geared electromagnetic motors. We collected and assessed data on available motors and gearing systems.

To maintain adequate control of driver - ARM motion required a tight system, i.e., no backlash. We evaluated commercially available low and zero backlash systems. The gear systems suitable were traction drives and harmonic drives. We assessed the characteristics and trade studied and ranked the candidate gear systems. The harmonic drives produced by Harmonic Drive were ranked over those produced by Dojen of Dolan-Jenner due to greater mechanical ruggedness.

ARM III required three prime movers, two at the shoulder and one at the elbow. We assessed the characteristics and trade studied and ranked the candidate motor systems. Brush and brushless DC motors were ranked highest. The motors for each of the articulations had slightly different requirements and, thus, specifications.

Elbow

The driver for selection of the elbow motor was weight. We sought to obtain the best torque to weight ratio. We selected Inland Motor of the Kollmorgen Corporation because of their ability to design to specification and experience in building space rated motors. The motor specified had a double shaft, one end fitted to a harmonic drive and the other to an encoder. Peak torque was on the order of 1600 oz.-in.

The Inland motor was coupled to a Harmonic Drive ISR Series 4M 200:1 speed reducer. This speed reducer was selected for two reasons. First, it was the greatest speed reduction - torque amplification unit available. Second, the housing and bearings had the capacity to handle the loads and torques exerted by the distal segment assembly and payload. Peak torque output, sub-second response, was on the order of 1700 ft-lb.

Critical to the operation of the DC brushless motor was the motor controller and driver. We evaluated three options; build our own, buy a

stock unit, and order a custom designed unit. We designed and prototype four generations of driver circuitry, each successive generation being more robust. The designs consisted of two portions, one was the controller and the other was the driver.

The controller portion receives user input commands and hall effect encoder outputs to determine current position and desired position. Decoding logic converted this information into necessary motor drive phase control and three sets of outputs, one for each phase. Based upon this information, a pulse width modulation circuit provided drive to the driver circuitry. The drive circuitry provided a current source or sink to each of the three windings of the motor. We successfully prototyped circuitry with the Motorola MC33034 brushless DC motor controller and the Sprague UDN-2937W 3 - Phase brushless DC motor controller/driver to perform the controller and pulse width modulation functions.

We had insurmountable problems with the driver circuitry. We evaluated discrete transistor and packaged power MOSFET designs with ultrahigh speed diode and snubber protection. We purchased the Gentron Powertherm ERM 133R-M18 3 phase MOSFET package rated for 30 amps. The net result was to blow the output transistors in one or more of each driver. Failure analysis was inconclusive being relegated to electrostatic discharge failure or excessively high back EMF.

We evaluated two commercial controller driver units. One was the SC 402012 Pacific Scientific 3-phase motor driver and the other was an Automotion Incorporated LC-4 3-phase motor driver. Both of these units functioned, however, peak drive amps were limited to less than half of the maximum required peak amperage for the motor.

We requested a quotation from Inland Motor for a driver suitable for use with our motor. The Model BDA5-24020-001 with 40 Amps peak current was priced at \$4,250.00 with 8 to 10 weeks delivery time.

Shoulder Elevation Articulation

We purchased a PMI MC 19P high pulse torque, low inertia, zero cogging, low armature inductance DC brush motor for the shoulder elevation driver. This was coupled with a Harmonic drive size 8M 100:1 speed reducer - torque amplification unit to provide a peak output torque on the order of 1800 ft-lbs. at 100 amps input current.

We have evaluated PWM, SCR, and linear drive controllers for this unit. Because of the initial planned restricted use of the ARM, reduced length and payload, we did not evaluate drivers with the full 100 amp peak output capacity. We evaluated an Apex PA-03 linear amplifier for driving this motor. It had a current capacity of +/- 30 Amps. We designed a voltage controlled current drive preamplifier stage suitable for analog input control. The operation was determined to be asymmetrical and had some instability around the zero operation voltage point. Although the operation was adequate, the amplifier was returned to the manufacturer for analysis. The analysis indicated that the unit was performing within its specifications. Therefore, additional modifications were required of the circuitry to further optimize performance.

Shoulder Azimuthal Articulation

For the azimuthal drive we have purchased a direct drive motor and controller from NSK. This unit had an 11 cm., 4.5 in., central orifice suitable for passage of the BP support segment. The motor has 180 ft. lb. of torque. The controller supported analog, RS-232 digital, and parallel port digital input. It had an integrated encoder positioning system with 2 arcsecond resolution.

The controller was semi-intelligent. It could be programmed to perform sets of operations on its own. It had primary and secondary servo loop digital filters which could be programmed to specific system modes of system vibration.

The megatorque motor was interfaced to a RS-232 port terminal and the basic functions were checked. The motor was operated in a minimal load configuration in both the torque and velocity control modes. The controller was programmed into a tight control loop suitable for stimulating the primary vibrational mode of the system/segment. These operations suggested that it was possible to utilize this motor controller for performing preliminary system shakedown experiments.

The analog drive control function was interfaced with a voltage controlled preamplifier. This amplifier was similar in design to the amplifier used to control the elevation motor controller. Together, these controllers were interfaced with a two dimensional joy-stick control. Use of the joy-stick allowed manual control of the two axes of the shoulder articulation. These inputs were suitable for interfacing with a digital to analog card on the VME bus computer to exercise computer control of the shoulder articulation.

ARM III

We have modeled vibrational modes for various segment sizes for various payloads. We first defined a set of two meter segments which have a primary mode of vibration consistent with the longer segment modes. We determined the behavior of these systems under acceleration and the behavior of the system under gravity.

We determined the first, second, and third order resonant frequencies for payloads ranging from 5 to 400 lb. Table 1. As expected, with this weight change, the primary frequency varied considerably, approximately an order of magnitude. The second order varied by about 15 %, and the third order by only about 3 %.

We selected a 34 Kg (75 lb.) payload capability for the distal segment; this should support the addition of the Oak Ridge joints. With counterweighting, the distal assembly, articulation, segment, beam rider and payload would mass about 182 Kg (400 lb.).

A 9 cm (4 inch) diameter aluminum segment used for the distal segment would have about a 1 cm static displacement and resonant frequencies of 6, 100, and 310 Hz. The same diameter steel segment used for the proximal segment would have a 2 cm static deflection and resonant frequencies of 8, 120, and 395 Hz.

The component specifications and the above described parameters were used to shape the design of the shoulder articulation. We hired a mechanical engineering consultant to render the drawings and develop the mechanical specifications. The components were manufactured, assembled, and made operational, Figure 16.

A consideration of the design for the articulation was a reactionless freewheeling drive configuration. For this project the freewheeling drive would have been bolted to the frame. In the future the drive could have been connected to a flywheel. This latter configuration would have then been suitable for use to investigate a "reactionless" drive configuration.

For the shoulder several options for counter rotating flywheels were examined. These would either attach to the harmonic drive unit or the motor. If the flywheel attached to the harmonic drive a pair of 2 meter diameter 500 Kg wheels would be required. This was determined to be unacceptable for the elevation axis. Because of the gear ratio of the harmonic drive 100:1 a flywheel mounted to the motor would be much smaller and spin faster. It was determine that the implementation of this option was beyond the scope of this project. However, the shoulder articulation was designed such that flywheels could be retrofitted at a later date.

TRACK III - CONTROL

Much of this project was a problem in real time autonomous robotic control. Our basic method of approach was similar to that defined by Dr. J. S. Albus in "Brains, Behavior, and Robotics" (1). The methodology was modeled on the functioning of the human brain and, as such, had an inherent degree of artificial intelligence.

This approach has been termed the hierarchical robot control system. The underlying structure of the system was one of task definition and prioritization. Unfortunately, tasks or actions which seem very simple to humans were incredibly complex to describe in a complete set of rules. By examining a goal and breaking it up into small units or events which must occur to attain the goal, we developed the necessary sets of rules. After analysis of the event units required for any problem of control, we found that certain events were generic, i.e., they were required events for attainment of most goals. The generic events were at the lowest level of the hierarchy.

At the top level of the hierarchy were the complete undecomposed goals, the main program. In between the top and bottom levels were a number of intermediate levels. Each new level was created by further breaking down the previous levels' tasks. These intermediate levels were responsible for a number of functions. These were:

1. System initialization
2. Data acquisition
3. Data decoding
4. Information and data storage
5. Data display
6. Control processing
7. Control input/output
8. Task scheduling

Below the generic procedure were the machine operating system and the run-time library. In general, the "power" or intelligence of the system can be considered to increase exponentially with the number of levels in the hierarchy.

The hierarchical approach also facilitated modularity. Cost effectiveness was the root of adapting modular programming. Modules made it easier to develop and debug software because they were more manageable. Reusable modules in separate compilation package meant that one modules had been coded, and thoroughly tested, they never needed to be rewritten. Software developed for this project was designed with reusability and maintainability as prime considerations.

Implementation of a modular approach placed numerous constraints on the

selection of hardware and software.

Hardware

A significant amount of time and effort was spent in accessing and evaluating the hardware selected. Several criteria were generated by the parameters of the project. The first of these criteria dealt with the resolution of the system. The accuracy sought mandated at least 21 bits of resolution. Therefore, we needed a data path of at least this width, which meant migrating to a 32 bit data bus. The second of these criteria dealt with multitasking. Because of the multitude of tasks required, it would be a definite advantage to be able to multitask or perform rapid task switches. Thirdly, because of the nature of robotic control, a real time operating system was required. These criteria served as a starting position for hardware selection.

Additionally, we identified eight general criteria of import in selecting our hardware. These were:

1. Availability - In order to adhere to the project timeline, equipment had to be available as required for development and use.
2. Flexibility - A wide variety of tasks must be performed by the controller; distributed processing works best in these situations.
3. Support - Experience, expertise, availability and capability of product backers and promoters were important factors and caused major problems.
4. Growth potential - Because of the rapid growth and change in this field we wanted a mature technology which could interface with new technology.
5. Software availability - a large software base encourages more widespread use and acceptance of a system which, in turn, encourages more products.
6. Processing power - Raw power, i.e., cycles per instruction, processor speed, and ability to interface with accelerators, coprocessors, or digital signal processors.
7. Bus - The bus strongly influences system layout, interconnection, processor support, ruggedness, and reliability.
8. Pricing - Components had to be cost effective and within budget.

Appendix B a list of the hardware evaluated. We trade studied and ranked these units. The top ranked central processing unit was manufacture by Intel, the 80386. The top ranked coprocessor was the Inmos transputer. The top ranked bus was the VME bus. The rest of the selection process involved selecting board level manufacturers who incorporated these devices.

We used the Intel processors, IBM XT, AT. and 386 clones on this project. The typical configuration was the CPU, a coprocessor, floppy and hard disks, extended memory, and appropriate I/O cards. The mainstay of

hardware was a 386 machine with a 64 k cache and 10 Meg of 32 bit RAM and the 80387 coprocessor. It had a 1.2 M floppy, 120 M hard disk, and 500 M WORM disk. It ran both MS-DOS and Unix. It was set up with a remote terminal link to the VME computer. For testing and experiments it used a MetraByte DASH board, A-D and D-A conversion, and a 32 bit wide digital interface card.

Because not much was known about the size of data sets required for control and other parameters, we did not know what kind of throughput we needed for ARM III hardware. We could not wait till all parameters were known about the controller as there would not be enough time left in the project to select and implement a system. Therefore, we needed to specify, purchase and assemble the ARM III computer system based on a number of assumptions and incomplete information. After we procured the ARM III control system, there were still significant problems in implementing it.

Therefore, because of the time constraints, we implemented the system without complete specifications. Furthermore, since the parameters effecting computing power were unknown, we had to implement a system with considerable flexibility. Thus, we designed a system such that throughput could be increased without impacting the rest of the system. Our solution was to design a system with a front end that only needed to execute the high level control and supervise slave hardware. It also had the capability to perform the mid to low level control processing off line.

Since it was the control processing units that required flexibility, the front end was fixed while the mid to low level processes were designed to be implemented as an expandable network of point to point connected computers. This solution minimized "trauma" by isolating the unknown and changing parameter problem logically and physically from the high level tasks. The high level tasks were developed without concern for the unknown parameters.

Hardware parameters definition, design and specification

1. High level control and system verification master computing unit

Because we coded in Ada, we were restricted by compatibility with compiler hosts and targets. Based upon current availabilities and costs we trade studied the Intel 386, NSC 332 & 532 and the MC 68020 & 030. Only the most widely supported MPU's were applicable for the front end unit. There was not enough specific information on system load to justify ranking in terms of specifications and performance alone. The NSC alternatives offer a good set of basic system support resources on chip and OEM modules offered. These should be tracked for ARM IV.

The 80836 was top ranked for front end use for many reasons. The flexibility of the addressing modes, larger address range, 64 k I/O address space and aspects of support for multi-tasking were high ranking attributes. The upward compatibility demonstrated by the company to date was important.

Other attributes that had an impact on the decision was cost and availability of:

1. evaluation boards for the product that were bus ready,

2. software and compilers,
3. memory
4. compatible storage and display controllers for peripherals,
5. compatible boards or subsystems for control processing
6. I/O boards and
7. I/O processing boards.

Even with all of this selection care there were significant problems because of the inability of manufactures to bullet proof hardware and software for the advanced technology being implemented. A second major problem was the redirection of companies after they had committed themselves to specific hardware and software.

We top ranked Multibus II and VME bus for consideration. Multibus II implementation was more uniform. Multibus II also supported message passing. Message passing varieties of and extensions to VME were available. There appeared to be more future for increased bandwidth and upward compatibility with the VME bus. A wider variety of products was available for the VME bus, often at a lower cost than Multibus II. While Intel was normally associated with Multibus I and II, we identified an 80386 VME bus ready board. Alternatively, an 80386 system board that was multibus II or AT compatible ready could be connected to a VME bus system through an adapter.

Logistics favored the VME bus. The program at LRC operated by our technical monitor used the VME bus. The use of the same bus should facilitate later interfacing.

We implemented control communication by interfacing through memory. This was via a hardware/software interface such that the control nodes processors command set appeared as an extension of the Master computing units instruction set. This required point to point links via one logical global memory which could exist in 2 to 3 physical locations. This was, in part, why the 80386 design used the protected memory scheme.

We purchased the Force Computer SYS 80K CPU 386 VME bus 80386 based board for the system board.

2. Control processing unit

The ability to add more throughput without bus bandwidth degradation was important. It was part of the solution to the general problem encountered when a general purpose bus is used. We wanted to be able to increase system throughput by bypassing the general bus.

One way of doing this was to add an additional bus known as a "sub-bus". Multibus II did specify a sub-bus. The VME specification did not define a sub bus, however, there was an extension to the VME specification which does.

Another method of avoiding possible bus overload used a modular computing unit, e.g., the Inmos Transputers. Transputers were the top ranked coprocessor. They were designed for parallel processing, point to point connection, and system bus connection. Each Transputer contained many of the support elements on chip that were normally implemented off chip. This included four transputer links that could be hardware and/or software configured and connected to other transputers. These links were also available at the edge of the board for external connection.

The Transputers could be purchased VME bus ready with different configurations, (number of transputers socketed for, amount of memory etc.), and were also available. There were other product lines that used the "building block" approach of Transputers but many aspects of the chip itself and the logistics of using it were very positive.

The instruction set was small and specifically oriented to real time control. A real time kernel was micro-coded in the chip. Timers and delays were controllable down to 1 microsecond. One instruction cycle was only 50ns at 20MHz. Some instructions were interruptable during execution so that interrupt latency was very short.

Because of delays in the availability and development of project hardware and software we did not reach the point where we were ready to implement the coprocessor units. Instead we selected the transputer as the preferred module and assumed that it would be available eventually. For current tasks we used the 80386 and 80387 off line with the assumption that they could be implemented on line in real time at a later date with the transputers.

3. I/O processing unit

There was a significant amount of I/O required for the ARM. We broke this down into digital, analog to digital, and digital to analog. For the analog to digital we chose the MetraByte VMECAI board. This was very similar to their DASH board we had been using on the AT bus. The major difference was that it did not have digital to analog capability. For the digital and digital to analog capability we selected Xycom. We purchase their XVME 201 card with 48 digital I/O lines. We evaluated their XVME 505 card with four channels of digital to analog capacity and suggest it use for future ARM development.

4. System memory subsystem

Because of conditions of memory unavailability and high cost, memory was a driving factor in computer hardware purchasing decisions. We have found that in recent months, versions of products were only deliverable in the foreseeable future if purchased with one or 2 MB of memory. Although the global memory was logically one block, using the 80386 it could be located in separate areas. We purchase the CPU card with 2 MB of 32 bit memory. We purchased the MM6230D memory board from Micro Memory Inc. with 4 MB on board. The board can accept another 4 MB on board and a daughter card for another 8 MB of 1024 k RAM chips.

5. Backplane, enclosure/connectors & power supply

We purchased a 20 slot VME bus cage with dividers and 3u and 6u prototype boards from Electronic Solutions. We bought a Powertec, Inc. Model 19F - E00 - ABD 500 watt power supply.

6. Peripherals

The VME bus based system was called the target system while our 386 based clone machine was the host computer. Programs were downloaded to the target from the host via a RS 232 port. We used a TeleVideo terminal to directly communicate with the target computer.

Xycom manufactures an XT short-card adapter card. We did not have an opportunity to evaluate this card. There are several possible uses for this card. One is for the adaptation of the DME Interferometer controller card to the VME bus. The other uses are to adapt XT display and controller cards to the bus.

Software

Ada was chosen to be the programming language for this project because it enforces many of the structural requirements for real time programming and supports the development of a hierarchical robotic control system. Several attributes of Ada made it an especially useful language. Among these were strong typing, generics, and tasking.

Typing refers to data type. In Ada each type of data was considered as unique and, therefore, must have its own specific set of operations. Because Ada was a strongly typed language, different versions of a subprogram module would have to be coded for each objects' type that we needed to pass to the module. The Generic feature of standard Ada avoided this. A generic module was a module which could accept any data type while still performing type checking. The process of instantiation of the generic module with a specific data type automatically created a version of the generic module that would accept that instantiated data type. Only one module template was required to be coded and versions of the module were created as needed with only one statement.

Scheduling was require to coordinate the control tasks. This required the design of a scheduler. The methodology for scheduler design was heuristic, i.e., developing rules by which other set of rules could be selected for use. This was one of the reasons we used the task construct for scheduling in Ada. The scheduling package of modules was the collection of tasks that direct traffic within the system.

A task was a process that runs concurrently with other processes. A task was not a compilation unit, as Ada packages were (a package is a compilation unit of related sub-program modules, including tasks). Tasks were structures that can be in the upper levels of the hierarchy as well as on a low level or nested within other tasks. They defined the interrelationships between events in terms of timing, importance, priority, or other rules or schedules that were necessary.

Various structure, e.g., arrays of tasks, were formed so that the software we designed was easier to analyze, test, and debug. The built in

scheduling features of Ada improved the level of reliability of the software produced.

Tasking was a great tool for preparing for coprocessor coordination. Provisions were made to declare particular high level tasks to coprocessors; the coprocessor was then viewed by Ada as a high level task. Tasks, as were other subprogram modules, were reusable. They were organized in compilation package for ease of reuse. Design of the scheduler package of tasks was implemented by first developing "production rules" and then determining an initial expected profile for the condition of the state table for the applicability of various production rules. Rules were the standard tool used to develop the "expertise" or "intelligence" of the system and were a set of ordered plans for producing the required results.

Initially, we used a hierarchical system to determine the production rules. The condition of the expected state table, which indicated the particular production rule or rules to be executed, was estimated. Experiments were performed to analyze the tasking and state table, and determined the exact values of variables in the state table of a particular task.

We determined that the preferred method of scheduling design on the macro level was to use the state machine. This was a non interrupt driven cyclic system, so that the program flow on the macro level was constant and did not allow any critical events to be missed by the system. This was true as long as the system had the appropriate resolution. System resolution was set using the timer on board the CPU board as part of the system initialization performed by the board support package and was basically a hardware function. Therefore, the software only needed to schedule and perform the tasks. When the execution speeds of the software were too slow, this was an indication of insufficient resolution, which indicated the need for a hardware fix, e.g., a smaller timer interval or more coprocessor power.

We developed a parasitic scheduler, a temporary main program, which functioned as a dumb controller to coordinate the off line tests supervised by the host machine. The parasitic scheduler scheduled the experiment, feed off of the state table, and saved the data. We used this method to perform experiments with the system constant but changing the event variables. This was done without making changes to the software.

Development of real time code was difficult. There were a large number of procedures which must be performed by the software; these were frequently complex interaction among modules. Besides being complex in interactions, because of the nature of the tasks, the flow patterns were continually changing. Debugging this code was difficult because of the interactions, the changing flows of interaction, and the large number of procedure which were considered. After debugging the code we applied the programs to the physical system using the host computer system.

Our real time robotic control system performed a number of procedures. The first was system initialization. This was a one time event which coordinated the various components, hardware, of the system. Hardware affected were the CPU, coprocessor, data linkers, memory, I/O cards and ports, and peripheral devices. Additionally, the physical ARM components had

to be initialized. Problems with the board support package for our target computer prevented any progress beyond this point on the target computer.

The second procedure was data acquisition. Sensors transmitted data to the acquired data area. The next task was the decoding of the data format such that it could be translated to the proper format for the next device. The decoded data was buffered or stored for access by the program procedure modules during run time and for analysis of the system off line.

Off line functions were data analysis and model development for the future runtime. From analysis of the input parameters the controller determined the instruction which were outputted to the drive elements of the ARM. These instructions were translated and encoded for use by the various actuators.

Finally, the workings of the program were displays such that the controller and the ARM could be monitored. These monitoring functions were performed internally and externally. Internal monitoring was required to keep the program on track and to provide breakpoints to evaluate program function. External monitoring was required to provide the operator with status information.

Programs

The software used for this project fell into two categories, acquired and written. The major acquired software packages were for the DME system, Matlab, Unix, and ADA. In addition, we acquired a variety of utility and upgrade packages. We programmed in ADA and wrote a variety of code to interface components and implement testing. The software generated was a basic set of tools which were designed to effect the implementation of a robust indirect adaptive controller. The general software control system design was developed, Figure 17. The tools also provided a mechanism for code additions and future alteration that will be required as more information is gained about the system.

Software to run the DME was provided with the hardware. It ran on an 8088 based machine. This system can be controlled as a task from the main program. Future developments would include rewriting the software in Ada and running the system from within the Ada environment as a task.

The Matlab program was simulation software. We used this to model the system. We purchased the package which runs on the 386 with a 387 coprocessor. We have formulated basic system models and an adaptive control model. The results of these simulations have been used to parameterize the system design.

Although it was not validated, we used a Janus ADA compiler for several years because nothing else was available. This approach allowed us to write code but, in some cases, had limited implementation. In December of 1987 the Janus compiler passed the validation suite and we received a validated compiler in February of 1988. We found that validation had little to do with the operation of the compiler. The validated version was so full of bugs that it was unreliable and, therefore, unusable.

We accessed, evaluated, trade studied, and ranked other Ada development systems. The top ranked system was that produced by Alysis. We ordered a

386 version in June 1988 but it turned out to be vapor-ware and we did not receive it until May of 1989. We did receive a 286 version of the Alysia compiler which we used to convert our Janus code and become familiar with the Alysia Ada environment.

We needed a Real Time Kernel (RTK) for the operating system. Several new RTKs and RTK development kits were available for the 80386. The Intel IRMK and the Hunter and Ready VRTX/32 386 were the most suitable. The Alsys RTK was not sold separately from the cross development system which was too expensive for the project.

We negotiated the purchase of the VRTX/32 386 RTK and board support package (BSP). It turned out to be vapor-ware; they delivered the VRTX/16 RTK and BSP. In late March of 1989 the VRTX/32 was ready and delivered. The BSP was unusable and they decided to drop the development of the required BSP for our CPU board and the Alysia environment, instead switching support to the Telesoft Ada environment for 68000 systems. Because of the problems associated with the receipt of the Alsys environment, we were able to negotiate for a Beta copy of their 386 cross development system. Although still under development, a sufficient portion was available to initiate work on a BSP. We were able to make sufficient progress to prepare to download from the host to target computer.

Most of our coding was of device drivers and low level primitives. This approach allowed us to implement basic system functions. We have designed the higher level programs. Our design follows the philosophy of the NASREM/NBS telerobotic control standard reference.

We have a collection of packages that take input from detector devices and encoders and outputs to the motors. We used a program made up from these packages to test the lateral effects detector from Hamamatsu.

The packages were :

1. Device specification packages

These were environmental specific device specifications. One was written for each device. They consist of global declarations of objects that were physically address ranges, port address ranges, values and/or structures that were transmitted to a device or its controller and other information required to use a specific device.

2. Device driver packages

These were packages of procedures and functions required to initialize a particular device and to operate that device on the lowest level. Device drivers were located in the logical map at the level of primitives and used the objects defined in the corresponding specification to satisfy requests for device use by units on the level of actions.

3. Actions level packages

Units at the action level were concerned with calling units in the primitives level to exchange information, as well as initiating jobs related to requests. Action level units were coded for all the basic system

services on the application level of the control system but nothing has been implemented for run time kernel level system services. So far these services have been handled by a standard operating system in connection with the run time kernel for the compiler we were using at the time. These system services are:

a. Display output, text based only

A "print data" template was used and all critical data objects existed in multiple types that have been derived from the base type of the low level I/O type of the particular object. The user can specify the format of data without altering the time interval of the output operation.

b. Permanent storage, standard disk drive storage

Rate and size of page dumps and data representation structures have been defined. The storage package was a special case in that it was written in a manner that was specifically tailored to the peculiarities of the compiler. Some of the structures have to be redefined.

c. Miscellaneous user interfaces

4. Task level code

We have designed tasking modules on paper but have not been able to adequately test tasking because of compiler difficulties. We have defined the task scheduling scheme, Figure 18. Task level units that will use the currently functioning sequentially linked units can be tested for performance and compared to the sequentially activated units once we have all units operating in the new APSE.

5. Event level code

We did not have the tools to implement multi-tasking and therefore event level programming was not appropriate at this stage of development.

6. Mission level code

Our "missions" have been to test various subsystems. We have assembled code from existing parts and written new parts as required for:

1. Control of the coil driver for the BR

This required levels 1, 2, and 3 for output of control of interface circuitry and the output of wave forms.

2. The lateral effects pin cushion detector testing.

This task actually has involved a mission that was in some ways a very simple model of a typical two node control unit. The detector node was simplified in that it consisted of the detector only. In reality we may add one or two more devices used for sensing of other parameters, e.g., temperature.

The actuator node consisted of two motors and two encoders. There was

no feedback from limit switches as there will be for ARM III from this node. In addition, the test used an x/y table and no vibrations were induced; it was not a realistic control node test. However, it did incorporate all of the support services required to implement control .

3. BR module

We tested and debugged the coil driver interface to the coil and completed testing and debugging the downloading of different data sets from the computer to the coil driver. Results were that the coil driver to coil interface functioned, as did downloading of various waveforms or data sets. We profiled timing attributes of the system.

Based on calculations, which used estimated figures for the 80386 machine at 16MHz, and assuming we were to write to each of 128 coils serially, we estimate that we could maintain update rates to the coil at frequencies below 7Hz. We investigated methods of offloading some of the cycle time into a parallel processing unit, (which would be the required implementation for ARM III), to increase estimated response time.

Target Dependent Programming

Once the target system is bootable, then the software can be used to run the ARM. This consists of the main program ARMCON and the device drivers. A large portion of this software has already been written. What is required now is to tailor it to the environment and test and debug the software.

Work to be done.

Device drivers.

Digital I/O card: The basic device driver routine has been written. It requires I/O port address specification be inserted and to then be compiled. The routine then must be tested and debugged incorporated into ARMCON.

Analog Input card: The basic device driver routine has been written. It requires I/O port address specification be inserted and to then be compiled. The routine then must be tested and debugged incorporated into ARMCON.

Analog Output card: The basic device driver routine must be written. It must then be compiled, tested and debugged incorporated into ARMCON.

ARMCON

A number of packages were used in this program. We have divided these into:

1) the ones that are required for the target system and what work is required to make them operational and

2) the ones which are running on the host system.

Work must be done on:

(The BP (Beam Positioning) routines retain the mirror designator because they were initiated when we were planning to use a mirror to position the beam. We now have a fiber optic and launch optics that delivers the beam to the beam directly to the BP.)

Mirror Azimuth: This routine receives input from a Canon encoder and directs the microstepper driver to reposition the beam positioner.

Mirror Elevation: This routine receives input from a Canon encoder and directs the microstepper driver to reposition the beam positioner.

Mirror test: This package uses the previous routines and other generic routine to test the BP module. With appropriate interfaces it will become part of the executable ARMCON program.

Shoulder Status: This routine needs to be written. It receives as input the current status of the two shoulder motors. Inherent to this program are the positional limits for the segment movement. These exceptions limit movement to the acceptable operating envelope.

ARM displacement: This routine needs to be written. It receives as input the current displacement of the segment from the reference beam. The input data is used to direct two activities. First, it is used to determine vibrations occurring within the system due to the forces, torques, exerted by the motors. Second, average displacement values are used to drive the BP to keep the reference beam centered in the segment (a closed loop low pass controller).

Shoulder Motor Torquer: This routine needs to be written. It receives as input user positioning commands. These are checked to verify they do not exceed operating limitations or the operating envelope. If the commands are valid they are routed to the motor drivers.

The following routines have been written and are operational on the host system.

User I/O: This routine accepts user input and gives the position of the beam positioner. It must be converted for use on the target system and modified to accept the required parameters.

Armrun: This routine operates in conjunction with MATLAB. MATLAB uses the physical parameters of the segment to generate a set of solutions to the first three modes of vibration. This routine predicts system response given a set of input parameters, i.e., motor torque. This is a portion of the adaptive control, i.e., given a set of input parameters it predicts system behavior.

In addition, in order to operate, a variety of generic routines are required:

Calendar - sets timing

Interrupt manager - manages interrupts

Communications interface - manages interface protocol

Unchecked conversion - error handling

Unsigned - unsigned numbers

Graphic functions:

Graphics

Graphing

Graphics Library

Mathematics Library

Input / Output

Text i/o

Generic i/o

Port i/o

i/o service

i/o exceptions

Modifications and enhancement of the program now running on the host computer will be required. These need to be performed in conjunction with the testing and debugging of the routines and programs required for the target computer.

Control

Adaptive Control

Adaptive control deals with the design of controllers which adjust to system uncertainties or time varying effects to ensure proper overall system performance. In this sense adaptive controllers are learning type controllers which monitor and learn about the unknown through input-output measurements of the unknown, a black box situation. In most cases adaptive controllers can be thought of as performing two functions. The first function is basically an identification process. The adaptive controller constructs a model of the unknown by looking at the response perturbations of the system stimulated by known input signals. The second function is, based on the most recent estimate of the unknown, to construct a controller which causes the system to behave as desired. Note that both identification and control occur simultaneously (or the identification could be completed first) so that, as the identifier zeroes in on the correct model, the control zeroes in on the proper controller to achieve the desired response of the overall system.

Adaptive control as applied to robotics is basically implemented as described above. Usually there exists a dynamic model of the manipulator, and generally, not every parameter of that model is known precisely. For example, friction coefficients may be difficult or impossible to measure or mass element terms may change due to the handling of various sized, unknown payloads. Thus, adaptive control techniques are used to identify any unknown terms in the model and then update a given controller to account for the change in system parameters.

To illustrate the concept of adaptive control, it is beneficial to review a paper by Craig, Hsu and Sastry (2) entitled, "Adaptive Control of Mechanical Manipulators." In this paper adaptive control techniques were used in the control of rigid link mechanical manipulators. The structure of the controller used was defined by the computed-torque method of control. Application of their method required a precise model of the dynamics of the manipulator because the control torques to be applied at each joint were calculated by plugging the desired response of the manipulator into the model of the system.

Specifically, most mechanical manipulators could be modeled by an equation of the form:

$$T = M(\Phi) + Q(\Phi, \dot{\Phi})$$

where Φ was a vector of joint angles, M was an inertia matrix which was dependent on manipulator position, Q was a function which accounted for torques arising due to centrifugal, Coriolis, gravity and friction forces and T was the vector of torques applied at each joint. If one knew every system parameter in the previous equation, then, to solve the equation for the necessary torques, all that was necessary was to plug into the given equation the desired joint angles, velocities and accelerations.

However, generally, not every parameter was known, thus, estimates for those parameters must be used. The adaptation came into play when one used the output of the real system and the model to make better and better estimates of the system's unknown parameters used in the model. It was the purpose of the previously mentioned paper to present a way to update estimates of the unknown parameters so that:

1. the controller maintained the stability of the system,
2. system performance improved, and
3. the correct values of the unknown parameters were identified.

We investigated the applicability of such techniques to the control of mechanical manipulators with flexible segments.

Control Considerations

We considered various ways to actively control the arm's end tip position through application of a torque at the base. Since accurate end tip positioning was the ultimate objective, it was logical to measure the end tip position and feed the position information back as the control variable. Such was the methodology used by Cannon & Schmitz in the control of a very flexible arm (3). In that paper an experimental set-up was described and analyzed. End tip position was measured by an optical sensor mounted above the arm. As the arm swung back and forth the optical sensor looked down on the arm and measured end tip position.

This position information was fed back, compared to the desired position and the resulting error signal was fed through a controller which was designed by Linear Quadratic Gaussian (LQG) methods (4). Controller

design was based on a sixth order model and achieved good performance. Hence, end tip position sensing was an important measurement and could be used to actively control an arm. However, external sensors are sometimes impractical to implement.

Therefore, we used a laser positioning system which measures arm end tip position through the use of a laser beam projected down the center of a hollow segment and detected the laser beam position at the end tip. The advantages to this type of end tip sensing were:

1. no external apparatus was needed,
2. one sensor for two axis of rotation - no transition problems between the multiple sensors that externally mounted sensing units required, and,
3. measurements of the manipulator behavior were made relative to a common base.

There were several configurations for laser mounting used on this project. The first had the laser mounted directly to the base of the single segment arm with the light beam shining directly down the center of the arm, ARM I. Under this configuration the laser coincides with the shadow beam and the end tip sensor measures directly the variable $u(X, t)$ -- vibrations of the arm relative to the shadow beam -- as defined in equations 1-6 of Appendix C, (ARM Model). This configuration was best suited for system identification and was simple to implement.

The second mounting configuration was to isolate the laser mount from the arm and used an independently controlled mirror, laser beam positioner, which directed the a light beam down the center of the arm, ARM II and ARM III. Under this configuration the difference between laser and arm end tip positions was measured and fed back as the control variable--see figure 19. The controller was designed so that the tip of the arm would track the tip of the laser. This set-up was used for the actual moving and positioning of the arm.

With the above described laser end tip positioning system a controller was designed which made the arm track the laser. The added constraint that the arm end tip not experience high accelerations, i.e., flex the segment more than one segment diameter, was also considered. We considered three basic design philosophies for the design of our controller. They were robust control design, direct adaptive control design, and identification/control design (indirect adaptive control). (Block diagrams showing the basic set-up of each type of control scheme as they apply to this situation are given in figures 19, 20, and 21 respectively.)

The idea behind the robust control design was to account for all system uncertainties in the design of a single, fixed controller. System uncertainties take the form of parameter variations, such as the change in payload mass, and unmodelled dynamics, such as the truncated modes and other system characteristics not included in the model. Hence, it was a worst case design scenario. The problem with using such a design technique in our situation was that it tended to lead to an overly conservative controller (under certain circumstances the arm would move more slowly than it needed

to move). The conservativeness arose due to the fact that the controller would have to be designed to ensure proper arm performance when the arm had a large or small payload.

The second type of a control scheme considered was adaptive control, (5). This type of controller was nonlinear and time varying. To implement this controller, first a model for the desired system response was chosen. Then, pre-filtering of the input and feedback of the output were used to force the resulting input/output properties of the controller plus real system to equal the input/output properties of the chosen model. The parameters of the controller were functions of an error signal created by taking the difference between the desired model output response and the controller plus real system output response. Update laws for controller parameters were chosen so that the just-defined error signal was driven to zero. Therefore, as real system parameters changed the controller parameters changed. Thus, the controller plus the real system always behaved like the chosen model.

There were, however, some very restrictive assumptions needed on the real system in order to ensure proper performance of the adaptive controller. One, for example, was that we know the order of the system -- the number of states. In our case the number of states was infinite and we could not implement an infinite dimensional controller of this form. Thus, direct adaptive control had some problems with application. Significant research would be required to modify this scheme for use on our infinite dimensional system.

More promising, however, was to use identification techniques, as given in Good (6), in conjunction with periodic control parameter updates. An identifier was placed around the real system to identify system parameters. Then, based on the value of those parameters, a controller was automatically designed and implemented. Since the system physical parameters changed only periodically, we updated the control parameters periodically. Thus, rather than continuously updating the controller, as was done in direct adaptive control, we only needed periodic updates, e.g., when a payload was picked up, of the control parameters. This generated a sequence of fixed controllers. Because this controller only adapted to a new situation indirectly as it occurred, this design was called Indirect Adaptive Control, Figure 22.

Modeled System Behavior

In order to predict expected system behavior we created a model of our system (Appendix C, equations 7-12) to calculate the first three modal frequencies of the system for rotation about the z-axis. We compared those modal frequencies to modal frequencies of several arm segment modeling configurations. Furthermore, we developed a model of the motor and gear box, Appendix D, which derived the transfer function between control voltage and torque to the segment. All together the arm segment configurations considered were:

1. a non-rotating cantilevered beam with no payload.
2. a non-rotating cantilevered beam with payload point mass m_p and no payload rotary inertia;

3. a non-rotating cantilevered beam with payload point mass m_p and payload rotary inertia I_p ;
4. a rotating beam with no base rotary inertia, payload point mass m_p and no payload rotary inertia;
5. a rotating beam with base rotary inertia I_h , payload point mass m_p and no payload rotary inertia.
6. a rotating beam with counterweights, base rotary inertia, payload point mass and payload rotary inertia.
7. a rotating beam driven from a motor/gear box with counterweights, base rotary inertia, payload point mass, and payload rotary inertia.

The last situation was the most complex of this series of models. This particular model was called SIMI and can be found in Appendix A. SIMI was used to generate the predicted behavior of a particular segment configurations based upon its physical parameters and characteristics. It was also used to scale the system. Thus, we were able to design systems with longer or shorter segments that would maintain the same primary mode of vibration and maintain similar response characteristics for the controller.

For the first case above, the modal frequencies were calculated assuming a 5 lb. mass payload then a 10 lb. mass payload. The other system parameters were generated from measurements of the actual system and are given in Table 2. Results of the modal frequency calculations are given in Table 3.

For the last case payloads in 1 to 100 Kg were calculated Table 1. Examination of this data reveals that for the segment of interest there is a primary mode under 10 Hz. In order to sense a particular mode one must sample at a frequency no less than twice that of the particular mode. Thus, for this system a sampling rate on the order of 400 - 800 Hz. would be necessary to sense the first 3 modes.

Stiffness

It was illustrative to make a few calculations to determine that we actually benefited by making the arm more flexible and accounting for those flexibilities in the analysis. As previously mentioned, every system has some degree of flexibility. Whether the flexibility was significant depended on the performance requirements. For space application it was beneficial to reduce overall system mass. Hence, we needed to determine if we could achieve a significant reduction in overall system mass by using lighter but more flexible materials while still maintaining reasonable overall system dimensions which allow the use of our laser positioning system.

The following were some approximate calculations we made to provide a rough idea of what was occurring in this situation.

The assumptions we made were:

1. The arm was massless in comparison to the size of the payload.
2. The arm consisted of a single segment of length L.
3. Beam deflections at the tip were governed by the equation, (7);

$$\delta = FL^3/3EI$$

where $F = ma$

$m =$ mass of the payload

$a =$ maximum acceleration of the payload

$L =$ length

$E =$ elastic modulus of the beam

$I =$ cross sectional moment area of inertia of the beam.

4. The maximum amount of stress experienced by the arm could be given by the following equation, (8);

$$\sigma = M * r_o/I$$

where

$$M = (m_p * a * L) + (m_b * a * L/2)$$

$m_b =$ mass of the beam.

5. System parameters were:

$$L = 10 \text{ m}$$

$$a = 1 \times 10 \quad g = 9.81 \times 10 \text{ m/sec}$$

$$m_p = 100 \text{ kg.}$$

beam cross-section was cylindrical

$r_i =$ beam inside radius

$r_o =$ beam outside radius

6. The maximum amount of allowable displacement for the "flexible" case was r_i .

7. The maximum amount of allowable displacement for the "stiff" case was 0.01 mm.

8. Material properties of the materials considered were:

| | Aluminum | Steel | Fiberglass |
|--|----------|-------|------------|
| density, ρ (kg./m) | 2770 | 7830 | 2081 |
| E (GPa.) | 75 | 200 | 11.4 |
| maximum allowable σ (MPa.) stress | 365 | 450 | (?) |

With the above assumptions an approximation for the first modal frequency, w_1 , was;

$$w_1 = (3EI/L^3 \rho)^{1/2}$$

Considering only first mode deflections the following equations must be satisfied for the "flexible" case conditions and the "stiff" case conditions:

$$r_i = FL^3 / 3EI \quad r_o^4 = .981*4 / (3r_i * E \pi) + r_i \quad \text{flexible case}$$

$$.00001 = FL^3 / 3EI \quad r_o^4 = 98100*4 / (3E \pi) + r_i \quad \text{stiff case}$$

The resulting beam mass was calculated by the following equation:

$$m_b = 10 (r_o^2 - r_i^2) \rho$$

Using the above assumptions and formulae we calculated the maximum stress, outside diameter, first mode frequency and mass of the resulting arm for various arm inside diameters made of the specified materials for both the "stiff" and "flexible" cases results in the numbers given in table 4.

Examination of the data in table 4 revealed that there was a significant savings in mass achieved by allowing the beam to be flexible, even if we compared materials which were light and flexible with materials which were slightly heavier but stronger. Furthermore, the resulting arm dimensions were reasonable. For example, an aluminum "flexible" arm with inside radius 1.5000 cm. and outside radius 1.5027 cm. had the mass that an aluminum "stiff" arm had and 1/50 the mass that a steel "stiff" arm had with comparable dimensions. Hence, we have achieved significant mass reduction by allowing a beam to be flexible. In addition, the ARM dimensions were reasonable enough to allow the use of the internal laser positioning system. It should be noted, however, that when a large mass moves at an extremely low acceleration, the system becomes very sluggish and has a low primary model frequency.

RESULTS

We have developed a preliminary design for a flexible two segment ARM using space rated technology. Because of the need to test and evaluate the ARM under earth gravity conditions a number of compromises were made. In general, the technology employed for prototyping is upwards migratable to space conditions.

We have identified the relevant parameters for the ARM. We have defined the pertinent parameters and defined the critical characteristics. Using this information we have specified and obtained the major critical system components.

The ten major systems have been prototyped and tested. The interrelationships between systems was considered and designs and schemes developed which would allow each system to operate independently and jointly with the other systems. Considerable flexibility was designed into the systems to allow latitude in their implementation. Simplicity was sought for each system to minimize failure effects and to ease interfacing between systems.

BR

A beam rider (BR) module was developed that used only one active component, the mirror positioner. The mirror position was controlled via a feedback loop from a quadrant detector that was located on the interferometer assembly and also used by the rotational measurement equipment. The other elements were passive in that they did not move. A single photodetector was employed which had a high resolution, 2000 x 2000 pixel, 10 x 10 micron, spot positioning capability. The photodetector automatically integrated the signal to determine the centroid of the spot. Beam spot diameter and size had no impact upon this ability as long as they were held constant. Signal processing was performed in real time using analog circuitry. A single optical component, a quarter wave plate, served to circularly polarize and unpolarize the beam and reflect the beam spot upon the detector. Thus, the BR module required only three elements and their associated electronics.

BP

A beam positioning (BP) module was developed that used a pair of high resolution microstepper motor/encoders. Motor operation and encoder read-out were setup for either manual or computer operation. Resolution, precision, and repeatability were all in the arc-second range. The greatest inaccuracies in the system were due to wobble and unorthogonality of the two axes stage; +/- several arc-seconds. The overall system pointing accuracy was well within the one part in 10,000 required for millimetric accuracy at 10 m; it was closer to one part in 1,000,000. A 1.4 +/- 0.7 degree power failure/system down - system up positioning accuracy was also provided by the system.

DME

A distance measuring equipment (DME) module was developed that had no moving parts and prealigned optical elements. The laser beam was delivered

to the interferometer using a single fiber optic. A single beam left and was retroflected colinearly to the interferometer assembly. Three optical fibers carried the interferometric information to the associated electronics. Submicron resolution was available from the system.

RME

The rotational measuring equipment (RME) module was the last system to be developed due to the need to finalize the configurations of the other systems. It utilized two photodetectors; one measuring the intensity of the output beam and the other the intensity of the return beam. The latter was a quadrant detector which also served as the positioning sensor for closing the loop of the mirror positioner unit. Because of the delay in implementing this system it was not possible to optimize its performance. There were deficiencies in the linearities and performance of the detectors and electronics. Resolution was, therefore, suboptimal, on the order of one part in 1000 to 3000.

Elbow

The elbow articulation was the basis for a single degree of freedom ARM testbed. A custom designed high torque-low weight brushless three phase motor was specified and obtained. A zero backlash 200:1 Harmonic drive gearbox was specified and obtained. The housings of these units were capable of mounting to the proximal segment and supporting the distal segment. The prototype motor and gearbox assembly were used to evaluate the performance of this combination and to determine the wind-up or spring constants inherent to the harmonic gearbox. This value was an important parameter in the motor/gearbox model.

Shoulder

The shoulder articulation was the most complicated of the systems developed. It consisted of a base assembly situated on a tripod. The azimuthal motor rested on the base and was surrounded by outrigger bearings. The fork bolted to the top motor plate, which also rode on the outrigger bearings. The two arms of the fork extended upwards and had bearings mounted on each distal end. The yoke pivot mounted to the fork bearings. The yoke accepted counterweight plates on each side of the back of the assembly. The front of the assembly was flanged to accept the mating piece from the segment. The central portions of the fork and yoke were empty to allow placement of the BP.

The shoulder required two different motors and drivers. The elevation motor was a DC brush motor coupled through a 100:1 harmonic gearbox. It was driven by a high current linear amplifier using a voltage controlled preamplifier. The azimuthal motor was a multipole direct drive annular motor with a semi-intelligent controller which could be operated in analog or digital torque or velocity modes. The two motors were connected to a two degree of freedom joy-stick for manual operation. The gain in the preamplifiers was adjustable so as to be able to equalize the torques applied to each axis.

Passing through the center of the azimuthal motor was the support segment for the BP. The shoulder and the BP support segment were each

bolted independently to a common base. The support segment was a rigid 9 cm. (3.5 in.) diameter steel tube.

Segments

Segments were designed to be of a non-critical design factor and interchangeable, i.e., the ARM was not sensitive in operation to any particular segment, only that the segments conform, in general, to a set of design parameters, and, in particular, design parameters determined by the particular task to be undertaken. The basic criteria for the selection of a segment was payload. (The payload, in this case, being the sum total of the "weight" applied to the distal end of a segment.) A minimum and maximum payload was determined for a segment. Two factors influenced these values. One was the frequency ranges of the modes of vibrations. The other was the range of travel on the counterweights required for operation.

We selected segments for use dependent upon the payloads they were required to carry. Most of the testing was performed using a 5 m. (15 ft.) long 9 cm. (3.5 in.) diameter aluminum segment. The elbow design parameter called for a 34 kg. (75 lb.) payload at the distal end of the distal segment. The shoulder design parameters called for a 182 kg. (400 lb.) payload at the distal end of the proximal segment. The elbow and shoulder design parameters were based upon a two meter articulation-to-articulation separation and, therefore, were actually indications of the maximum torques. Longer segments would have reduced payloads and shorter segments greater payloads.

Calculations were performed to compare a "flexible" and a "stiff" segment. There was a significant savings in mass achieved by allowing the beam to be flexible, even when we compared materials which were light and flexible with materials which were slightly heavier but stronger. For example, an aluminum "flexible" segment with inside radius 1.5 cm. and an outside radius of 1.5027 cm. had 1/20 the mass of an aluminum "stiff" arm and had 1/150 the mass that a steel "stiff" arm.

Calculations were performed to compare segments made of five different materials; titanium, aluminum, E-glass/Epoxy, UHM Graphite/Epoxy, and Beryllium. For a 7 m. segment with a 10 cm. internal radius capable of carrying the same payload the following were obtained:

| Material | Outside Radius (cm.) | Weight (kg.) |
|--------------------|----------------------|--------------|
| Titanium | 11.06 | 221.31 |
| Aluminum | 11.51 | 197.61 |
| E-Glass/Epoxy | 11.93 | 181.14 |
| UHM Graphite/Epoxy | 10.50 | 37.56 |
| Beryllium | 10.44 | 35.89 |

Hardware

A 20 slot VME bus Intel 80383 based computer system was implemented. A Force CPU 386 main computer board with 2 megabytes of memory was used. A Micromemory board with 4 megabytes on board, expandable to 16 megabytes, was obtained. A Metrabyte VMECAI 16 digital I/O board, a Xycom XVME-201 analog input board, and one 6u and two 3u prototyping boards were purchased. A

Powertec, Inc power supply served to supply the system. A TeleVideo monitor and keyboard served for user I/O to the system.

Software

A variety of software packages were used on the project. The computer had a ROM based Force Debug program which initialized the CPU board to protected mode and allowed user control of low level functions and debugging capability. Matlab, a matrix algebra program, was used for performing the modeling calculations. Programming was done in ADA. Initially, a Janus ADA compiler was used. We migrated into the Alsys compiler from the 286 to the 386 version. Ultimately, we used a beta version of the 386 cross compiler to implement a real time operating system on the target computer.

A Ready Systems VRTX 32 real-time operating system was purchased for the system. This was, ultimately, found to be unimplementable. This was because the board support package for our computer was not available and support for the Alsys environment was never developed.

An assembly based board support package was written using the Phar Lap 386 ASM/LinkLoc assembler for the Alsys 386 cross compiler. The package initialized the environment for the Alsys run time kernel. It initialized the clock and I/O ports and initiated the down load procedure.

The low level device drivers were written using the Alsys 286 compiler environment. These included driver specification packages, device driver packages, and action level packages for the I/O boards. A variety of generic routines were generated. These were a Calendar to set timing, an Interrupt manager to manage interrupts, a Communications interface to manage interface protocol, an Unchecked conversion to handle errors, an Unsigned to handle unsigned numbers, graphic functions, and mathematics library, and I/O routines.

The high level programs were "mission" level code. These were written for particular "missions", e.g., control of the linear voice coil driver for the BR module, for testing the lateral effects diode, and control of the BP module.

A system design for ARM III was configured, Figure 23. At the top, using a single data format, were the:

1. Main System Tasks
2. Initialization Tasks
3. High Level Control Tasks
4. Low Level Control Tasks
5. Internal Format Buffers.

At the bottom, using variable data formats, were the:

1. Device Buffers

2. Interfaces and Filters
3. Device Nodes
 - A. Actuators
 1. shoulder
 2. elbow
 3. BP
 4. BR
 - B. Encoders and Detectors
 1. DME
 2. RME
 3. shoulder
 4. elbow
 5. BP
 6. BR

Intermediate to these system portions were the translation and filters. These were responsible for the interconversion of data from a uniform format to the device specific formats and vice versa. In addition, from this stage, was the interface to the data storage area.

Adaptive Control

An adaptive control program ARMCON was written to model the behavior of a single link flexible segment. Four steps were required for execution. These are explained in detail in Appendix I. The first was to run ARMMODEL. The second was to run MATLAB. The third was to translate the files for the fourth program, SIMIAC. The translated output of the simulation was presented as a graphic output to the screen. The screen graphics provide three moving displays. One was an emulation of the segment rotating about a center pivot. The second, coordinated with the first, provided an appropriately labeled graph showing end tip displacement response. U2, from the normal position. The third was the DC driving voltage. Additional data displayed was the time after initiation, the endtip velocity, and the endtip acceleration.

ARMMODEL had six options. These were:

1. Input Values
2. Calculate Coefficients
3. Display Calculated Data
4. Display Matrices
5. Print Data to Disk (For Printer Output)
6. Save Matrices for MATLAB.

Input parameters were the:

1. Base rotary inertia
2. Tube inside radius
3. Tube outside radius
4. X-sectional inertia of beam
5. Payload mass
6. Mass/length of beam material

7. Elastic modulus of beam
8. Length of beam
9. Beam material damping coefficient

The program calculated the coefficients and saved the matrices for use with MATLAB.

The MATLAB execution had four parts. The first part, ARMMOD, modeled the behavior of the segment, base, and counterweight assembly. The second part, MOTGER, Figure 24a, modeled the behavior of the motor and gear box. The third part, COMBINE, combined these models and the fourth part, SIMCOMB, Figure 24b, allowed for the insertion of the operating parameter. A further MATLAB operation, TRANSLATE, translated the matlab product files to flat ASCII files for use with SIMIAC.

SIMCOMB allows for operator input of the control voltage. Provisions have been made for a time varying DC voltage for the prime control and up to three decaying time and phase varying AC voltages at different frequencies for vibration control. A set of simulations was run for a 2 m segment. The input data was printed out as an ARM MODEL data file, see Table 5. Different input voltages were used to drive the model. Figures 25 and 26 were examples of a single DC kick start and a DC kick start with an exponentially decaying signal. The step DC voltage starts exhibited a characteristic set of oscillations at the end tip. A exponentially ramped up voltage input, $1 - \exp(-3t)$, provided a relatively smooth start, Figure 27, however, a second order oscillation was observable. The addition of a quickly decaying, large amplitude, phased sinusoidal input, Figure 28, substantially reduced these oscillations. Further refinements were possible using AC inputs of various frequencies, phases, amplitudes, and duration.

SIMIAC ran a simulation of the behavior given DC and AC input parameters. It was present as an updated animated moving graphics display. For a tuned adaptive controller, the ARM would exhibit the same behavior as that shown on the screen. Figures 29a and b were the SIMIAC final screen of the function shown in Figure 27 and 28; the end tip displacement was shown in greater resolution and exhibits ringing upon startup. Figure 29 b showed the effect of adding a second order decaying AC control voltage to actively damp the induced vibrations.

Safety

A safety assessment of the ARM was performed. A number of recommendations were made. A list of these is contained in Appendix E.

DISCUSSION

Within the results section of this report we have covered many topics. Let us first discuss why it was necessary to take into account the effects that compliance has on the behavior and control of a mechanical manipulator. The main reasons were derived in the presentation of a system model. These were:

1. As positioning requirements become more precise the significance of compliance in the system increases and
2. To reduce overall system mass it was necessary to use lighter and, therefore, more compliant materials.

Because the major goal of this project was the precise positioning of long, flexible manipulators, there was significant compliance in the system. We avoided the approach of using a massive rigid body to precisely position the end tip. Instead we relied upon an essentially massless beam of light to act as our rigid frame of reference.

This approach also facilitated the need to reduce overall system mass. Because of the need to launch the system into space, reducing system mass became a prime objective. The more compliant the system was allowed to be, the less mass that was required in the segment. Although the articulations were required to be rigid bodies, reducing the segment mass reduced the forces on the articulations and, therefore, reduce their massiveness.

We derived a mathematical model of the system which took into account the flexure of the segment. Previous work by Cannon and Schmitz (9) demonstrated that the segment end tip position could be used in a closed loop feedback system to actively control the ARM. The experimental set-up used by Cannon's group required external sensors to measure end tip position for feedback control. However, external sensors are difficult to implement in practice. Therefore, we implemented a concentric laser positioning system to measure end tip position. This approach had several advantages:

1. No external peripheral apparatus was required,
2. A reduced number of sensors was required; there was no transition problems between multiple sensors that externally mounted sensing units require, and
3. Measurement were made relative to a common frame of reference.

Track I - Positioning System

To be meaningful, we had to know the position of the end tip to six degrees of freedom, Figure 30. In other words, we were required to know the current position, three degrees of freedom, and point to a new location, three degrees of freedom. Such precise positioning was demanding under any set of conditions; we made it more difficult. We wanted to accomplish our positioning with a single laser beam.

The simplicity of the concept of using a single laser beam was compelling. We evaluated a large number of single and multiple beam

positioning schemes. As a scheme became more convoluted and complex it was dropped. We distilled the essence of the various schemes into the final approach. The final design used one beam reflected within a cavity defined by the rigid bodies of each of two articulations. Theoretically, it was not even necessary for the two ends to be physically connected. In reality, the physical connection between the two ends defined the limits of operation and simplified design of the system.

BR

At the distal end of the segment was the beam rider (BR) module. The original design of the BR was a rather complicated affair, Figure 5. It used a pair of quadrant diodes with center orifices to monitor beam position. Beam displacement was used in a feedback mode to actively reposition the module in two dimensions. Two problems were defined for this scheme. The first was the need for a precise linear positioner and the second was for some mechanical linkage between the beam rider and the articulation.

We evaluated the status of linear positioners and found nothing that met our requirements. Therefore, we developed a scheme for a multi-voice coil linear positioner with variable waveform drive capacity. Although this driver functioned well, the signal processing required to implement its motion was incredibly complex. Extrapolating from the 8088 based system we used initially to a 16 MHz 80386 based machine and to a 128 coil configuration, we estimated that we could update drive rates to the coils at frequencies at or below 7 Hz. Our design objective was in the 500 to 1000 Hz. range.

We developed a more simple scheme for the BR. We had identified some highly accurate, 2000 x 2000, pixel lateral effect diodes that avoided the image recognition problems associated with a CCD type matrix. The centroid of the beam spot was automatically provided and, within limits, the size of the beam spot was irrelevant, i.e., the beam spot was small compared to the size of the active surface of the diode. A beamsplitter could be used to split a portion of the beam to the diode and transmit the rest for the other positioning sensors. This portion of the system could then be passive, i.e., no moving parts.

Our positioning concept required the retroreflection of the incident beam. Originally, a mirror attached to the active BP would be positioned to do this by the linear positioners. With the elimination of the linear positioners an alternative scheme was required. The technical name for this unit was a Fast Steering Mirror. Three suitable units were identified, one was too expensive, one was not yet in production, and the third was purchased.

The piezoelectric unit was not yet in production. Preliminary data from prototype units indicated that it was ideal for our application. It should be seriously considered for any future development in this area.

The quadrant voice coil unit we used functioned after significant development effort. It had the frequency response required but required a lightweight mirror. The weight requirement affected the quality of the mirror and, therefore, degraded system performance.

The other element employed in the BR was a quarter waveplate. It had a triple duty. The polarized incident beam was split by mounting the plate at an angle. The split beam was reflected onto the lateral effects diode. The transmitted beam was circularly polarized. The circularly polarized beam reflected by the mirror was converted to a polarized beam orthogonal to the polarization of the incident beam. Rotation of the segment and, thus, the articulation and wave plate changed the efficiency of the orthogonal polarization conversion. This principal was used to measure rotation.

BP

We were fortunate enough to find a space rated BP unit with the required arcsecond pointing capability required. This unit, built for the Hubble telescope was ideal for our current and future space needs. Unfortunately, the cost of a ground based unit was that of our total equipment budget and, thus, beyond our means. Therefore, we had to develop our own unit.

Initially, the BP was to position a mirror which would reflect the laser beam down the segment. For this concept to function, it was necessary to have a hollow central orifice in the azimuthal axis of rotation. This requirement restricted the drive and encoder designs which could be incorporated into the unit. Ultimately, we modified the laser beam delivery system such that the laser beam was delivered to the beam positioner through a fiber optic. This greatly simplified design considerations. The price we paid was in beam intensity.

DME

The DME was interferometric in nature. Polarized light was used so that, by detecting its orthogonal components, P and S, two signals were derived which were in phase quadrature. These signals enabled normal bi-directional counting techniques to be employed. Both signals consisted of sine waves which related to the path difference in the two arms of the interferometer. The sine wave was superimposed on a DC level, which was related to the light which does not produce interference.

Misalignment of the system decreased the amount of light producing interference. This was seen electronically as a decrease in the sine wave component and a increase in the DC level. In order to trigger a counter it was essential to have a stable DC level. Two systems have been developed which overcome this problem. One was patented by Hewlett Packard. The other was based on a design developed by M. Downs and K. Raine at the National Physical Laboratory. The line was initially commercialized by Barns and Stroud in England. Subsequently, the line was purchased by Coherent Radiation Labs and, after several years, dropped by them. We used this latter system.

In this system, plane polarized light from a single frequency stabilized laser was split by a single plate so that each beam had equal intensity. Each beam contained an equal amount of P polarized and S polarized light. The polarization content was achieved by rotating the plane of polarization of the laser to approximately 45 degrees. On recombination, the interference pattern could be viewed either in

transmission or reflection.

Two quadrature signals were produced by examining the P and S components. By introducing a one-eighth wavelength mica retardation plate, it was possible to retard either the P or S component by 90 degrees. An additional polarizing beam-splitter and selective polarizers were used to produce three signals, each having the same DC and AC levels but having phase angles of 0, 90, and 180 degrees. Subtraction of the 0 and 90 degree signals and the 90 and 180 degree signals results in two further signals. These latter two signals had a zero DC level and were in quadrature. Any changes in the DC levels did not affect the bi-directional counter because it was set at a trigger level of zero.

The standard HeNe laser had three main limitations in its use in an interferometer.

1. Multiple modes of oscillation,
2. Frequency stability, and
3. Sensitivity to optical coupling back in the laser cavity.

Multiple modes were controlled by using a short tube which supported only two modes. These were linearly and orthogonally polarized. Laser stabilization was achieved by maintaining a constant distance between the laser mirrors. The tube was heated to adjust the cavity length so that, by using polarizing beamsplitter and photo-detectors, the intensity of the two modes could be adjusted and maintained equal.

Normally, the use of retroreflectors and the displaced return beam eliminates the possibility of any coupling back into the laser cavity. For our application it was necessary to use a single beam. The beams were decoupled by utilizing the polarized nature of the beam. The lateral displacement prisms reflected and transmitted the S and P waves differently. Therefore, by rotating the plane of polarization by 90 degrees in the BR module, the input and output beams were decoupled.

RME

The RME also relied on beam polarization. Any rotation of the distal end tip affected the efficiency of the conversion of the S and P waves. If the return beam intensity was monitored, all other parameters held constant, changes in beam intensity indicated a rotation of the distal end tip.

As previously mentioned, the output beam intensity varied because of a number of reasons. One of these reasons was the movement of the fiber optic delivering the beam to the BP during movements of the physical ARM. Because of the nature of operation of the DME decoding operation, it was not particularly sensitive to these intensity changes. On the other hand, the RME, which relies on beam intensity, was quite sensitive to these changes. Therefore, we needed to develop a scheme which would be immune to beam output intensity variations.

The scheme selected was to measure the intensity of the beams up and

back from the segment. Theoretically, the ratio of these two should remain constant. In practice we encountered several problems. These problems related to the sensitivity, linearity, and dynamic range of the detectors and to the electronics.

The Basic difficulty was the same reason that the scheme worked well for the DME. Small rotations about the optimal quarter wave plate orientation, impact the beam intensity very slightly. For example, about the optimal orientation, the return beam detector output amplifier produced a 12 volt signal. Rotations of one or two degrees resulted in a signal change of one or two millivolts. When a rotation was chosen further from the optimal operating position, the signal changes were more dramatic, i.e., hundreds of millivolts. Unfortunately, when operated far from optimum, the DME loses signal intensity and, thus, count. Additionally, coupling back into the laser cavity was possible.

We have evaluated some high dynamic range, i.e., one to a million range, detectors from Dalsa. Initially, their responses were deemed to be too nonlinear over the entire range to be of use. However, we would require only a small portion of the entire range for rotation measurement. Therefore, the large dynamic range detectors could provide a solution. In operation, the two beams being analyzed would be coupled into fiber optics. The fibers would deliver the beams to the detector board with their integrated electronic circuitry.

There were several electronic signal processing schemes which could be used to isolate the signal portion of the detector input, i.e., the changes associated with intensity variations. An automatic gain control circuit or a differential amplification circuit could be used. There were two problems which must be considered however. The first was if the dynamic range of the detectors currently being used was satisfactory. The second was that we need to work with the ratios of the up and back beams and not their absolute values.

Track II - Physical ARM

The original design scheme for the ARM envisioned a hollow structure in which a light beam would pass from the base of the shoulder, through the elbow, and out to the distal end tip of the distal segment. The structure was a folded cavity with positioning mirrors located within the shoulder and elbow articulations. The elbow would have had a 90 degree freedom of rotation and the segments would be approximately 7 m. in length.

The final design scheme for the ARM confines the laser beam to a single segment and used a solid articulation at the elbow. This design had the advantage of simplifying the positioning system in that it was no longer necessary to accurately reflect the beam through the elbow. Rather, the positioning system would be cloned for each segment.

A second advantage to the new design was that it could use shorter segments. By increasing the freedom of rotation of the elbow to 360 degrees, a pair of 5 m. segments could be used to obtain the desired 10 m. reach. An advantage to a shorter segments was in the amount of flex or compliance. The flex of the segment was proportional to the cube of the length. Therefore, shortening of the segment resulted in a segment with 64%

less compliance. This significantly decreased the rigidity required of the segment for a given payload positioned at the same rate. Decreasing the rigidity of the segment also decreased the mass of the segment and, ultimately, that of the entire system.

Elbow

The elbow articulation was the first one prototyped. It consisted of a yoke with the segment attached to one end and counter weights at the other. The yoke assembly balanced upon the shaft of the motor gear box unit. The assembly mounts above the plane of the proximal segment in order to have a clear field of rotation. Because of cabling the rotation was limited to +/- 180 degrees. For safety sake, to avoid possible collision with the shoulder articulation, rotation was limited to +/- 170 degrees. However, because of budget and time limitations the connection between the proximal segment and elbow articulation was never implemented.

To accommodate a reactionless drive requires a modification of the motor gearbox/harmonic drive coupling. There are two positions where a flywheel can be mounted. One location would rotate the flywheel at the rate of segment rotation while the other would rotate at the speed of the motor rotation. The latter would rotate 200 times faster than the former with a concomitant decrease in the required mass of the flywheel. If the motor is decoupled from the gearbox and surrounded by a flywheel, it can then free-wheel in reverse of the torque provided to the drive shaft. Therefore, the torque required to rotate the distal shaft is not transmitted to the proximal segment and the base. Thus, we have a reactionless drive.

Douglas Rohn at NASA Lewis Research Center has developed several traction drives. There are several advantages to traction drives in the area of backlash. To accommodate traction drives required the latter design configuration for the ARM, since the traction drive designs tend to have solid centers, i.e., no central orifice,.

Shoulder

The shoulder was a robust assembly capable of dealing with the weights of the components required to function under earth gravity conditions. Among these are the massive counterweights required to balance the payload. Each prong of the yoke carries 102 kg. of counterweight for a total of 204 kg. The yoke itself must act as a rigid body, therefore it was designed massive enough not to flex when subjected to the forces required to position the ARM. From here down the structure becomes progressively more massive at each piece had to bear the weight of the structures above it and contributed its own weight to the structure.

One advantage to this massive structure is its inertia. Being massive, small forces and torques exerted upon it have little affect and tend to dampen. This dampening effect can further be aided by the use of vibrational isolation components. A number of these are available. Elastomers can be used between components and on the mountings. A sound dampening material can be applied to all of the free surfaces. Because of our desire to initially characterize the basic system, none of these steps have been implemented.

In general, the response of the assembly to vibration was small. The components most affected were the segments. This suggests that it may be desirable to coat them with vibrational dampening materials or to include an absorptive material in their construction. The BP support segment was especially susceptible to vibrations transmitted from the base.

Segments

We have characterized the requisite parameters for segment design and developed a program to model their performance. We have analyzed their performance as a function of length and of material. Based upon the objective of a 10 m. reach our design utilizes two 5 m. segments. Because the articulations require some space, the actual length required of the segments was somewhat less than 5 m.

In the results section we presented data on the parameters for a "stiff" and a "flexible" segment. We found that there was a significant savings in mass achieved by allowing the segment to be flexible. We also presented data on the required cross section for segments of different materials with similar length, inside radius, and payload capabilities. The most exotic materials, UHM Graphite/Epoxy and beryllium, were significantly lighter, only 20% of the weight of a more common material such as aluminum. Therefore, a flexible segment of an exotic material can easily be justified for space use even with the significant increase in the production cost over more common materials.

Using the 5 m. value we determined the principal modes of vibration for segments of different material. In scaling the system the primary objective was to match the primary modes of vibration between the segments of different length. An interesting phenomena was the behavior of the resonant frequencies with changes of payload mass. Table 1 presents data for aluminum and steel segments of the dimensions we used. The second set of data in the table was for a 9 cm. diameter segment of the type we used. Payloads modeled ranged from 2.27 kg (5 lb.) to 181.3 kg (400 lb.). with these different payloads the first mode frequency ranged for 3 to 18 hz., a 500 % increase. The second mode ranged from 95 to 110 hz., a 16 % increase. The third mode ranged for 309 to 327 hz., a 6 % increase. The principal mode was, thus, determined to be of prime importance in scaling.

Track III - Control System

Our control problem for this project was one of real time robotic control. The real time aspect was the driving force behind hardware and software selection. Real time was used to define a time frame of action or response from the control system. In general, the response time had to be faster than any particular set of movements such that the system could react before any untowards event occurred. The second general timing factor was the bandwidth required to sample events. For example, it was necessary to sample at twice the frequency of an event in order to accurately determine the frequency of the event. Therefore, for a third order mode in the 400 hz. range, sampling was required at 800 hz. Thus, a timing factor on the order of one millisecond was indicated.

In order to increase the time of response, a mixture of analog and digital technology was used. In general, much of the low level control and

sensing was performed using analog circuitry. The mainstay of the position detection systems were the lateral effect diode and the quadrant diode. These each had four output signals. These signals were buffered, summed, subtracted, multiplied, and divided using analog components. This approach yielded microsecond response times. The greatest problems associated with this circuitry was the generation of unstable high frequency oscillations. Although a number of fixes were possible, we chose to degrade the response times to submillisecond to stabilize the circuitry.

Most of the driver circuitry was analog. Motor or driver control signals were, in general, a voltage. A particular input voltage corresponded to a particular output current and, therefore, torque produced by the prime mover. Some of the driver circuitry was modified to act in a semi-digital fashion, e.g., the use of pulse width modulation. Conversely, some of what might be considered as digital technology, i.e., stepper motors, were operated in a more analog format, microstepping. Where possible, a feedback controlled loop was established using analog technology, e.g., the loop between the mirror mover and the quadrant diode.

In a sense the control system was modeled after the human nervous system. Actions which required quick response were set in a reflex arc with information of the events that transpired being passed to the higher cognitive functions of the computer. The higher order functions were executed by the computer. These included mission level tasks such as predicting how the system would respond to a certain set of stimuli, i.e., modeling, planning and sequencing a set of moves to generate a path from point A to point B, tracking the path of the move and determining the need for midcourse correction, unilateral system shutdown, and communication with the operator.

Hardware

The computer hardware will be more useful in the future than it was in the present. The process of system definition, design, selection, and implementation of the target computer system consumed the allocated time and left none for actual operation. However, the host computer system was essentially identical to that of the target computer system. The major difference was that the host operated under the interrupt driven MS DOS while the target operates with a real time kernel. Thus, the work performed on the host was directly applicable to the operation of the target.

The engineering impetus for switching to a VME bus was reliability. Because of the planned application of the ARM safety and reliability became an obsession with the engineers. The development of the dedicated computer system consumed resources in excess to its current utility. It was a much more difficult and complex task than was ever allocated for in the original proposal. However, given its current operational status and our boost along the learning curve, we are in an excellent position to implement the control system. Thus, the hardware is more of a Phase III tool that it was a Phase II tool.

Software

The availability of 32 bit microprocessors with their four Gigabyte address space allow for the creation of embedded systems incorporating truly

gargantuan programs. Popular programming languages are hard pressed to support programs forged with mega-lines of code, but Ada meets that challenge. NASA has adopted Ada as the official programming language of the Space Station Freedom Project, and expects the computerized system aboard the space station to require millions of lines of code. Ada appears to be the language of the future.

Unfortunately, the development of the Ada language and its implementation has been slower than expected. The Ada development systems have been less than promised and their deliveries have lagged their schedule by years, i.e., vapor-ware. We adopted the Ada language over four years ago and have ridden this rocky path.

Some of the strong points of the Ada language were the following:

1. Top-down development
2. Strong data typing
3. Abstraction
4. Information hiding and encapsulation
5. Separation of specification from implementation
6. Reusability
7. Separation of physical realization from logical concepts
8. Portability
9. Modularity
10. Readability

We were able to make good use of the strong points of the Ada language to develop code. The code we developed years ago, using using a now obsolete development system and compiler, were upgradable to our present system. After a year of vapor-ware, we finally received our validated 386 compiler and programming environment. In summary, we have a great tool for Phase III but lacked what was actually required for Phase II.

Fortunately, because of the vapor-ware problem, Alsys owed us a favor. Therefore, we were able to evaluate a beta copy of their 386 cross compiler (not released in a final form as of the date of this report). With this package we were able to design a board support package which should initialize the target computer to allow the downloading of the runtime executive program. While the executive does support Ada tasking, it does not support the tasking attribute of the 386 protected mode.

MATLAB has lived up to its claims. This matrix algebra program was very useful for our model implementation. Unfortunately, we had difficulties implementing matlab from our programming environment. This was because our "386" Ada compiler was actually a 286 version and required a 287 math coprocessor. MATLAB was a 386 version and required a 387 math coprocessor. Although our host computer supported both the 287 and the 387, we had to physically toggle a switch between the two. Therefore, we had to choose which of the programs would be run before turning on the computer.

The Microport System V/386 Unix environment functioned well. It was utilized by the engineers familiar with Unix from their work at the University of California, Berkeley. It facilitated the transfer of programs from the university based computers.

We utilized both the Microsoft assembler MASM and the Phar Lap assembler, ASM/LinkLoc. Although MASM was quite functional it used slightly different terminology than LinkLoc. Because the real time kernels were written with the Phar Lab LinkLoc environment, this environment was required to effectively write the board support package and implement downloading.

The DME program was something of an anachronism. It was written in basic and performed a variety of function not required for this project. We were able to obtain a source code listing. Therefore, we have the capacity to rewrite the program if required. Because of the defunct state of this product, a VME based board or a revision of the software does not appear likely. Currently, the system runs off of a dedicated 8088 computer system. The simplest solution to bring it onboard the VME bus is to use one of Xycom's XT short card adapter boards.

The VRTX/32 was of no use to us. Originally, they shipped VRTX/16 and a board support package adaptable to the Force CPU 386. By the time they created the VRTX/32 support of the Force CPU 386 and the Alsys environment had been dropped. Creation of the BSP was beyond the abilities of this project.

Adaptive Control

We have analyzed how our system model could be used in the design of a controller for the active control of the ARM end tip position. The end tip position was controlled by the application of a torque at the base. It was noted that, because the model required an infinite numbers of dimension, it was necessary to truncate it. (An infinite dimensional system was difficult to deal with because it required an infinite dimensional controller.)

We covered the concepts of robust control design, direct adaptive control design, and adaptive control design techniques for use in the design of our controller. It was determined that indirect adaptive control was the best option because a robust control design would lead to an overly conservative design, and direct adaptive control had technical implementation problems.

We made some approximate calculations to determine if making an arm "flexible" as opposed to "stiff" really resulted in the desired objective of reducing the overall system mass. We found that for a 10 m. long single segment arm which could move 100 kg. payloads at microgravity accelerations, the mass of the arm could be reduced by a factor of roughly 20 by allowing it to be flexible. For higher accelerations the mass ratio was further increased. Another result of these calculations was that the mass of the segment, compared to that of the payload was not negligible. Therefore, for modeling, the segment mass needed to be considered.

Preliminary to the design of our system, we modeled the behavior of a single segment flexible ARM. We developed a program to calculate the first three modal frequencies based upon a variety of input parameters. We compared this data for different configurations of base and counterweight, segment materials, diameters, and lengths, and payloads. We determined, for our design, sets of segments which would have approximately equal first modes of vibration and third order modes under 500 Hz.

The model was adjusted for a typical set of operation parameters. Simulations were subsequently run to predict the displacement of the segment end tip. The kick start simulation ran, as expected, with easily discernible modes of vibration. Soft start configurations had less pronounced oscillations. These secondary oscillations could be exacerbated or reduced by driving at the proper phase and frequency. Controlled wave shaped starts not only decreased the initial end tip displacements, but also reduced the energy channeled into secondary modes of vibration.

In general, the model behaved as expected for simple conditions. Thus, in the general sense, we validated the model. We were not able to validate the model against the physical ARM; this would be the next logical step. There was some problem with model "run away" in the long term. This was a linear increase in the end tip displacement at a rate of 1 to 2 micrometers/second. We were not able to locate the source of this problem; we could add a linear term in the voltage formulation to compensate for this drift.

The purpose of the simulation model was to form the basis of the indirect adaptive controller. The model appeared to be suitable for this function. The simulation model must be consolidated into a software package suitable for operation with the computer system. Initially, variables were hand entered; these would actually be derived from ARM sensors. The system must then be taught the proper or preferred responses to these stimuli, i.e., scaling factors and selection criteria. This would create the required smart or intelligent system.

As we have previously mentioned the degree of artificial intelligence of a system depends upon the hierarchical level of the system. Our system requires a number of levels. These vary from the low level reflex closed loops to the higher level control and mission functions. Thus, our system can be considered to possess some intelligence.

An expert system depends upon production rules to determine the best solution to a particular problem. We have developed a protocol to model the behavior of the system. The parameters of the model can be varied to produce a response similar to the actual responses of the system, validation. The validated model can be used to predict the response of the system. This ability provides a mechanism for path planning. Once the path has been determined, the model stores the parameters. At this point the model becomes the controller and drives the motors to move and position the end tip.

The actual end tip position was determined by the positioning system. The physical placement of the ARM was an approximation to the desired position. This was because the resolution of the arm drivers was limited by mechanical factors to be much less than that required for the desired positioning accuracy. Therefore, it fell upon the positioning system to accurately determine the actual position of the end tip. Given the actual position, fine positioners on the distal end tip can be used to manipulate the payload into the exact position required.

CONCLUSION

We have developed the preliminary designs for the critical systems necessary for a flexible two segment Articulated Robot Manipulator (ARM) using space rated technology. These systems were breadboarded, or prototyped, and tested and evaluated under earth gravity conditions.

The principle goal of the project was to demonstrate the feasibility of using a laser beam for determining, with millimetric precision, the position of the distal ARM endtip in six degrees of freedom over a 10 m. distance. We developed a scheme which allowed as to accomplish this using only a single laser beam per segment.

The second goal was to develop a control scheme which would allow active control over the Physical ARM based upon the laser reference system. We adopted a control theory which allowed for the positioning of the physical ARM based upon the distance d between the nominal static reference beam position and the actual reference beam position under dynamic conditions, the vector U_2 . We identified a type of controller, the indirect adaptive controller, suitable for the pick and place duty of the ARM. We constructed a model of the system which served both to define the needs of the physical ARM and act as the basis of the indirect adaptive controller.

The third goal was to prototype the physical ARM in order to test and evaluate the requisite concepts. We prototyped three versions of the ARM. The first had a static base and was used to evaluate the properties of the segment. The second rotated with one degree of freedom and served as the basis of the elbow articulation. A zero backlash motor-harmonic gear box was used as the driver. The output torque of the unit was a function of the control voltage/motor drive current. The behavior of this unit was used to identify and define the motor-gearbox transfer function. The third version was the shoulder articulation. It rotated on two mutually orthogonal axis. The center of this articulation was hollow such that the laser guidance system could be located collinear with, but independent of, the physical ARM.

We developed, defined, and breadboarded or prototyped ten systems for this project. Four of these were for the positioning system. Three of these exceeded the positioning requirements. These were:

1. The Beam Rider Module - measured two dimensions, x_1 and y_1 , and retroflected the laser beam.
2. The Beam Positioning Module - measured two angles which corresponded to two dimensions, x_2 and y_2 , pointed the laser beam, and contained the DME and RME systems.
3. The distance Measurement Equipment - measured changes in path length between the ends of the segment and provided the measurement of length.

The fourth system was not optimized and provided only one-third to one-tenth of the desired resolution. This was the:

4. Rotational Measurement Equipment - measured changes in rotation of the axis of the segment.

Three systems related to the physical ARM were developed and prototyped. These were prototyped using space ratable technology or materials. These were the:

5. Segment - connected the articulations and supported the beam positioning module.
6. Elbow - this was a single degree of freedom articulation located between the two segments and designed to hold one beam rider and one beam positioning module.
7. Shoulder - a two degree of freedom articulation built around the beam positioning module.

Three systems relating to the control of the ARM were designed, specified, and implemented. These were:

8. Hardware - An Intel 80386 based computer system responsible for the overall control and operation of the ARM.
9. Software - These were the programs which ran the computer, the ARM, and comprised the controller model.
10. Indirect Adaptive controller - This program modeled system behavior, which duplicated the behavior of the physical ARM, and generated the control information necessary to move from one point to another.

In addition, a variety of circuitry was developed and breadboarded to support the devices used in the various systems. These included:

1. Lateral effects diode decoder circuitry
2. Quadrant diode decoder circuitry
3. RME diodes decoder circuitry
4. DC brush motor controller and driver
5. DC brushless motor controller
6. Mirror positioner driver and controller

Several other breadboards and prototypes were built, tested, and evaluated. These include a:

1. A twenty coil linear voice coil positioner unit with associated circuitry, computer interface, and associated software.
2. The lateral effects diode test jig drivers, controller, computer interface, and associated software.

CONCLUDING REMARKS

Using a concentric laser positioning reference system is a elegant solution the the problem of controlling long flexible manipulators. Significant reductions of mass are possible by using a flexible manipulator. Moving this concept from the laboratory to a production environment is nontrivial. Numerous difficulties remain to be resolved. The technology necessary for this transition is available.

This project took the fist several steps required for the implementation of this concept. A period of testing and refinement of the various systems is required. No insurmountable obstacles lie in the development path, i.e., it is feasible.

There is alternative technology available which would improve to performance of the various systems. Where appropriate, reference has been made in the text. There are, however, tradeoffs in adopting alternative technology, e.g., a time of flight DME system would require a different solution to the RME system. A large amount of time and effort was spent in developing a self-consistent set of system which would interrelate and work well together.

The concept we have championed is feasible, its implementation is a challenge for the future.

APPENDIX A

Documentation of the Segment Modeling/Simulation Software

I. Overview

There are three principle programs associated with the segment modeling/simulation software. These are:

- 1) ARMMODEL.EXE and its corresponding source files. This program is given, as input, the physical parameters of the segment to be modeled. The core of the model was written in FORTRAN translated into Microsoft C. Functions were added to find the roots of the characteristic equation, output the resulting model's data to screen and printer, and to produce MATLAB-readable matrix files for the simulator.
- 2) MATLAB FILES. These files are executed under the MATLAB environment and take, as input, the output matrices of ARMMODEL, as well as parameters specifying the duration of the simulation, the time-wise resolution of the simulation, and the voltages to the motor (DC and AC). MATLAB is a linear algebra applications program. The files originally produced a plot of end-displacement against time; Code was modified to output data describing segment travel and approximate endtip velocity and acceleration, for input to the ARMSIM program.
- 3) ARMSIM.EXE and its corresponding source files. This program takes as input the model data from the MATLAB files and outputs to the display time-variant graphic and numeric representations of segment travel, endtip displacement, voltage, approximate endtip velocity and acceleration.

II. Notes Regarding the Science behind and limitations of ARMMODEL

The mathematical model implemented in ARMMODEL was designed based on a cantilevered beam (fixed at one end, payload at the free end) will approximate the true configuration (the beam's base fixed to a motor). As an approximation, if the base moment of inertia is large with respect to the mass of the payload then the two configurations probably generate model frequencies which are similar. If the mass of the segment is large compared to the payload mass the approximation degenerates. These relationships need to be determined experimentally based upon the actual system.

ARMMODEL determines the first three resonant frequencies of a single segment in two dimensions. Rotational resonances are not modeled.

III. Using ARMMODEL

The executable file is ARMMODEL.EXE. Once run, the program displays six options:

1) Input Values

This option executes a procedure that prompts the user for input

parameters. Current/default parameters are displayed and may be retained by inputting a number less than zero. See below for explanations of each input parameter.

2) Calculate Coefficients

This option executes the procedures that calculate the coefficients of the output matrices used by MATLAB, as well as the resonant frequencies of the segment, based on the input parameters. Once the coefficients are calculated, the program displays all relevant data produced. In order to display all the data on one screen, the descriptors are rather terse; it is suggested that the data be viewed with Option 3 or 5.

3) Display Calculated Data

This option displays the data calculated by option 2.

4) Display Matrices

This option displays the matrices used by MATLAB (Matrices A, B, C)

5) Print Data to Disk (For Printer Output)

This option writes a file to disk that can be PRINTed or TYPed at DOS. It is more verbose than the output of option 2 or 3. The user is prompted for a filename.

6) Save Matrices for MATLAB

This option writes the matrices to disk. The user is prompted for filenames, though MATLAB expects the filenames to be a.mat, b.mat, c.mat for the matrices A, B, C, respectively.

The only option that needs elaboration is Option 1. Option 1 prompts for a number of input parameters, described below (all units are SI):

1) Base Rotary Inertia - This value is the sum of:

counterweight rotary inertia
yoke rotary inertia
payload rotary inertia
segment rotary inertia

2) Tube Outside Radius (in meters)

3) Tube Inside Radius (in meters)

4) Mass per Unit Length (kilogram/meter)

5) Payload Mass (in kilograms)

6) Elastic Modulus of Beam (in Pascals)

7) Length of Beam (in meters)

8) Damping Coefficient of Segment

IV. Using the MATLAB files

NOTE: some familiarity with MATLAB is useful but not necessary.

Once ARMMODEL has been run, and appropriate matrix files have been saved, the MATLAB files can be executed. Once in the MATLAB directory, make sure the matrix files are approximately named (am.mat, bm.mat, cm.mat). Enter MATLAB by typing 'matlab' at the DOS prompt. The files to be run, in order of use, are as follows:

- 1) armmod.m - this loads the three matrices into the MATLAB environment.
- 2) motger.m - this loads the data related to the motor/gearbox parameters/state space model.
- 3) combine.m - combines the arm model (the three matrices) with the motor/gearbox model. You will be prompted to input the length of the segment.
- 4) simcomb.m - this file runs the simulation. You will be prompted to input:
 - a) tmin - the starting time (in seconds)
 - b) tmax - the ending time (in seconds)
 - c) tinc - the time increment (in seconds)

As an example, a simulation with a running time of ten seconds might have tmin = 0.00, tmax = 10.00, and tinc = .01; MATLAB will generate a matrix, to be used in the simulation, something like this:

```
t = [0.01 0.02 ... 9.98 9.99 10.00]
```

You will then be prompted to input voltages:

- d) dc voltage - a numerical constant (i.e. 100) or a function of time (i.e. $1/\exp(-t)$).
- e) ac voltages - up to three amplitudes and corresponding frequencies. (input zeroes if no ac input wanted).

MATLAB will generate another matrix, whose i-th entry is the voltage at the time corresponding i-th entry in the time matrix.

To run the simulation, the commands are entered in the following order:

```
armmod
motger
combine
simcomb
```

MATLAB will then run the simulation, display a plot of end-tip displacement versus time, and write two files to disk: model.mat and header.mat. These two files contain the information needed by ARMSIM.

Before these files can be used by ARMSIM, they must be translated into 'flat' ascii files. To do this, leave the MATLAB environment with the 'exit' command.

The files are translated from a MATLAB format to a flat ascii file through the program TRANSLATE, a MATLAB utility. Invoke the program by typing `translate` at the prompt. The use of TRANSLATE is self-explanatory: you will be prompted for input filename (model.mat or header.mat) input filetype (.mat) output filename (model.dat or header.dat) and output filetype (flat ascii). See MATLAB manual for more information.

Once the files header.mat and model.mat are translated, you can run ARMSIM.

V. Using ARMSIM

The graphics used in ARMSIM require an IBM CGA-compatible graphics card.

ARMSIM's executable file is called SIM1AC.EXE. To run, make sure that the files header.dat and model.dat are in the working directory. Type `sim1ac`. You will be presented with the program's graphics screen. Hit `<RETURN>` to start the simulation. Subsequent `<RETURN>`s will pause and continue the simulation. These are the only controls.

The display is divided into three graphics windows and several text lines. The large, leftmost window displays a representation of the segment. The upper right window displays the voltage, and the lower right window displays the end-tip displacement.

The text lines are labeled and include time, voltage, the length of the arc scribed by the endtip around the base, endtip displacement, and approximate endtip velocity and acceleration.

When the simulation halts at `time=tmax`, you may exit with `<RETURN>`.

APPENDEX B - HARDWARE

DSP HARDWARE - PRODUCT:

| | |
|---|---|
| AT & T Technologies Dept. 50AL203140 555 Union Blvd. Allentown, PA 18103 1-800-372-2447 WE DSP32C | LSI Products Division TRW Electronic Components Group P.O. Box 2472 La Jolla, CA 92038 (619) 457-1000 TMC3032/3033 |
| Bonschul International, Inc. 11000 Cedar Avenue, Ste. 212 Cleveland, OH 44106 (216) 421-2380 MSP320 | Mercury Computer Systems, Inc. Wannalancit Technology Center 6600 Suuffolk Street Lowell, MA 01854 (617) 458-3100 (415)847-2025 MC3200 |
| Definicon Systems, Inc. 31324 Via CXolinas, Ste. 108 Wastlake Village, CA 91362 (818) 889-1646 DSI-32E | Metme Corp. 4623 Morganford St. Louis, MO 63116 (314)353-3869 TMS320 |
| General Instrument Microelectonics 3080 Olcott Street, Ste. 230C Santa Clara, CA 95054 (408) 496-0844 DSP320C10 | Micon systems Co. 1800 Avenue of the Stars, Ste.10 Los Angeles, CA 90067 (213) 282-8570 Micon's M8096-1 |
| Imapro U.S. Inc. P.O. Box 67 Suffern, NY 10901 (914) 368-2787 Master Vector Processor Plus (MVP+) | Micro Way P.O. Box 79 Kingston, Mass. 02364 (617)746-7341 Accelerators XXX86 |
| Intersil, Inc. 10600 Ridgeview Court Cupertino, CA 95014 (408) 996-5000 IM29C325 | Microstar Laboratories, Inc. 2863 152 Avenue N.E. Redmond, Washington 98052 (206) 881-4286 DAP1200 |
| Keithley Instruments, Inc. 28775 Aurora Road Cleveland, OH 44139 (216) 248-0400 Series 500 | NEC Electronics Inc. 10080 N. Wolfe Road, SW3 Ste.360 Cupertino, CA 95014 (408) 446-0650 |
| LSI Logic Corp. 1551 McCarthy Blvd. Milpitas, CA 95035 (408) 433-8000 L64000 Series | Oki Semiconductor 650 North Mary Avenue Sunnyvale, CA 94086 (408) 720-1900 M6992 |
| | Omega Engineering, Inc. One Omega Drive, Box 4047 Stamford, CT 06907-0047 1-800-826-6342 |

Opto 22
15461 Springdale Street
Huntington Beach, CA 92649
(714) 891-5861
I/O System Components

Paracom Inc.
Bldg. 9, Unit 60
245 W. Roosevelt Rd.
West Chicago, IL 60185
(312)293-9500

Sota Technology, Inc.
657 N. Pastoria Blvd.
Sunnyvale, CA 94086
MotherCard 5.0

Spectrum
240 H Street
Blaine, WA 98230
1-800-663-8986

Altos Computer Systems
2641 Orchard Parkway
San Jose, CA 95134
(408) 432-6200
Altos 386 Series 1000

American Micro Technology
14751-B Franklin Ave.
Tustin, CA 92680
(714) 731-6800

BBN Advanced Computers Inc.
10 Fawcett Street
Cambridge, MA 02238
(617) 873-6000
Butterfly 1000

CCI
17830 State Road 9
Miami, FL 33162
800-331-5150

Computer Dynamics, Inc.
2201 Donley, Ste. 365
Austin, TX 78758
800-722-8304

Concurrent Computer Corp.
197 Hance Ave.
Tinton Falls, NJ 07724
(201) 758-7000
Series 3200

Systolic Systems, Inc.
2240 North First Street
San Jose, CA 95131-2310
(408) 435-1760
PC-100

Texas Instrument Inc.
P.O. Box 809066
Dallas, TX 75380-9066
1-800-232-3200
VLSI 32-bit

Weitek Corp.
1060 E. Arques Avenue
Sunnyvale, CA 94086
(408) 738-8400
ACCEL 8000 Series

Zoran Corp.
3450 Central Expwy.
Santa Clara, CA 95051
(408) 720-0444
ZR34161 VSP, ZR33891

386 HARDWARE

DFE Electronic Data Systems
5820 Stoneridge Mall Rd. Ste. 115
Pleasanton, CA 94566
(415) 847-2024
TIGER-32

Digital Research Inc.
OEM Sales
4401 Great America Parkway Ste. 200
Santa Clara, CA 95054
(408) 982-0700

Dyna Computer Inc.
3081 N. First St.
San Jose, CA 95134
(408) 943-0100
SX386

General Micro Systems, Inc.
4740 Brooks Street
Montclair, CA 91763
(714) 625-5475
GMS V07

Hauppauge Computer Works, Inc.
358 Veterans Memorial Highway, Ste. MSI
Commack, NY 11725
800-443-MATH

Hertz Computer Corp.
325 Fifth Ave
New York, NY 10016
(212) 684-4141

Hyundai Electronics America
4401 Great America Parkway, 3rd Fl.
Santa Clara, CA 95054
(408) 986-9800

Intel Corp.
3065 Bowers Ave.
Santa Clara, CA 95051
(408) 987-8080
System 120 Real time 386

JMI Software Consultants, Inc.
P.O. Box 481
904 Sheble Lane
Spring House, PA 19477
(215) 628-0846

Lloyd I/O Inc.
P.O. Box 30945
Portland, OR 97230
(503)666-1097
Omega 68020

National Semiconductor Corp.
2900 Semiconductor Drive
P.O. Box 58090
Santa Clara, CA 95052-8090
(408) 721-5000
Series 32000

Performance Semiconductor Corp.
610 E. Weddell Drive
Sunnyvale, CA 94089
(408) 734-9000

Perkin-Elmer
Data Systems Group
2 Crescent Place
Oceanport, NJ 07757
(800) 631-2154
32-BIT Minicomputers
Plessey Microsystems
22931 Triton Way
Laguna Hills, CA 92653
(714) 855-4947
PMM 8M

Pro-Log Corp.
2560 Garden Rd.
Monterey, CA 93940
(408) 372-7082
System 1

TeleVideo Systems, Inc.
1170 Morse Ave.
P.O. Box 3568
Sunnyvale, CA 94088-3568

Zaiaz
2225 Drake Ave.
Huntsville, AL 35805
(205) 881-2200
ZAI AZ 933

Zeos International
530 5th Ave, NW Ste. 1000
St. Paul, MN 55112
800-423-5891
ZEOS 386/M

INTERFACES & BUSES

| | | |
|-----------------------|--------|------------|
| G-64 | VME | MULTIBUS I |
| MULTIBUS II | S-100 | STD |
| UNIBUS | Q BUS | BIT BUS |
| SCSI | ESDI | ST/506 |
| SUPER-BUS | NU-BUS | IBM/AT BUS |
| IBM MICRO CHANNEL BUS | | |

AT & T
Dept. KB, 55 Union Blvd.
Allentown, PA 18103
1-800-372-2447

Acromag
30765 wixom Rd.
Wixom, MI 48096
(313) 624-1541

Advanced Electronics Design
440 Potrero Ave
Sunnyvale, CA 94086
(408) 833-3555

Alcyon
5010 Shoreham Pl.
San Diego, CA 92122
(619) 587-1155

Analog Devices
One Technology Way
Norwood, MA 02062
(617) 777-4500

Anasco
42A Cherry Hill Dr.
Danvers, MA 01923
1-800-826-2726

Applied Control Concepts
6589 N Sidney Pl.
Glendale, WI 53209
(414) 351-2550

Arcom Control Systems
Unit 8 Clifton Rd.
Cambridge, U K
0223 242 226

Ariel Systems
8545 Arjons Dr. Ste. I
San Diego, CA 92126
(619) 549-0134

Auscom
2007 Kramer Ln.
Austin, TX 78758
(512) 836-8080

Basu
c/o Dage Precision Industries
2914 Scott Blvd.
Santa Clara, CA 95054
(408) 727-1932

Beal Communications
9794 Forest Ln., Ste. 246
Dallas, TX 77801
(409) 775-5009

Bicc-Vero
1000 Sherman Ave.
Hamden, CT 06514
(203) 288-8001

Burr-Brown
6730 Tucson Blvd.
Tucson, AZ 85706
(602) 746-1111

Central Data
1602 Newton Dr.
Champaign, IL 61821
(217) 359-8010

Chrislin Industries
31352 Via Colinas
Westlake Village, CA 913662
(818) 991-2254

Ciprico
2955 Xenium Ln
Plymouth, MN 55441
(612) 559-2034

Clearpoint
99 South St.
Hopkinton, MA
1-800-253-2778

Communications Machinery
1421 State St.
Santa Barbara, CA 93101
(805) 963-9471

Comcontrol B V
P.O. Box 193]
Eindhoven, Holland
31-40-124955

Computer Modules, Inc.
2348 C Walsh Avenue
Santa Clara, CA 95051
(408) 496-1881

Data Translation
100 Locke Drive
Marlborough, MA 01752
(617) 481-3700

Datel
11 Cabot Blvd.
Manssfield, MA 02048
(617) 339-9341

Dual Systems
2530 San Pablo Ave.
Berkeley, CA 94702
(415) 549-3854

Dy-4 Systems
1475 S Bascom Ave., Ste.202
Campbell, CA 95008
(408) 377-9822

Educational Microcomputer System
One Clear Spring
Irvine, CA 92715
(714) 854-8545

Electronic Modular Systems
Capital Center Plaza, Ste. 109
1325 Capital Pkwy.
Carrollton, TX
(214) 446-2900

Eltec Electronix GMBH
Galileo-Galilei-Strabe 11
D-500 Mainz 42 PO Box 65
West Germany
49(6131)50631

Excelan
2180 Fortune Drive
San Jose, CA 95131
(408) 434-2296

Force Computers
727 University Ave.
Los Gatos, CA 95030
(408) 354-3410

GalilMotion Control
1928A Old Middlefield Way
Mountain View, CA 94043
(415) 964-6494

General Micro Systems
4740 Brooks St.
Montclair, CA 91763
(714) 625-5475

Grant Technology, Computer Prod
321 Billerica Rd.
Chelmsford, MA 01824
(617) 256-8881

Graphic Strategies
549 Weddell Dr.
Sunnyvale, CA 94086
(408) 745-6500

Heurikon
3201 Latham Dr.
Madison, WI 53713
1-800-356-9602

High Technology Electronics
303 Portswood Rd.
Southampton SO 2 1LD
U K
(703) 581555

Ikon
2617 Western Ave
Seattle, WA 98121
(206) 728-6465

ILC Data Device
105 Wilbur Pl.
Bohemia, NY 11716
(516) 567-5600

Imaging Technology
600 W Cummings Park
Woburn, MA 01801
(617) 938-8444

Imagraph
800 W Cummings Park
Woburn, MA 01808
(617) 938-5480

Integrated Micro Products
No.1 Ind Est,
Consett Co Durham DH8 6TJ
England
0207-503481

Integrated Solutions
1140 Ringwood Ct.
San Jose, CA 95131
(408) 943-1902

Interactive Circuits & Systems
3101 Hawthorne Rd., Ottawa
Ontario, Canada K16 3V8
1-800-267-9794

Integrated Scientific Systems
1181 Aquidneck Ave
Middletown, RI 02840
1-800-847-4797

ms

ucts

| | |
|---|---|
| Interphase 2925 Merrell Rd. Dallas, TX 75229 (214) 350-9000 | Microdesigns 1874 Forge St. Tucker, GA 30084 (404) 493-6318 |
| Introl 2675 Patton Rd. St. Paul, MN 55113 (612) 631-7600 | Microproject 4676 Admiralty Way Ste. 617 Marina Del Rey, CA 90292 (213) 306-8000 |
| IOtech, Inc. 23400 Aurora Rd. Cleveland, OH 44146 (216) 439-4091 | Microproject V.V. Clams Sluterweg 125 2012 WS Haarlem The Netherlands, 023-292084 |
| Ironics 798 Casadilla St. Ithaca, NY 14850 (607) 277-4060 | Microvoice 23362 Peralta Dr. Laguna Hills, CA 92653 (714) 859-1091 |
| Iskra VME Technologies 222 Sherwood Ave Farmingdale, NY 11735 (516) 753-0400 | Mini Computer Technology 696 East Trimble Rd. San Jose, CA 95131 (408) 435-2032 |
| Logical Design Group 541 Pylon Dr. Raleigh, NC 72606 (919) 834-8827 | Mizar 20 Yorkton Ct. St. Paul, MN 5517 (612) 224-8941 |
| Matrix 1203 New Hope Rd. Raleigh, NC 27502 (919) 833-2000 | Mizar/Kontron Mikrocomputer Oskar Von Miller STS 8057 Eching B Munchen West Germany * |
| Matrox Electronics Systems 1055 St. Regis Dorval Quebec, Canada H9P 2T4 (514) 685-2630 | Monolithic Systems 84 Inverness Cir East Englewood, CA 80112 (303) 790-7400 |
| Mercury Computer Systems 600 Suffolk st. Lowell, MA 01854 (617) 458-3100 | Motorola 2900 S Diablo Way Tempe, AZ 85282 (602) 438-3501 |
| Micro Memory 9540 Vassar Ave Chatsworth, CA 91311 (818) 998-0070 | National Instrument 12109 Technology Blvd. Austin, TX 78727 (512) 250-9119 |
| Micro/Sys 1011 Grand Central Ave Glendale, CA 91201 (818) 244-4600 | NCR 3325 Platt Springs Rd. W Columbia, SC 29169 (803) 791-6800 |

Nectronix
1372 McDowell Blvd.
Petaluma, CA 94952
(707) 72-2703

Nimbus
1420 N. Claremont Blvd.
Bldg. 102-A
Claremont, CA 91711
(714) 625-0017

Owl Computers
640 Crest Drive
Encinitas, CA 92024
(619) 436-4214

Pacific Microcomputers
6730 Mesa Redge Rd.
San Diego, CA 92121
(619) 453-8649

Parallax Graphics
2500 Condensa St
Santa Clara. CA 95051
(408) 727-2220

PEP Modular Computers
00 N Bell Ave
Pittsburgh, PA 15106
(412) 279-6661

Performance Technologies
435 West Commercial St.
East Rochester, NY 14445
(716) 586-6727

Philips/Signetics Microsystem
811 Arques Ave.
sunnyvale, CA 94088
(408) 991-3544

Plessey Microsystems
One Blue Hill Plaza
Pearl River, NY 10965
(914) 735-4661

Psi Tech Inc.
18368 Bandilier Circle
Fountain Way, CA 92708
(714) 964-7818

Recognition Technology
335 Fiske St.
Holliston, MA 01746
(617) 429-780

saimet/Pascot
17981 Skypark Cir Ste. B
Irvine, CA 92714
(714)261-5220

SBE
2400 Bisso Lane
Concord, CA 94520
(415) 964-5700

Scanbe Unit of Zero Corp.
3445 Fletcher Avenue
El Monte, CA 91731
(818) 579-2300

Scientific Micro Systems
339 N Bernardo Ave.
Mountain View, CA 94043
(415) 964-5700

Stollmann
Max-Brauer-Allee 79-8
D-200, Hamburg 50
West Germany
040/389003-0

Storage Concepts
3198-G Airport Loop Dr.
Costa Mesa, CA 92626
(714) 557-1862

Syscon
3990 Sherman St.
San Diego, CA 92110
(619) 296-0085

Tadpole Technology
Unit 151, Science Park
Cambridge, England
0(0223)861688

Tadpole Technology/Pascot
17981 skypark Circle, Ste. B
Irvine, CA 92714
(714) 761-5220

Thomson Semiconducteurs Microsy
45 Av De L'Europe
78140 Velizy, France
(1) 39.46.97.19

T L Industries
2541 Tracy Rd.
Toledo, OH 43619
(419) 666-8144

Wespercorp
1821 E Dyer Rd.
Santa Ana, CA 92705
(714) 261-0606

VME Inc
560 Valley Way
Milpitas, CA 95035
(408) 946-3833

Xycom
750 N Maple
Saline, MI 48176
(313) 429-4971

VME Microsystems International
12121 NS Memorial Pkwy
Huntsville, AL 35803
(205) 880-0444

Xylogics
144 Middlesex Tnpk
Burlington, MA 01803
(617) 272-8140

VME Specialists
558 Brewster Ave #1
Redwood City, CA 94063
(415) 3664-3328

Zendex
6700 Sierra Lane
Bublin, CA 94568
(415) 828-3000

ADA COMPILERS DATABASE

Aetech Inc.
Solana Beach, CA
(619) 755-1277

Meridian Software Systems, Inc
23141 Verdugo Drive, Ste. 105
Laguna Hills, CA 92653
(714) 380-9800

Alsys, Inc.
1432 Main Street
Waltham, MA 02154
(617) 890-0030

Meridian Technology Inc.
7 Corporate Park, Ste. 100
Irvine, CA 92714
(714) 261-1199

Alsys, Inc.
Western Regional Office
5000 Birch Street
Suite 3000, West Tower
Newport Beach, CA 92660
(714) 476-3683

Mikros Systems Corp.

Artek Corp.
100 Seaview Drive
Syracuse, NJ 07094
(201) 867-2900

David Marguardt
Marketing Director
General Systems Corp., W. Coast
815 Marilyn Drive
P.O. Box 1114
Campbell, CA 95009
(408) 866-9455

Gould, Inc.
Computer Systems Division

Oasys
Federal Systems Group
60 Aberdeen Avenue
Cambridge, MA 92138
(617) 491-4180

Harris Corp.
Computer Systems Division
2101 W. Cypress Creek Rd.
Ft. Lauderdale, FL 33309-1892s

SofTech, Inc.
460 Totten Pond Road
Waltham, MA 02254
(617) 890-6900

High Intensity Systems, LTD
England

Intellimac, Inc.
6001 Montrose Road, 6th Floor
Rockville, MD 20852
(301) 984-8000

TeleSoft
10639 Roselle Street
San Diego, CA 92121-1506
(619) 457-2700

OPERATING SYSTEMS

Award Software, Inc.
130 Knowles Dr.
Los Gatos, CA 95030
(408) 370-7979
286/386 MODULATOR BIOS

Interactive
2401 Colorado Ave. 3rd Fl.
Santa Monica, CA 90404
800-453-8649

LSI Logic Corp.
1551 McCarthy Blvd.
Milpitas, CA 95035
(408) 433-8000

Lynx Real-Time Systems, Inc.
550 Division Street
Campbell, CA 95008
(408) 370-2233

Microsoft Corp.
16011 NE 36th Way
Box 97017
Redmond, WA 98073-9717
MS OS/2

NASTEC Corpp.
24681 Northwestern Highway
Southfield, MI 48075
(313) 353-3300
Case 2000

Oasys
60 aberdeen Avenue
Cambridge, MA 02138
OASYS PC/VADS
(617) 491-4180

Orion Instruments, Inc.
702 Marshall St., Ste. 614
Redwood City, CA 94063
(415) 361-8883
UniLab II

Relational Technology Inc.
1080 Marina Village Parkway
P.O. Box 4006
Alameda, CA 94501-1041
INGRES

Recognition Technology, Inc.
335 Fiske St.
Holliston, MA 017466
(617) 429-7804
RTI Station

SoftLogic Solutions, Inc.
530 Chestnut St.
Manchester, NH 03101
800-272-9900
Software Carousel

Softguard Systems, Inc.
2840 San Tomas Expressway, Ste. 201
Santa Clara, CA 95051
(408) 970-9240
80386 DOS

The Software Link, Inc.
3577 Parkway Lane
Atlanta, GA 30092
(404) 448-5465
PC-MOS/386

Sophia Computer Systems, Inc.
3337 Kifer Rd.
Santa Clara, CA 95051
(408) 733-1571
Microprocessor

Tektronix, Inc.
Case Division
P.O. Box 1752
Portland, OR 97214
1-800-342-5548

Telesoft
10639 Roselle St.
San Diego, CA 92121-1506
(619) 457-2700
VAX/VMS

Wind River Systems
1351 Ocean Ave.
Emeryville, CA 94608
(415) 428-2623

APPENDIX C

ARM MODEL

1. Introduction

The performance specifications placed on the behavior of any mechanical system dictates the relative significance of the various physical parameters of the system. As the required performance of a system increases, more of the physical aspects of the system impact the system's response in comparison to the increased performance requirements.

Successful use of mechanical manipulators in space to perform careful, accurate positioning of delicate payloads, such as the transfer of micro-gravity experiments from the NASA space station to free-flying platforms, will depend on the ability of designers to take into account previously assumed negligible effects in robotic systems such as joint friction and system compliance. In particular, space based mechanical manipulators will need extremely high positioning accuracies (on the order of 0.1 mm.) and relatively low overall system mass. Beside the obvious benefit of lifting less mass into space, the additional benefits derived from the decrease in mechanical manipulator's mass are:

- 1) the need for smaller actuators,
- 2) quicker response and
- 3) less energy consumption during operation.

(Note that these increased requirements also result in the same benefits for earth-based robots.) To achieve the stated objectives of accurate end point positioning and a reduction in overall system mass lighter materials and more sophisticated control schemes must be used. Lighter materials usually result in a more compliant system while an increase in positioning requirements mean that system compliance is no longer a negligible effect.

Therefore, in this section of the report we will analyze and discuss the effects that the flexibility of the main segments of a robot arm has on the behavior and control aspects of the overall system. To begin with, we shall first consider an analytical model of a single segment arm which takes into account the flexibility of the segment. Then, we will discuss methods of controlling such a system to achieve accurate end tip positioning under low acceleration constraints.

2. Analytical Modeling of a Flexible Single Segment Mechanical Manipulator

The basic set up is a flexible single segment arm capable of rotation about two axis which intersect at a point on the base of the arm. For the modeling of this system we make the following assumptions:

- A1) Rotation about each axis is accomplished by independent torques applied at the base.
- A2) Arm segment response about each axis is assumed to be decoupled.
- A3) At the tip of the arm is a payload possessing point mass m_p and no rotary inertia.
- A4) At the base is a mass possessing rotary inertia I_{h_x} and I_{h_y} about each axis of rotation respectively.
- A5) Shear effects and beam cross-section rotary inertia effects are negligible.
- A6) Elongation effects are negligible.
- A7) Tip displacement due to bending is small in comparison to the overall length of the beam: geometrically linear beam theory.
- A8) The beam experiences relatively slow rotational speeds: i.e. $\dot{\psi}^2$ terms are negligible.
- A9) The beam material stress-strain relationship is linear.

A schematic diagram of the physical system being modeled and the definition of specific quantities is given in fig. A. Since it is assumed that the response of the arm about the two axis of rotation is decoupled, it is sufficient to model rotation about one axis. Thus, with the above assumptions, use of Hamilton's principle in a manner similar to that given in [Simo] results in the following partial differential equation (PDE) and boundary value/initial value problem (BV/IVP) describing the behavior of the system.

$$Elu_2''''(X_1,t) + m_a \ddot{u}_2(X_1,t) + \ddot{\psi} X_1 m_a = 0 \quad (1)$$

$$Elu_2'''(L,t) = m_p \ddot{u}_2(L,t) + \ddot{\psi} L m_p \quad (2)$$

$$I_h \ddot{\psi} = T(t) + Elu_2''(0,t) \quad (3)$$

$$u_2''(L,t) = 0 \quad (4)$$

$$u_2(0,t) = 0 \quad (5)$$

$$u_2'(0,t) = 0 \quad (6)$$

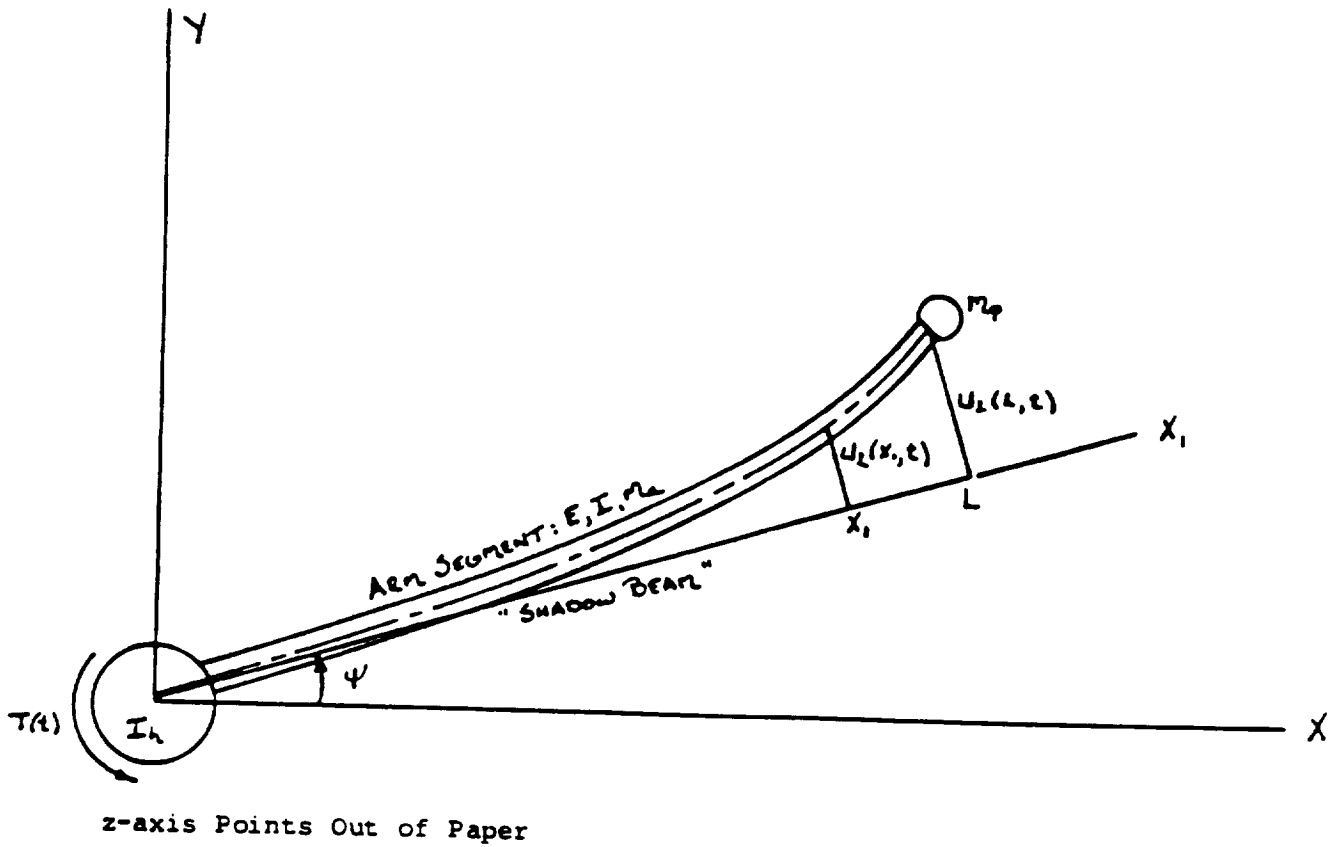


Figure A Schematic of Arm Segment

In the previous equations;

$u_2(X_1, t)$:= displacement due to bending of the beam

m_a := mass per unit length of the beam

I := beam cross-section moment area of inertia

E := elastic modulus of the beam material

ψ := angle of shadow beam with respect to the X-axis (the XY axes form an inertial reference frame)

I_h := rotary inertia of base mass (can be I_{h_x} or I_{h_y})

m_p := point mass of payload

g := acceleration due to gravity

superscript "''" denotes derivative with respect to X_1

superscript " " denotes derivative with respect to t

Following a common convention we term the straight line segment at an angle ψ with the X-axis and emanating from the origin the "shadow beam". The shadow beam is basically the position of the beam had it been perfectly rigid. Thus, $u_2(X_1, t)$ defines bending displacements relative to the shadow beam position. Also, note that eqn.(1) is applicable for all $X_1 \in (0, L)$ while eqns. 2-6 define end point conditions. Furthermore, notice that Eqn.(2) is basically $F=m*a$ applied at the tip, eqn.(3) is simply $I_h * \ddot{\psi} = \sum \text{Torques}$ experienced at the base, eqn.(4) says there is no external moment applied at the tip, eqn.(5) specifies that there is no translation of the base and eqn.(6) enforces the cantilevered nature of the beam with respect to the shadow beam. In addition, eqn.(1) is basically the Euler-Bernoulli beam equation with the additional inertia term $\ddot{\psi} X_1 m_a$ to account for the rotating behavior of the beam. As was previously mentioned, this model applies to both axis of rotation independently. Furthermore, models used for earth-based mechanical manipulators will include the gravity term $g m_p \cos(\psi)$ on the right hand side of eqn.(2) when considering rotation about an axis that is perpendicular to the earth. For our analysis we neglect such a term; equivalently the axis of rotation is perpendicular to the earth.

Now that a model for the system has been established we will

- 1) determine the system's inherent properties from an analysis of the model and
- 2) study how the use of this model impacts the design of a controller which will actively control end tip position by application of a torque at the base.

To simplify the derivation of a solution to our model we make the following transformation $y(X_1,t) := \psi X_1 + u_2(X_1,t)$ so that rewriting eqns. 1-6 in terms of y gives:

$$E I y''''(X_1,t) + m_a \ddot{y}(X_1,t) = 0 \quad (7)$$

$$E I y'''(L,t) = m_p \dot{y}(L,t) \quad (8)$$

$$I_h \ddot{y}(0,t) = T(t) + E I y''(0,t) \quad (9)$$

$$y''(L,t) = 0 \quad (10)$$

$$y(0,t) = 0 \quad (11)$$

$$y'(0,t) = \psi \quad (12)$$

3. Analysis of Model

The above model is a PDE and BV/IVP. Solution to such a system of equations is typically arrived at using modal analysis. For background material on modal analysis techniques and definition of terms used in this section see [Mer.]. The real essence of modal analysis lies in the fact that any solution to a self-adjoint BV/IVP, such as the one above, can be represented by an infinite series of functions which separate time and spatial dependence. Specifically, the solution to the above problem can be given as $y(X_1,t) = \sum_{i=0}^{\infty} f_i(X_1) g_i(t)$. The f_i 's are called the "eigenfunctions" of the system and define the "mode shapes". The g_i 's are referred to as the "generalized coordinates". The f_i 's are determined by solving the eigenvalue problem;

$$E I f_i''''(X_1) = \omega_i^2 m_a f_i(X_1) \quad (13)$$

$$-E I f_i'''(L) = \omega_i^2 m_p f_i(L) \quad (14)$$

$$-E I f_i''(0) = \omega_i^2 I_h f_i'(0) \quad (15)$$

$$f_i''(L) = 0 \quad (16)$$

$$f_i(0) = 0 \quad (17)$$

In the above equations the ω_i^2 's are real-valued parameters known as the "eigenvalues" while the ω_i 's are called the "modal frequencies". If we let $\beta_i^4 := \omega_i^2 m_a / EI$ then eqn.(13) has a solution of the form

$$f_i(X_1) = C_1 \sin(\beta_i X_1) + C_2 \cos(\beta_i X_1) + C_3 \sinh(\beta_i X_1) + C_4 \cosh(\beta_i X_1)$$

The four boundary conditions, eqns. 14-17, are used to solve for the 3 constants C_2 , C_3 , and C_4 , and establish an equation for determining the β_i 's. The equation which determines the β_i 's, and therefore the ω_i 's, is referred to as the characteristic equation. The characteristic equation

for the above PDE and BV/IVP is:

$$[\beta_i^4 I_h m_p - m_a^2][\sinh(\beta_i L) \cos(\beta_i L) - \sin(\beta_i L) \cosh(\beta_i L)] \\ + \beta_i^3 I_h m_a [1 + \cos(\beta_i L) \cosh(\beta_i L)] + 2m_a m_p \beta_i \sin(\beta_i L) \sinh(\beta_i L) = 0$$

This equation must be solved numerically and, as mentioned, determines the modal frequencies which are infinite in number.

In addition to the solution form just given, eqns (13) - (17) also have a rigid body solution of the form

$$f_0(X_1) = C_4 X_1^3 + C_3 X_1^2 + C_2 X_1 + C_1$$

Application of this solution to the boundary conditions yields $f_0(X_1) = C_2 X_1$.

The real benefit to using modal analysis techniques is that each $f_i(X_1)g_i(t)$ pair contributes independently to the response of the system due to the effect of initial conditions or the action of the input function $T(t)$. Hence, in order to determine the resultant response, $y(X_1, t)$, one simply adds the "component" responses -- the response of each mode. For this to be valid however, the modes must be decoupled and orthogonal to one another in some sense. For this problem the proper orthogonalization requirement is as follows:

$$\int_0^L f_i(X_1) m_a f_j(X_1) dX_1 + f_i'(0) I_h f_j'(0) + f_i(L) m_p f_j(L) = \begin{cases} 1 & i=j \\ 0 & i \neq j \end{cases} \quad i, j = 0, 1, 2, \dots \quad (18)$$

When $i \neq j$ it can easily be shown, using the boundary conditions imposed on the f_i 's and f_j 's, that the above equation is automatically satisfied, and since as of yet the C_{1_i} 's for the first solution form and C_{2_0} are unspecified, they are calculated to fulfill the above orthogonalization condition when $i=j$. Thus, with the given orthogonalization condition the solution can be calculated and is simply given as $y(X_1, t) = \sum_{i=0}^{\infty} f_i(X_1) g_i(t)$.

To determine the g_i 's one simply substitutes the series form of the solution, $y(X_1, t) = \sum_{i=0}^{\infty} f_i(X_1) g_i(t)$, into eqns. 7, 8 and 9 and does some rearranging to get;

$$EI \sum_{i=0}^{\infty} f_i''''(X_1) g_i(t) + m_a \sum_{i=0}^{\infty} f_i(X_1) \ddot{g}_i(t) = 0 \quad (7a)$$

$$-EI \sum_{i=0}^{\infty} f_i''''(L) g_i(t) + m_p \sum_{i=0}^{\infty} f_i(L) \ddot{g}_i(t) = T(t) \quad (8a)$$

$$-EI \sum_{i=0}^{\infty} f_i''(0) g_i(t) + I_h \sum_{i=0}^{\infty} f_i'(0) \ddot{g}_i(t) = 0 \quad (9a)$$

Now multiply eqn.(7a) by $f_j(X_1)$ and integrate from 0 to L; multiply eqn.(8a) by $f_j(L)$ and; multiply eqn.(9a) by $f_j'(0)$. Adding the resulting three equations and using the relationships defined by the eigenvalue problem yield;

$$\sum_{i=0}^{\infty} \left[\int_0^L f_i(X_1) m_a f_j(X_1) dX_1 + f_i'(0) I_h f_j'(0) + f_i(L) m_p f_j(L) \right] [\ddot{g}_i(t) + \omega_i^2 g_i(t)] = f_j'(0) T(t) \quad j=0, 1, 2, \dots$$

(In the above manipulations we rather indiscriminately interchanged integration, summation and differentiation. For proof as to why this is ok see [Gar.] Use of the orthogonality condition, eqn.(18), in the above equation then results in;

$$\ddot{g}_j(t) + \omega_j^2 g_j(t) = f_j'(0) T(t) \quad j=0, 1, 2, \dots$$

which is an infinite set of ordinary differential equations. Recall that in compact notation one can express the end tip position as

$$y(L,t) = \sum_{i=0}^{\infty} f_i(L) g_i(t)$$

In addition, $y'(0,t) = \psi$. This too can be expressed in compact notation as

$$\psi = \sum_{i=0}^{\infty} f_i'(0) g_i(t)$$

Because of the choice of the orthogonality condition, both of the above quantities are outputs of infinite-dimensional, linear, time-invariant systems with completely decoupled modes, and in matrix form they are expressed as

$$\begin{bmatrix} \dot{g}_0(t) \\ \ddot{g}_0(t) \\ \dot{g}_1(t) \\ \ddot{g}_1(t) \\ \dot{g}_2(t) \\ \ddot{g}_2(t) \\ \vdots \\ \vdots \\ \vdots \end{bmatrix} = \begin{bmatrix} 0 & 1 & 0 & 0 & 0 & 0 & \dots \\ 0 & 0 & 0 & 0 & 0 & 0 & \dots \\ 0 & 0 & 0 & 1 & 0 & 0 & \dots \\ 0 & 0 & -\omega_1^2 & 0 & 0 & 0 & \dots \\ 0 & 0 & 0 & 0 & 0 & 1 & \dots \\ 0 & 0 & 0 & 0 & -\omega_2^2 & 0 & \dots \\ \vdots & \vdots & \vdots & \vdots & \vdots & \vdots & \dots \\ \vdots & \vdots & \vdots & \vdots & \vdots & \vdots & \dots \\ \vdots & \vdots & \vdots & \vdots & \vdots & \vdots & \dots \end{bmatrix} \begin{bmatrix} g_0(t) \\ \dot{g}_0(t) \\ g_1(t) \\ \dot{g}_1(t) \\ g_2(t) \\ \dot{g}_2(t) \\ \vdots \\ \vdots \\ \vdots \end{bmatrix} + \begin{bmatrix} 0 \\ f_0'(0) \\ 0 \\ f_1'(0) \\ 0 \\ f_2'(0) \\ \vdots \\ \vdots \\ \vdots \end{bmatrix} T(t)$$

and

$$\begin{bmatrix} y(L,t) \\ \psi(t) \end{bmatrix} = \begin{bmatrix} f_0(L) & 0 & f_1(L) & 0 & f_2(L) & 0 & \dots \\ f_0(0) & 0 & f_1(0) & 0 & f_2(0) & 0 & \dots \end{bmatrix} \begin{bmatrix} g_0(t) \\ \dot{g}_0(t) \\ g_1(t) \\ \dot{g}_1(t) \\ g_2(t) \\ \dot{g}_2(t) \\ \vdots \\ \vdots \\ \vdots \end{bmatrix}$$

The above then composes our model of the system where $T(t)$ is the input and $y(L,t)$ and ψ are the outputs. Notice that the above model does not include structural damping terms. Such terms may be included here by simply adding the terms $-2 \zeta_i \omega_i$ to the $(2i+2,2i+2)$ elements of the matrix containing the ω_i^2 's for $i=1,2,3,\dots$ where ζ_i is the damping coefficient for the i^{th} mode.

Numerical Calculation of the System Model

To numerically calculate the linear model just derived one needs to calculate the quantities β_i , ω_i , C_{1_i} , C_{2_i} , C_{3_i} and C_{4_i} . From these quantities $f_i(L)$ and $f_i(0)$ can be calculated.

- The β_i 's (and consequently the ω_i 's) are calculated from the characteristic equation. Then the relationship $\beta_i^4 = \omega_i^2 m_a / EI$ is used to get the ω_i 's.
- To calculate C_{1_i} , C_{2_i} , C_{3_i} and C_{4_i} we use the orthogonalization condition and the boundry conditions.

+ Eqn. (17) gives that $C_{2_i} = -C_{4_i}$

+ Eqns. (15) + (16) give that

$$C_{2_i} = bC_{3_i} \quad \text{and} \quad C_{1_i} = aC_{3_i}$$

where

$$a := \frac{2m_a \sinh(\beta_i L) - \beta_i^3 I_h (\cos(\beta_i L) + \cosh(\beta_i L))}{2m_a \sin(\beta_i L) + \beta_i^3 I_h (\cos(\beta_i L) + \cosh(\beta_i L))} \quad \text{and} \quad b := \frac{(1+a)\beta_i^3 I_h}{2m_a}$$

- + To get the last remaining coefficient the normalization condition is used. Recall that this condition is

$$\int_0^L m_a f_i^2(x) dx + f_i^2(0)I_h + f_i^2(L)m_p = 1$$

Using our previous expressions for the coefficients we get

$$f_i^2(0)I_h = I_h \beta_i^2 (a+1) C_{3_i}^2$$

$$f_i^2(L)m_p = 4m_p \left[\frac{a \sin(\beta_i L) \cosh(\beta_i L) + \sinh(\beta_i L) \cos(\beta_i L)}{\cos(\beta_i L) + \cosh(\beta_i L)} \right] C_{3_i}^2$$

$$\int_0^L m_a f_i^2(x) dx = C_{3_i}^2 \frac{m_a}{2\beta_i} \left[a^2 (L\beta_i - \cos(\beta_i L) \sin(\beta_i L)) + b_2 (L\beta_i + \cos(\beta_i L) \sin(\beta_i L)) \right.$$

$$\left. + (\sinh(\beta_i L) \cosh(\beta_i L) - \beta_i L) + b^2 (\sinh(\beta_i L) \cosh(\beta_i L) + \beta_i L) \right.$$

$$\left. + 2ab(\sin^2(\beta_i L)) + 2a(\sin(\beta_i L) \cosh(\beta_i L) - \cos(\beta_i L) \sinh(\beta_i L)) \right.$$

$$\left. - 2ab(\sin(\beta_i L) \sinh(\beta_i L) - \cos(\beta_i L) \cosh(\beta_i L) + 1) \right]$$

$$+ 2b(\sin(\beta_i L)\sinh(\beta_i L) + \cos(\beta_i L)\cosh(\beta_i L) - 1)$$

$$- 2b^2(\sin(\beta_i L)\cosh(\beta_i L) + \cos(\beta_i L)\sinh(\beta_i L)) - 2b(\sinh^2(\beta_i L))$$

Summing the above three expressions, setting that quantity equal to 1 and solving for C_3 , gives the expression for C_3 .

- Then to calculate $f_i(0)$ and $f_i(L)$ we note that

$$f_i(0) = (C_1 + C_3)\beta_i$$

and

$$f_i(L) = C_3(a \sin(\beta_i L) + b \cos(\beta_i L) + \sinh(\beta_i L) - b \cosh(\beta_i L))$$

- THE RIGID BODY MODE PARAMETERS MUST ALSO BE CALCULATED.

THE RIGID BODY MODE IS

$$f_0(x) = C_{20} x$$

NOTE THAT THIS MODE IS ORTHOGONAL TO ALL OTHER MODES AND C_{20} IS CHOSEN TO SATISFY THE NORMALIZATION CONDITION ↗ In the sense of Eqn 18

$$\int_0^L m_a C_{20}^2 x^2 dx + C_{20}^2 I_h + C_{20}^2 L^2 m_p = 1$$

WHICH TURNS OUT TO GIVE

$$C_{20}^2 = \frac{1}{\frac{1}{3} L^3 m_a + I_h + L^2 m_p}$$

4. Considerations for the use of the Beam Model for Controller Design

Most control design techniques can only deal with finite dimensional systems. Also, infinite dimensional controllers are difficult, if not impossible, to implement. Therefore, the above model must be truncated to a finite number of states for use in the design of the controller. There are several techniques for determining a finite dimensional model from an infinite dimensional system. These techniques are nicely outlined in [Bal.]. For this problem, even when structural damping effects are taken into account, model order reduction will entail the exclusion of certain modes. Which modes to exclude will depend on;

- 1) the sensitivity of the sensors,
- 2) the responsiveness of the actuators,
- 3) the frequencies of potential disturbances and
- 4) the "quality" of the model.

Even though we deemed the affect of compliance significant, we can not model its influence perfectly. Therefore, we had to make certain assumptions about the system in order to account for any type of compliant affects. As it turns out, the assumptions we made yield a model which is not necessarily representative of system high frequency behavior. This is because neglected effects like shear and beam cross section rotary inertia effects have a greater impact on high frequency modes. However, we feel that the model is good enough to be used for system analysis and controller design to achieve the desired system behavior requirements. We also feel that the model is valid in the bandwidth that disturbances are likely to occur namely low frequencies. Therefore, the reduced order model should include the lowest frequency modes. How many of those low frequency modes it needs to contain will probably be determined by experimentation.

Use of a truncated model raises a very crucial question concerning resultant controller implementation. And that is;

Given that the controller was designed for a specific set of modes, how will it respond to the modes it wasn't designed for (i.e. the truncated modes) but are present in the "real" system? e.g. Will it destabilize any or all of the truncated modes ?

Such a concern was addressed by Balas in [Bal]. In that paper it was pointed out that the sensor and actuator dynamics play a key role. One way to provide for proper performance of the controller when implemented on the real system is to minimize the amount of interaction between the controller and the unmodeled modes. Since, in this case, the modes contained in the truncated model are low frequency, the best way to "shield" the controller from the high

frequency unmodeled modes is to make the sensor and actuator low pass. A low pass sensor is one which is too slow to measure high frequency variations and a low pass actuator is one which is too sluggish to excite high frequency vibrations. Thus, use of low pass sensors and actuators yields a system which is designed to sense and control low frequency vibrations. As mentioned, if disturbances are present they are likely to be low frequency thus the designed controller can damp them out quickly. So overall, our truncated model will contain the lowest frequency modes because that is the bandwidth of potential disturbances, the model is valid in that range, and the sensors and actuators can measure and affect those modes.

APPENDIX D MOTOR AND GEAR MODELS

Motor Model

The same basic principles are used in both the conventional permanent magnet DC motor and the brushless DC motor. The basic motor constants are also the same as long as some caution is used in applying the constants.

A simplified electrical equation of a brushless DC motor is:

$$V = IR + L \frac{dI}{dt} + K(E) \omega \quad 1$$

where

- I is the sum of the phase currents
- R is the resistance of a phase winding
- L is the inductance of a phase winding
- K(E) is the voltage constant of a phase winding over the conduction angle
- ω is the angular velocity of the motor shaft

These relationships hold well for the common brushless motor structures, although there are lower order effects due to mutual inductance between windings, overlapping conduction angles and unequal rise and fall times of current (due to differing charge and discharge paths). However, for practical applications eq. 1 is adequate.

The dynamic equation for a motor coupled to a load is:

$$K(T)I = (J_m + J_l) \frac{d\omega}{dt} + D + T_f + T_l \quad 2$$

Where

- K(T) = torque constant of motor winding
- J_m = motor moment of inertia
- J_l = load moment of inertia
- D = viscous damping coefficient
- T_f = motor friction torque
- T_l = load friction torque

In a brushless DC motor T_f is small, usually only due to bearing drag, the viscous damping coefficient is also very small, and both items can usually be ignored in dynamic performance calculations.

Motor equations and Transfer function

The motor impedance at stall is equal to a resistance, R, in series with a parallel combination of an inductance, L_a, and another resistance, R_l. When the motor rotates, the armature coils move in the stator magnetic field. The induced emf appears across the armature terminals as internally generated voltage (counter emf), E_g. Therefore, the equivalent electric circuit of the motor is the impedance at stall, connected in series to a voltage source, E_g. The physical explanation for this model is that R_l represents the losses in the magnetic circuit. This model was found to be accurate for the motor. However, the resistance R_l is usually larger than R (typical, about 5-10 times), and hence, the effect of R_l on the motor operation is insignificant. Therefore, it is possible to ignore this

resistance in most practical applications, and approximate the motor equivalent circuit by R , L_a , and E_g . Let the motor voltage and current be V and I_a , respectively. The relation between these variables is given by

$$V = L_a \frac{dI_a}{dt} + R I_a + E_g \quad 3$$

where E_g , the internally generated voltage, is proportional to the motor velocity; w .

$$E_g = K(E)w \quad 4$$

Equations 3 and 4 can be combined to give:

$$V = L_a \frac{dI_a}{dt} + R I_a + K(E)w \quad 5$$

Equation 5 is known as the electrical equation of the motor.

Since the magnetic field in the motor is constant, the current produces a proportional torque:

$$T_g = K(T)I_a \quad 6$$

Let us denote the moment of the motor by J_m , and let T_f represent the constant friction torque in the motor. Also, denote all the viscous friction torques and other torques which are proportional to the velocity by Dw . Then, the opposing torque in the motor, T_m , is given by:

$$T_m = T_f + Dw \quad 7$$

Now assume that the motor is coupled to a load. Denote the load moment of inertia by J_l and the load opposing torque by T_l . The relation between the torques and velocity is the following:

$$T_g = (J_m + J_l) \frac{dw}{dt} + Dw + T_f + T_l \quad 8$$

Equation 8 is the dynamic equation of the motor, and along with 5 and 6, it describes the relations between the electrical and mechanical variables. This equation is based on a tacit assumption that motor velocity is the same as that of the load.

For high-performance servo systems, since the mechanical parts of the system are elastic, they deflect under torque. Consequently, the instantaneous velocities of various parts are different, and at some frequencies will be in opposite directions. This condition allows the system to store a large amount of mechanical energy, which results in noticeable angular vibrations. This phenomenon is called torsional resonance.

For our purposes we represent the motor and segment as two solid bodies coupled by an inertialess shaft. (Further couplings for, e.g., a tachometer, can be denoted by additional values $n = m, 1, 2, \dots$) Let us denote the moments of inertia and angular positions of the load and the motor by J_l, θ_l and J_m, θ_m , respectively. Also, denote the stiffness and damping factors of the shaft by K_l and D_l . Note that this model is an overall approximation and, hence, K_l and D_l may be influenced by characteristics of the motor armature, shaft, coupling, or the load.

In order to derive the dynamic equations for this system, let T_1 be the torque delivered from the motor to J_1 . The dynamic equations are:

$$T_g = J_m \ddot{\theta}_m + D \dot{\theta}_m + T_1 \quad 9$$

$$T_1 = J_1 \ddot{\theta}_1 \quad 10$$

The deflections of the shaft is describe by the following equation:

$$T_1 = K_1 (\theta_m - \theta_1) + D_1 (\dot{\theta}_m - \dot{\theta}_1) \quad 11$$

If we substitute 10 for torque T_1 the dynamic equations become:

$$T_g = J_m \ddot{\theta}_m + D \dot{\theta}_m + J_1 \ddot{\theta}_1 \quad 12$$

$$J_1 \ddot{\theta}_1 + D_1 \dot{\theta}_1 + K_1 \theta_1 = D_1 \dot{\theta}_m + K_1 \theta_m \quad 13$$

Now consider the electrical equations 1 and 6 with:

$$I = I_a \quad \text{and}$$

$$w = \dot{\theta}$$

which describe the behavior of the system. To simplify the analysis, we substitute 6 and 12 and apply the Laplace transformation to all the equations. (The laplace transform of $x(t)$ is $x(s)$).

$$(sL_a + R)I_a(s) + K(E)s \theta_m(s) = V(s)$$

$$-K(T)I_a(s) + (s^2J_m + sD) \theta_m(s) + s^2J_1 \theta_1(s) = 0$$

$$(sD_1 + K_1) \theta_m(s) - (s^2J_1 + sD_1 + K_1) \theta_1(s) = 0 \quad 14$$

Equations 14 are the motor model system equation and may be written in matrix form for simplification. For use in MATLAB we have rearranged these terms and let $l = g$ for the harmonic drive gearbox flex, $gr =$ gear ratio, and $C =$ inertia and damping terms.

$$\text{Let } I \theta = \begin{bmatrix} I \\ \dot{\theta} \\ \theta \end{bmatrix}$$

Thus:

$$\begin{bmatrix} \dot{I} \\ \ddot{\theta} \\ \dot{\theta} \end{bmatrix} = \begin{bmatrix} -R/L & -K(E)/L & 0 \\ K(T)/I_m & -Cg/I_m gr^2 & -Kg/I_m gr^2 \\ 0 & 1 & 0 \end{bmatrix} \begin{bmatrix} I \\ \dot{\theta} \\ \theta \end{bmatrix} + \begin{bmatrix} 1/L \\ 0 \\ 0 \end{bmatrix} V$$

and

$$I \dot{\theta} = A_{I\theta} I\theta + B_{I\theta} V$$

where the output is:

$$\begin{bmatrix} I \\ \dot{\theta} \\ \theta \end{bmatrix}$$

This operation is executed by MOTGER.M.

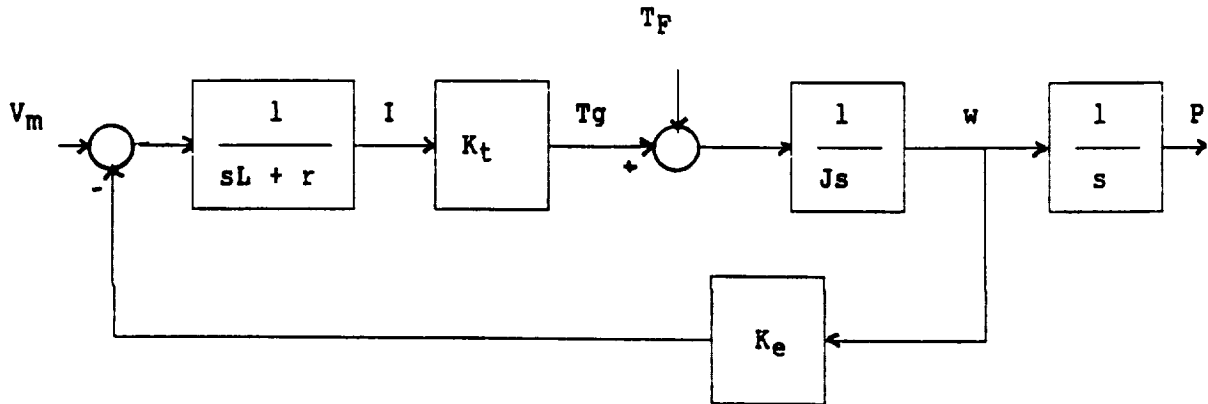
The transfer function is denoted by G. From the Beam (segment) model:

$\dot{G} = AmG + BmT(A)$ where $T(A)$ is the torque delivered to the beam or segment. γ is the rotation of the segment.

$$\begin{vmatrix} \dot{\gamma} \\ \gamma \end{vmatrix} = \begin{vmatrix} C_m \end{vmatrix} G$$

This operation is executed by ARMMOD.M.

BLOCK DIAGRAM OF MOTOR MODEL



Motor Transfer Function

$$\frac{w}{V_m} = \frac{\frac{K_t}{Js(sL + r)}}{1 + \frac{K_e K_t}{J(sL + r)}} = \frac{K_t}{J(sL + r) + K_e K_t}$$

Let: $T_m = \frac{rJ}{K_t^2}$ and $T_e = \frac{L}{r}$

Then:

$$\frac{w}{V_m} = \frac{1/K_e}{(s T_m + 1)(s T_e + 1)}$$

MODELING COMBINATION

(Series of commands: `motger`, `armmod`, `combine`; to simulate, type: `simcomb`)

MOTOR MODEL: (executed by `motger.m`)

$$I\theta = \begin{bmatrix} I \\ \dot{\theta} \\ \theta \end{bmatrix}$$

$$\begin{bmatrix} \dot{I} \\ \ddot{\theta} \\ \dot{\theta} \end{bmatrix} = \begin{bmatrix} \frac{-R}{L} & \frac{-K_E}{L} & 0 \\ \frac{K_T}{I_M} & \frac{-C_g}{I_M g_r^2} & \frac{-K_g}{I_M g_r^2} \\ 0 & 1 & 0 \end{bmatrix} \begin{bmatrix} I \\ \dot{\theta} \\ \theta \end{bmatrix} + \begin{bmatrix} \frac{1}{L} \\ 0 \\ 0 \end{bmatrix} V$$

$$= [A_{I\theta}] [I\theta] + [B_{I\theta}] V \quad \text{output is } \begin{bmatrix} I \\ \dot{\theta} \\ \theta \end{bmatrix}$$

BEAM MODEL: (executed by `armmod.m`)

$$\dot{G} = A_M G + B_M T_A$$

$$\begin{bmatrix} y \\ \dot{\psi} \\ \psi \end{bmatrix} = \begin{bmatrix} - & C_y & - \\ - & C_{\dot{\psi}} & - \\ - & C_{\psi} & - \end{bmatrix} G$$

$$= [C_M] G$$

PUTTING THE TWO TOGETHER: (executed by `combine.m`)

$$\begin{bmatrix} \dot{I}\theta \\ \dot{G} \end{bmatrix} = \begin{bmatrix} A_{I\theta} & A_{C1} \\ A_{C2} & A_{Ma} \end{bmatrix} \begin{bmatrix} I\theta \\ G \end{bmatrix} + \begin{bmatrix} B_{I\theta} \\ 0 \end{bmatrix} V$$

$$=[A_c] \begin{bmatrix} I\theta \\ G \end{bmatrix} + [B_c] V$$

$$\begin{bmatrix} I\theta \\ y \\ \dot{\psi} \\ \psi \end{bmatrix} = \begin{bmatrix} I_A & 0 \\ 0 & C_y \\ 0 & C_{\dot{\psi}} \\ 0 & C_{\psi} \end{bmatrix} \begin{bmatrix} I\theta \\ G \end{bmatrix}$$

$$=[C_c] \begin{bmatrix} I\theta \\ G \end{bmatrix}$$

$$T_A = \frac{K_g}{g_r} \theta + \frac{C_g}{g_r} \dot{\theta} - K_g \psi - C_g \dot{\psi}$$

$$= \frac{K_g}{g_r} \theta + \frac{C_g}{g_r} \dot{\theta} - K_g C_{\psi} G - C_g C_{\dot{\psi}} G$$

$$A_{c1} = \begin{bmatrix} \dots & 0 & \dots \\ \dots & \frac{C_g}{I_M g_r} C_{\dot{\psi}} + \frac{C_g}{I_M g_r} C_{\dot{\psi}} & \dots \\ \dots & 0 & \dots \end{bmatrix}$$

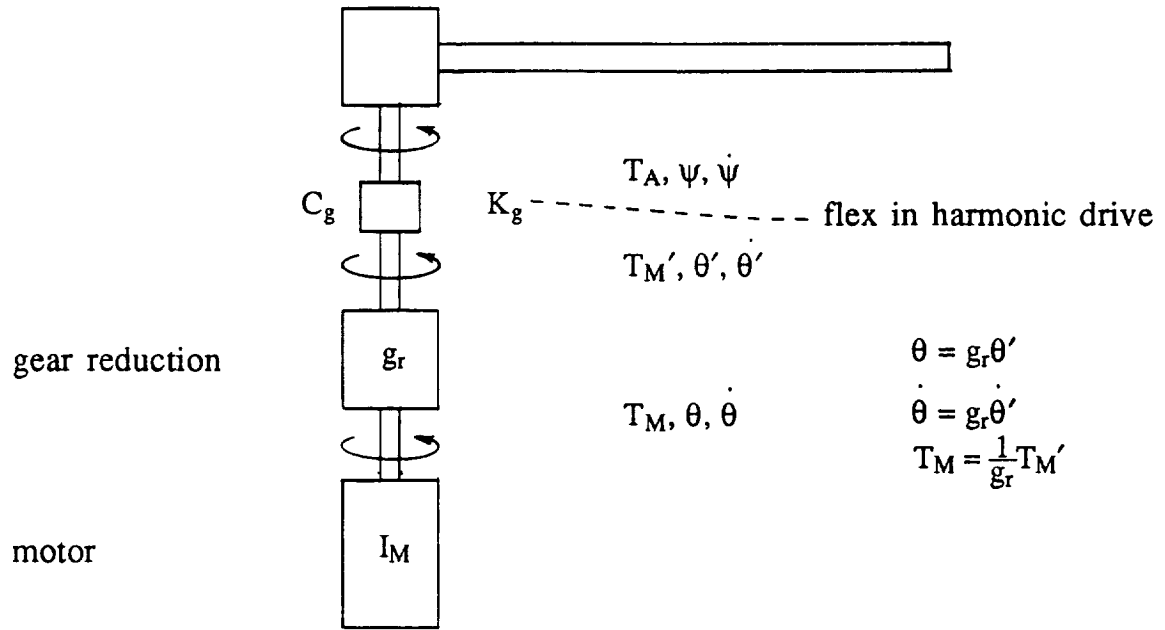
$$A_{c2} = \begin{bmatrix} \dots & \dots & \dots \\ 0 & \frac{C_g}{g_r} B_M & \frac{K_g}{g_r} B_M \\ \dots & 0 & \dots \end{bmatrix}$$

$$A_{Ma} = A_M - K_g B_M C_{\psi} - C_g B_M C_{\dot{\psi}}$$

$u_2 \equiv$ quantity which the end tip detector measures

$$u_2 = \begin{bmatrix} 0 & C_y - LC_{\psi} \end{bmatrix} \begin{bmatrix} I\theta \\ G \end{bmatrix}$$

$$=[C_{u2}] \begin{bmatrix} I\theta \\ G \end{bmatrix}$$



$$T_A = K_g(\theta' - \psi) + C_g(\dot{\theta}' - \dot{\psi}) = K_g\left(\frac{1}{g_r}\theta - \psi\right) + C_g\left(\frac{1}{g_r}\dot{\theta} - \dot{\psi}\right)$$

For motor

$$\frac{-T_A}{g_r} + T_M = I_M \ddot{\theta}$$

or

$$T_M = I_M \ddot{\theta} + \frac{K_g}{g_r} \left(\frac{1}{g_r}\theta - \psi\right) + \frac{C_g}{g_r} \left(\frac{1}{g_r}\dot{\theta} - \dot{\psi}\right)$$

Motor Parameters

L_R = Inductance of motor = 4.1 *mH* +/-30%

R = Motor electrical resistance = 1.788 *ohms* +/-12% @25°C & 2.48 *ohms* +/-12% @125°C

K_T = Motor torque sensitivity = 71.36 *oz-in/A* +/-10%

K_E = Motor voltage constant = 0.504 *v-sec/rad*

J_m = Motor rotor rotary inertia = .064 *oz-in-sec²*

V = Voltage to windings

I_A = Current to windings

$\theta, \dot{\theta}$ = Motor angular position and rotational speed, respectively

T_M = Torque generated by motor

System Parameters

d = Difference between laser end tip position and arm end tip position as measured by the sensor

T_A = Torque applied to the ARM

$C(s)$ = Controller

g_R = Gear box ratio = 200

$M_A(s)$ = Arm model (Torque in; end tip position, base angular velocity out)

$F_L(s)$ = Laser positioning system model

$G_s(s)$ = Sensor model

L = Length of segment

ψ_c = Desired segment angular position

ψ_L = Laser angular position

$\psi, \dot{\psi}$ = Segment base angular position and rotational speed, respectively

Flexible segment model for modeling configuration 1; input: T , output: y and $\dot{\psi}$

$$A = \begin{bmatrix} 0 & 1 & 0 & 0 & 0 & 0 & 0 & 0 \\ 0 & 0 & 0 & 0 & 0 & 0 & 0 & 0 \\ 0 & 0 & 0 & 1 & 0 & 0 & 0 & 0 \\ 0 & 0 & -\omega_1^2 & 0 & 0 & 0 & 0 & 0 \\ 0 & 0 & 0 & 0 & 0 & 1 & 0 & 0 \\ 0 & 0 & 0 & 0 & -\omega_2^2 & 0 & 0 & 0 \\ 0 & 0 & 0 & 0 & 0 & 0 & 0 & 1 \\ 0 & 0 & 0 & 0 & 0 & 0 & -\omega_3^2 & 0 \end{bmatrix}$$

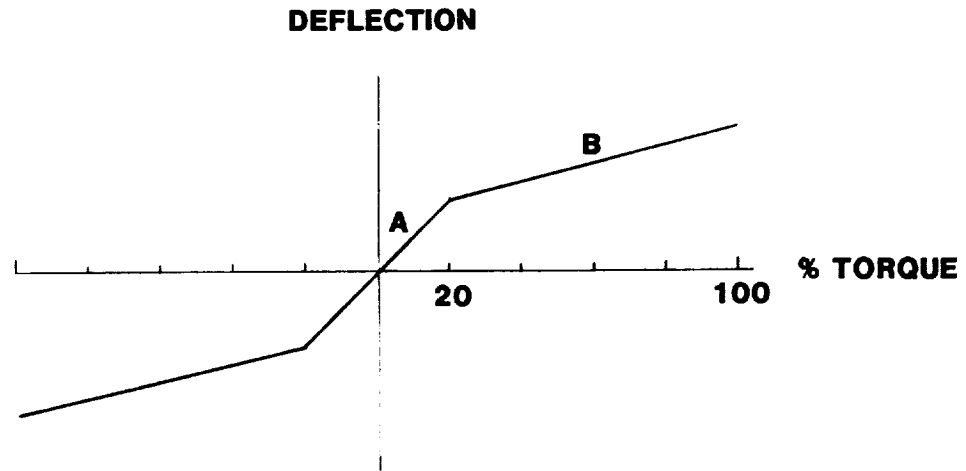
$$B = \begin{bmatrix} 0 \\ f_0'(0) \\ 0 \\ f_1'(0) \\ 0 \\ f_2'(0) \\ 0 \\ f_3'(0) \end{bmatrix}$$

$$C = \begin{bmatrix} f_0(L) & 0 & f_1(L) & 0 & f_2(L) & 0 & f_3(L) & 0 \\ 0 & f_0'(L) & 0 & f_1'(L) & 0 & f_2'(L) & 0 & f_3'(L) \\ f_0'(L) & 0 & f_1'(L) & 0 & f_2'(L) & 0 & f_3'(L) & 0 \end{bmatrix}$$

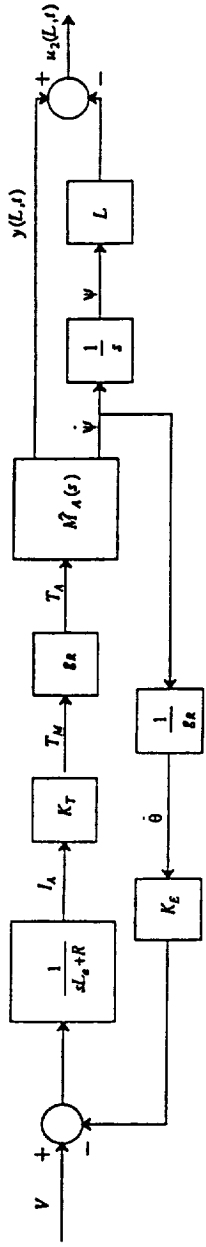
$$A = \begin{bmatrix} 0 & 1 & 0 & 0 & 0 & 0 & 0 & 0 \\ -\omega_0^2 & -2\zeta_0\omega_0^2 & 0 & 0 & 0 & 0 & 0 & 0 \\ 0 & 0 & 0 & 1 & 0 & 0 & 0 & 0 \\ 0 & 0 & -\omega_1^2 & -2\zeta_1\omega_1^2 & 0 & 0 & 0 & 0 \\ 0 & 0 & 0 & 0 & 0 & 1 & 0 & 0 \\ 0 & 0 & 0 & 0 & -\omega_2^2 & -2\zeta_2\omega_2^2 & 0 & 0 \\ 0 & 0 & 0 & 0 & 0 & 0 & 0 & 1 \\ 0 & 0 & 0 & 0 & 0 & 0 & -\omega_3^2 & -2\zeta_3\omega_3^2 \end{bmatrix}$$

HARMONIC DRIVE SPRING RATE CHARACTERISTICS

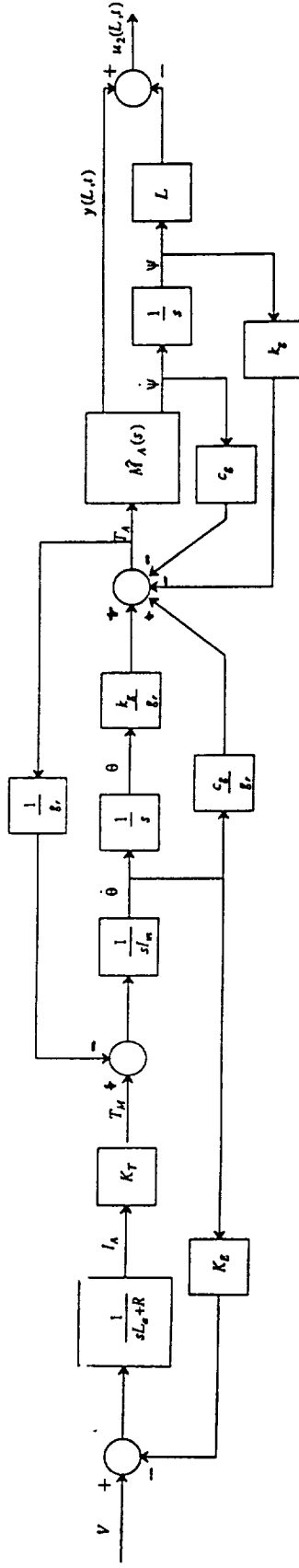
These spring rates are found by fixing the input shaft and torquing the output shaft. 100% rated output torque @1750 rpm input of a 200:1 4M drive is 4100 in-lb (463.2 N-m).



Slope A: $1/K_A = 345,000 \text{ in-lb/rad}$ (38,979 N-m/rad)
Slope B: $1/K_B = 1.88 \times 10^6 \text{ in-lb/rad}$ (212,410 N-m/rad)

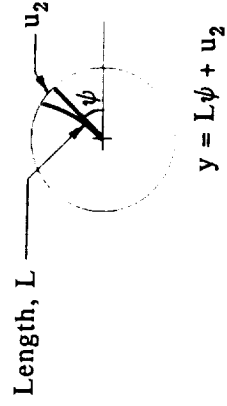


Block diagram of open loop system: DC Motor, Gear Box and Single Segment Flexible Arm.



Block diagram of open loop system: DC Motor, Gear Box and Single Segment Flexible Arm.

There is also a spring and damper included to account for the flex in the Harmonic drive.



CALCULATION OF END TIP POSITION

APPENDIX E - SAFETY ASSESSMENT

Safety and Health Plan

The Objectives of the Health and Safety Plan are to:

1. Provide a safe work environment for personnel.
2. Prevent injuries
3. Monitor compliance with Federal, State, and local Safety Regulations including OSHA.
4. Provide a set of preferred responses to emergencies.
5. Provide a means for recording and reporting accidents, incidents, and injuries to the administration and to the safety committee.
6. Provide a set of Safety and Health requirements for subcontractors.
7. Determine the structure of the Safety and Health Organization and Programs.

Organization

Implementation of the Health and Safety Plan will be the responsibility of the Health and Safety Officer. The Safety Officer will consult with the Laser Safety Specialist in matters of laser safety and with the safety committee as required. The Safety committee is open to all employees and will function as the forum for Health and Safety matters. The safety committee will meet as required to review injury reports and to evaluate and change the Health and Safety Plan.

Responsibilities

CCE recognizes the importance of the Safety and Health of its employees and will comply with Federal, State (OSHA), and local Safety Regulations. To demonstrate its commitment CCE will operate a Safety Program and employ a Safety Officer to oversee and manage the program.

An injury report will be completed for all reported injuries. A copy of the injury report will be sent to:

1. the Principal Investigator,
2. the Safety Officer,
3. the Safety File/Administration.

The Safety officer will have responsibility for compliance with Federal, State, and Local Safety Regulations including OSHA. The Safety Officer will conduct a monthly inspection of the facilities.

The Safety Officer is responsible for the evaluation of the safety aspects of incoming equipment and materials and recommending safety policy. Hazardous or dangerous materials and equipment will be logged in the Safety File along with recommended actions.

The safety officer will review injury reports, evaluate their cause and suggest rules, means, or procedure which could eliminate or reduce risk of future injuries. For serious accidents the Safety officer will convene the Safety committee and present the situation for their review.

Laser Safety Program

I. Laser hazard analysis and control.

The safety procedure necessary for any laser operation vary with three aspects:

1. Laser hazard classification
2. Environment of use
3. Operating personnel

The safety procedures are best presented by relating them to the laser hazard classifications.

II. Laser hazard classification

Class I - The lowest powered lasers. These lasers are not considered hazardous even if the output laser beam can be collected by 80 mm collecting optics and concentrated into the pupil of the eye or if the radiation at its maximum possible concentration on the skin or eye will not cause injury at the maximum exposure duration possible during one day of laser operation.

Class II - Those lasers which are only hazardous if the viewer overcomes his or her natural aversion response to bright light and continuously stares into the source.

Class III - Those lasers which can cause injury within the natural aversion response time, i.e., faster than the blink reflex (0.25 s). They are not capable of causing serious skin injury or hazardous diffuse reflections under normal use.

Class IV - Those lasers which present a "High Risk" of injury and can cause combustion of flammable materials. They may cause diffuse reflections that are eye hazards and may also cause serious skin injury from direct exposure.

III. Safety precautions

Class I - No user safety rules are necessary.

Class II -

a. Never permit a person to continuously stare into the laser source if exposure levels exceed the applicable permissible exposure level for the duration of intended staring.

b. Never point the laser at an individual's eye unless a useful purpose exists and the exposure level and duration will not exceed the permissible limit.

Class III -

- a. Do not aim the laser at an individual's eye.
- b. Permit only experienced personnel to operate the laser.
- c. Enclose as much of the beam path as possible. Termination should be used at the end of the useful paths of the primary and any secondary beam.
- d. Shutters, polarizers and optical filters should be placed at the laser exit port to reduce the beam power to the minimal useful level.
- e. Control spectators.
- f. A warning light or buzzer should indicate laser operation.
- g. Do not permit laser tracking of nontarget vehicles or aircraft.
- h. Operate the laser only in a restricted area. Place a warning sign on the door.
- i. Place the laser beam path well above or well below the eye level of any sitting or standing observers when possible. Make sure that the laser is secure and that the beam travels only along the intended path.
- j. Always use proper laser eye protection if required.
- k. A key switch should be installed.
- l. The beam or its specular reflection should never be directly viewed with optical instruments without sufficient protective filters.
- m. Remove all unnecessary mirror-like surfaces from within the vicinity of the laser beam path.

Class IV -

- a. Restrict personnel access.
- b. Operate only within a localized enclosure or in a controlled workplace.
- c. Eye protection is required for all personnel in the controlled area.
- d. Remote firing and viewing (video) should be used when feasible.
- e. Tracking systems should have positive stops to limit irradiated areas to predefined control areas.
- f. Beam shutters, beam polarizers, and beam filters should be used to mask or obstruct beams to limit use of laser beam to authorized personnel.
- g. Backstops should be diffusely reflecting-fire resistant target materials where feasible. Safety enclosures should be used around work areas. Viewing systems used should ensure against hazardous levels of reflection of laser irradiation back through optics.

IV. Application of safety procedures.

The Safety Officer (SO) and the Laser Safety Specialist (LSS) are responsible for interpretation of safety controls and determining which control safety rules are applicable to the particular situation and environment. Specific safety guidelines are available in the Handbook "Safety with Lasers and other Optical Sources" by D. Sliney and M. Wollbarsht, Plenum Press, New York (1982) or the "Laser Safety Reference Book" by the Laser Institute of America. Performance standards for laser products are covered in the Code for Federal Regulations (21CFR1040) and ANSI Z-136.1 (1986) Standard "Safe Use of Lasers" or their revisions.

To use these rules the laser must first be classified. This is usually found on the manufacturer's label. If the laser classification cannot be determined from the label, the manufacturer's literature, or if the laser has been modified, then its classifications must be determined by calculations and measurements as detailed in the Handbook.

All helium-neon lasers with an output power below 0.4 microW are classified as Class I. Those with a power below 1 mW are classified as Class II. Those with outputs of 1-2 mW and those with a power below 5 mW and an output irradiance below 2.5 mW/cm² are Class 3A; others are Class 3B. All continuous wave lasers with an output above 0.5 W are classified as Class IV.

A "Laser Equipment Survey Form" will be completed for each laser in use and kept in the Laser Safety File. For Class III and Class IV lasers a "Laser Installation Survey Form" will be completed and kept in the Laser Safety File. A monthly safety inspection will be made of the installation and will be recorded in the Laser Safety File log. One copy of the Report of Injury for any laser related injury will be kept in the Laser Safety File.

V. Laser Safety Training

Laser safety training will be provided employees based upon the Class lasers they use. A general orientation on laser hazards and laser safety will be provided to employees. The "Industrial Laser Safety Program Management" and the "Laser Safety" Professional Advancement Course Notes in the "Laser Safety Reference Book" will form the basis for the training program.

Robotics

The American National Standard Institute (ANSI) has safely developed a set of standards for industrial robot systems safety requirements. These standards are intended for industrial situations and are not necessarily appropriate or sufficient for space robots used in or for teleoperations. A complete analysis of the interaction of the ARM, spacecraft, astronaut, computer, and hardware is required before promulgating specific safety standards for space or teleoperations. Analysis should be conducted for each situation and usage.

We recommend that NASA comply with the appropriate portions of ANSI/RIA R15.06-1986 and the recommendations of our safety consultant for ARM III operations. These recommendations are:

1. The main power disconnect should be outside the operating work envelope.
2. The main power disconnect should be locked out prior to entering the barrier.
3. The personnel barrier gate should be interlocked and shut off all power and safe the robot if breached.
4. A presence sensing should be installed on the barrier such as trip cord to an interlock switch to prevent inadvertent passage over the barrier and as an emergency stop mechanism.
5. The area should be posted with warning signs.
6. The barrier should enclose the maximum potential reach of the robot through normal and potential failure sequences.
7. The robot operator station must have an emergency stop switch of the mushroom button type.
8. Provide means to prevent unintended motion of the robot while personnel are inside the barrier.
9. Assure the barrier is high enough and strong enough to contain loose or flying parts.
10. Prepare a written safe work and maintenance procedure.

We propose that a physical means of separating personal from the restricted work envelope, a barrier, be in place before operation. A circuit, using hardware-based components, that overrides all other robot controls, removes drive power from the robot actuators, and causes all moving parts to stop, an emergency stop should be in place. Power supply to the physical ARM should be sufficient to prevent access during operation, the stopping process, and configuration failure.

The ARM was designed to eliminate, where possible, the hazards associated with moving parts during assembly or operation. Because of the research nature of ARM III, special care is required to insure safe use. The ARM must be maintained and inspected before and after each use. Operating procedure review should be conducted prior and subsequent to each configuration modification.

References

ANSI Z-136.1 (1986) Standard "Safe Use of Lasers"

Burton, J. , "Industrial robotics: Hazards, accidents, safety applications and advanced sensor technology" Professional Safety, 28-33, Nov. 1988.

Code for Federal Regulations (21CFR1040)

Laser Institute of America, "Laser Safety Reference Book"

Sliney, D. and :M. Wollbarsht "Safety with Lasers and other Optical Sources" Plenum Press, New York (1982)

REFERENCES

1. Albus, J. S. "Brains, Behavior and Robotics" 1981.
2. Craig, J.J., P. Hsu, and S.S. Ssastry, "Adaptive control of mechanical manipulators" College of Engineering, U. C. Berkeley, Memo # M86/3, (1986)
3. Cannon, R.H. and E. Schmitz, "Precise Control of Flexible Manipulators," Robotics Research; The First International Symposium, Edited by; M. Brady and R. Paul, MIT Press, 1984, pp. 841-861.
4. Kwakernaak, H. and R. Sivan, Linear Optimal Control Systems, John Wiley & Sons, Inc., 1972.
5. Goodwin, G.C. and K.S. Sin, Adaptive Filtering Prediction and Control, Prentice-Hall Inc., 1984.
6. Ibid. Goodwin et. al., 1984.
7. Popov, E.P., Mechanics of Materials, 2nd Ed., Prentice-Hall Inc., 1976.
8. Ibid. Popov, 1976.
9. Ibid. Cannon et. al. 1984.

Bibliography

- Ahmad, Shaheen, "Real-time Multiprocessor Based Robot Control", IEEE International Conference on Robotics and Automation, San Francisco, April, 1986.
- Allan, Roger, "Nonvision Sensors", Electronic Design, June 27, 1985.
- Allen, Peter K., "Sensing and Describing 3-D Structure", IEEE International Conference on Robotics and Automation, San Francisco, April, 1986.
- Angermeyer, J and Kevin Jaeger, "MS-DOS Developers Guide" The Waite Group (1986)
- Asada, H. and T. Kanado, "Design of Direct-drive mechanical arms" Robotics Institute of Carnegie-Mellon university ADA 1266 347, 1981.
- Baillieui, John, "Avoiding Obstacles and Resolving Kinematic Redundancy", IEEE International Conference on Robotics and Automation, San Francisco, April, 1986.
- Balas, M. J., "Trends in Large Space Structures Control Theory: Fondest Hopes, Wildest Dreams," IEEE Transactions on Automatic Control, Vol. AC-27, No. 3, June 1982, pp. 522-536.
- Bania, Christopher F., and James C. Lin, "Theory and Implementation of a High Capacity 3-D Recognition System", IEEE International Conference on Robotics and Automation, San Francisco, April, 1986.
- Bronez, M.A. and Margaret M. Clarke, "Requirements Development for a Free Flying Robot - the "Robin"" Rockwell International Space Station Systems Division, 12214 lakewood Blvd. Downey, Ca 90241
and
Alberta Quin, NASA, Marshall Space Flight Center EL15, Huntsville, AL 35812, 1986 IEEE
- Brown, Michael K., "On Ultra-sonic Detection of Surface Features", IEEE International Conference on Robotics and Automation, San Francisco, April, 1986.
- Cannon, R. H. and E. Schmitz, "Precise Control of Flexible Manipulators," Robotics Research; The First International Symposium, Edited by; M. Brady and R. Paul, MIT Press, 1984, pp. 841-861.
- Cernuschi-Frias, Bruno, et al., "3-D Object Position Estimating and Recognition Based on Parameterized Surfaces and Multiple Views", IEEE International Conference on Robotics and Automation, San Francisco, April, 1986.
- Chester, Michael, "Surveying the array-processor landscape" Electronic Products, 42, July, 1986.
- Chiu, Stephen L, et al., "Sensor Data Fusion on A Parallel Processor", IEEE International Conference on Robotics and Automation, San Francisco, April, 1986.

- Dario, P. et al., "Geometrical Optimization Criteria for the Design of Tactile Sensing Patterns", IEEE International Conference on Robotics and Automation, San Francisco, April, 1986.
- Doyle, J.C. and G. Stein, "Multivariable Feedback Design: Concepts for a Classical/Modern Synthesis," IEEE Transactions on Automatic Control, Vol. AC-26, no. 1, Feb. 1981, pp. 4-16.
- Elfes, Alberto, "Sonar Based Mapping and Navigation System", IEEE International Conference on Robotics and Automation, San Francisco, April, 1986.
- Ellis, R. E., "Multiple-scale Measure of Static Tactile Texture", IEEE International Conference on Robotics and Automation, San Francisco, April, 1986.
- Garabedian, P.R., Partial Differential Equations, John Wiley and Sons Inc., 1964.
- Goel, P. K. "The inverse kinematics solution, closes-form dynamics and simulation of adept one industrial robot" Proceeding of 1988 IEEE International Conference on Robotics and Automation, 1688-1693, 1988.
- Goodnic, S. E. and Y. Y. Lau "Adaptive Control Algorithm Self-tunes Industrial Servo", PCIM 26-32, Sept. 1989.
- Goodwin, G. C. and K. S. Sin, Adaptive Filtering "Prediction and Control, Prentice-Hall Inc., 1984.
- Haberman, N. A. and Dewayne E. Perry, "Ada for Experienced Programmers" Addison Wesley 1983
- Haggood, Fred, "Inside a Robotics Lab: The Quest for Automatic Touch", Technology Illustrated, April 1983.
- Hawker, J. S., R. N. Nagel, R. Roberts, and N. G. Odrey, "Multiple Robotic Manipulators - Designing a task-oriented control system for multiple manipulators" Byte 203-219 Jan. 1986.
- Haynes.L. S. and A. J. Wavering, "Real Time Control System Software, Some Problems and an Approach" Real-Time Control Group
- Hillis, W. D., "A High Resolution Image Touch Sensor", The International Journal of Robotics Research, Vol. I, No.2, Summer 1982.
- Hsia, T. C., "Adaptive Control of Robot Manipulators - A Review", IEEE International Conference on Robotics and Automation, San Francisco, April, 1986.
- Huang, Y. Y., et al., "Region Filling Operations for Mobile Robot Using Computer Graphics", IEEE International Conference on Robotics and Automation, San Francisco, April, 1986.
- Johnston, A. R. "Automatic guidance for lremote manipulator", NASA Tech Brief 9 - 4 - #74 1985.

- Kent, Ernest W., et al., "Building Representations from Fusions of Multiple Views", IEEE International Conference on Robotics and Automation, San Francisco, April, 1986.
- Koivo, A. J., "Force-Position-Velocity Control with Self-tuning for Robotic Manipulators", IEEE International Conference on Robotics and Automation, San Francisco, April, 1986.
- Kresselmeier, G., "Adaptive Observers With Exponential Rate of Convergence," IEEE Transactions on Automatic Control, Vol. AC22, 1977, pp. 2-0.
- Kreutz, K. "On nonlinear control for decoupled exact external linearization of robot manipulators" NASA Tech Vrief 11 - 8 #114, 1987.
- Krogh, Bruce H., and Charles E. Thorpe, "Integrated Path Planning and Dynamic Steering Control for Autonomous Vehicles", IEEE International Conference on Robotics and Automation, San Francisco, April, 1986.
- Lin, Xueyin, and William G. Wee, "SDFS: A New Strategy for the Recognition of Objects Using Range Data", IEEE International Conference on Robotics and Automation, San Francisco, April, 1986.
- Luo, Ren C., and Wen-Hsiang Tsai, "Object Recognition Using Tactile Image Array Sensors", IEEE International Conference on Robotics and Automation, San Francisco, April, 1986.
- Marcus, M. A., "Ferroelectric polymers and their applications" Fifth International Meeting on Ferroelectricity, Penn State University, 1981.
- Mahalingam, Subbiah, and Anand M. Sharan, "The Optimal Balancing of the Robotic Manipulators", IEEE International Conference on Robotics and Automation, San Francisco, April, 1986.
- Medioni, Gerald, and Yoshio Yasumoto, "Corner Detection and Curve Representation Using Cubic B-Splines", IEEE International Conference on Robotics and Automation, San Francisco, April, 1986.
- Narerdrad, K. S., and L. S. Valavari, "Stable Adaptive Observers and Controllers," Proc. IEEE, Vol. 64, pp 1198-1208, August 1976.
- Palmin S. "New approach for the control of DC servo motors", Motion 3-13, Jan 1989.
- Pennwalt, "Kynar piezo film technical manual" Pennwalt Corp, Pa. 1983.
- Rajaram, S. and J. L. Junkins, "Identification of Vibrating Flexible Structures," AIAA Journal of Guidance, Control, and Dynamics, Vol. 8, July-August 1985, pp 463-470.
- Schwartz, Lawrence M, "CD ROM offers cost effective alternative for large databases" Computer Technology Review 75-83, Winter, 1985
- Seraji, H. "Simplified linear multivariable control of robots", NASA Tech Brief 13 - 4 #89, 1989.
- Shu, David B. et al., "Approach to 3-D Object Identification Using Ranging Images", IEEE International Conference on Robotics and Automation, San Francisco, April, 1986.

- Slotine, J.-J. E., "On Model and Adaptation in Robot Control", IEEE International Conference on Robotics and Automation, San Francisco, April, 1986.
- Sontag, Edwardo D., and Hector J. Sussman, "Time-Optimal Control of Manipulators", IEEE International Conference on Robotics and Automation, San Francisco, April, 1986.
- Sundararajan, J. P., J. P. Williams and R. C. Montgomery, "Adaptive Modal Control of Structural Dynamic Systems Using Recursive Lattice Filters," AIAA Journal of Guidance, Control, and Dynamics, Vol. 8, March-April 1985, pp 223-229.
- Vranish, John M., "Magnetoinductive Skin For Robots", IEEE International Conference on Robotics and Automation, San Francisco, April, 1986.
- Wallace, W. et al., "Progress in Robot Road-following", IEEE International Conference on Robotics and Automation, San Francisco, April, 1986.
- Waxman, Allen M., et al, "A Visual Navigation System", IEEE International Conference on Robotics and Automation, San Francisco, April, 1986.
- Zhaung, X., and T. S. Huang, "From 2-View Motion Equations to 3-D Motion Parameters and Surface Structure: A Direct and Stable Algorithm", IEEE International Conference on Robotics and Automation, San Francisco, April, 1986.
- "A Report on the 12th ISIR in Paris", Robotics Today, Vol. 4, No. 4, August 1982.
- "Touch Sensor Responds to Contact Pressure", NASA Tech Briefs, Summer 1981.
- "Touch Sensor for Robots", NASA Tech Briefs, Fall 1985.
- National Bureau of Standards (1986).
- Kwakernaak, H. and R. Sivan, Linear Optimal Control Systems, John Wiley & Sons, Inc., 1972.
- Meirovitch, L., Analytical Methods in Vibrations, Collier-MacMallian Canada, LTD, 1967.
- NASA Tech Briefs, Technical Support Package for "Finding Bright-Spot Coordinates in Television Images" Vol. 9, No. 1, MFS-25999 George C. Marshall Space Flight Center Marshall Space Flight Center, Alabama 35812 (1984)
- Popov, E.P., Mechanics of Materials, 2nd Ed., Prentice-Hall Inc., 1976.
- Rector, Russel and George Alexy, "The 8086 Book" Osborne/McGraw Hill Berkeley, Ca. 1980
- Simo, J.C. and L. V. Quoc, "A Novel Approach to the Dynamics of Flexible Beams Under Large Overall Motions--The Plane Case," Electronics Research Laboratory Memorandum No. UCB/ERL/M85/63, University of California, Berkeley, 1985.

Results of Segment Modeling

Material : Aluminum
 Outside Radius : 2.917 cm
 Inside Radius : 2.619 cm

| Payload Mass | Static Displacement | Resonant Frequencies (hz) | | |
|----------------|---------------------------|---------------------------|------|-------|
| | | 1st | 2nd | 3rd |
| 2.267 kg | 3.95 x 10 ⁻³ m | 8.38 | 66.9 | 207.5 |
| 2.267 kg (-CW) | 3.95 x 10 ⁻³ m | 8.94 | 66.9 | 207.5 |
| 4.534 kg | 7.92 x 10 ⁻³ m | 6.36 | 64.9 | 205.3 |
| 9.068 kg | 1.58 x 10 ⁻² m | 4.68 | 63.8 | 204.0 |
| 45.34 kg | 7.92 x 10 ⁻² m | 2.17 | 62.8 | 203.0 |
| 90.68 kg | 1.58 x 10 ⁻¹ m | 1.54 | 62.7 | 202.9 |
| 181.36 kg | 3.16 x 10 ⁻¹ m | 1.09 | 62.6 | 202.8 |

Material : Aluminum
 Outside Radius : 4.5 cm
 Inside Radius : 3.92 cm

| Payload Mass | Static Displacement | Resonant Frequencies (hz) | | |
|--------------|---------------------------|---------------------------|-------|-------|
| | | 1st | 2nd | 3rd |
| 2.267 kg | 5.78 x 10 ⁻⁴ m | 18.2 | 110.2 | 326.8 |
| 4.534 kg | 1.16 x 10 ⁻³ m | 14.3 | 104.3 | 318.9 |
| 9.068 kg | 2.31 x 10 ⁻³ m | 11.4 | 100.4 | 314.2 |
| 45.34 kg | 1.16 x 10 ⁻² m | 5.59 | 96.4 | 309.8 |
| 90.68 kg | 2.31 x 10 ⁻² m | 4.01 | 94.8 | 309.3 |
| 181.36 kg | 4.62 x 10 ⁻² m | 2.85 | 95.5 | 308.9 |

Material : Steel
 Outside Radius : 3.65 cm
 Inside Radius : 3.25 cm

| Payload Mass | Static Displacement | Resonant Frequencies (hz) | | |
|----------------|---------------------------|---------------------------|--------|-------|
| | | 1st | 2nd | 3rd |
| 2.267 kg | 5.68 x 10 ⁻⁴ m | 20.58 | 147.2 | 449.8 |
| 2.267 kg (-CW) | 5.68 x 10 ⁻⁴ m | 21.8 | 147.4 | 449.9 |
| 4.534 kg | 2.27 x 10 ⁻³ m | 16.06 | 141.6 | 443.0 |
| 9.068 kg | 4.55 x 10 ⁻³ m | 12.04 | 138.2 | 439.3 |
| 45.34 kg | 2.27 x 10 ⁻² m | 5.68 | 135.12 | 436.0 |
| 90.68 kg | 4.55 x 10 ⁻² m | 4.05 | 134.7 | 435.6 |
| 181.36 kg | 9.09 x 10 ⁻² m | 2.87 | 134.5 | 435.4 |

TABLE 1

Material : Steel
 Outside Radius : 4.445 cm
 Inside Radius : 3.8894 cm

| Payload Mass | Static Displacement | Resonant Frequencies (hz) | | |
|--------------|-------------------------|---------------------------|------|-------|
| | | 1st | 2nd | 3rd |
| 45.34 kg | 4.66×10^{-3} m | 8.44 | 94.4 | 299.7 |
| 90.68 kg | 9.33×10^{-3} m | 6.16 | 93.0 | 298.2 |
| 181.36 kg | 1.87×10^{-2} m | 4.43 | 92.3 | 297.5 |

Material : Steel
 Outside Radius : 5.8738 cm
 Inside Radius : 5.1594 cm

| Payload Mass | Static Displacement | Resonant Frequencies (hz) | | |
|--------------|-------------------------|---------------------------|-------|-------|
| | | 1st | 2nd | 3rd |
| 45.34 kg | 1.57×10^{-3} m | 13.98 | 127.2 | 399.2 |
| 90.68 kg | 3.13×10^{-3} m | 11.09 | 124.5 | 396.1 |
| 181.36 kg | 6.26×10^{-3} m | 7.57 | 122.8 | 394.5 |
| 181.36 (-CW) | 6.26×10^{-3} m | 8.12 | 122.9 | 394.5 |

Table 2 - System Parameters

| Length L m | ARM Segment Mass/length Kg/m | Elastic Modulus GPa | Cross Section Circular | | Payload Rotary Inertia, Ip Kg.m ² | Base Rotary Inertia, Ib | |
|---------------|------------------------------------|---------------------------|---------------------------|-------|--|----------------------------|--------|
| | | | OD cm | ID cm | | 5 lbs. | 10lbs. |
| 1.86 | 1.0971 | 11.375 | 6.350 | 5.715 | 8.897 x 10 ⁻³ | 3.210 | 5.557 |

Table 3 - Modal Frequencies




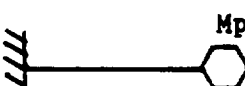
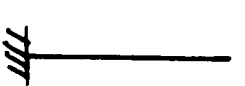
| ARM Segment Modeling Configuration | Modal Frequencies Mp = 2.267 Kg (5 lbs.) | | | Modal Frequencies Mp = 4.534 Kg (10 lbs.) | | |
|---|---|----------------|----------------|--|----------------|----------------|
| | W ₁ | W ₂ | W ₃ | W ₁ | W ₂ | W ₃ |
| 1  | 7.34 | 40.4 | 124 | 5.52 | 39.2 | 124 |
| 2.  | 26.0 | 99.0 | 220 | 25.0 | 97.0 | 216 |
| 3.  | 3.66 | 39.7 | 125 | 2.71 | 38.8 | 124 |
| 4.  | 3.66 | 39.2 | 122 | 2.71 | 38.4 | 121 |
| 5.  | 8.63 | 54.1 | 151 | | | |

Table 4: Arm Sizing; Flex/Stiff

| | Material | r_1 (cm) | r_0 (cm) | Arm Mass (kg) | Approx. 1 st Mode ω_1 (Hz) | Max. Stress (k pa.) |
|------------------------|------------|---------------|---------------|------------------|--|------------------------|
| "FLEXIBLE" CASE | Fiberglass | 1.0000 | 1.0811 | 1.103 | .00498 | 3.9 |
| | | 1.5000 | 1.5178 | 0.3503 | .00407 | 7.9 |
| | | 2.0000 | 2.0057 | 0.1491 | .00352 | 13 |
| | Aluminum | 1.0000 | 1.0136 | 0.2383 | .00448 | 23 |
| | | 1.5000 | 1.5027 | 0.0714 | .00407 | 51 |
| | | 2.0000 | 2.0009 | 0.0302 | .00352 | 90 |
| | Steel | 1.0000 | 1.0052 | 0.2547 | .00498 | 61 |
| | | 1.5000 | 1.5010 | 0.0758 | .00407 | 136 |
| | | 2.0000 | 2.0003 | 0.0320 | .00352 | 240 |
| "STIFF" CASE | Fiberglass | 1.0000 | 2.4763 | 33.6 | .0498 | 0.23 |
| | | 1.5000 | 2.5406 | 27.5 | .0498 | 0.21 |
| | | 2.0000 | 2.5931 | 21.3 | .0498 | 0.19 |
| | | 3.0000 | 3.2931 | 12.1 | .0498 | 0.18 |
| | Aluminum | 1.0000 | 1.6000 | 13.6 | .0498 | 0.60 |
| | | 1.5000 | 1.8050 | 8.77 | .0498 | 0.58 |
| | | 2.0000 | 2.1546 | 5.59 | .0498 | 0.62 |
| | | 3.0000 | 3.0501 | 2.64 | .0498 | 0.78 |
| | Steel | 1.0000 | 1.3249 | 18.6 | .0498 | 1.5 |
| | | 1.5000 | 1.6349 | 10.4 | .0498 | 1.5 |
| | | 2.0000 | 2.0621 | 6.21 | .0498 | 1.6 |
| | | 3.0000 | 3.0191 | 2.83 | .0498 | 2.1 |

TABLE 4

Table 4: 1.5 g.; Arm Sizing

| | | r_i (cm) | r_o (cm) | Arm Mass (kg) | Approx. 1 st Mode ω_1 (Hz) | Max. Stress (k pa) |
|------------------------|------------|---------------|---------------|------------------|--|-----------------------|
| "FLEXIBLE" CASE | Fiberglass | 10.000 | 15.961 | 1011 | 1.93 | 0.0187 |
| | | 15.000 | 17.186 | 460 | 1.58 | 0.0141 |
| | | 20.000 | 20.808 | 215 | 1.37 | 0.0111 |
| | Aluminum | 10.000 | 11.635 | 307 | 1.93 | 0.0286 |
| | | 15.000 | 15.395 | 105 | 1.5 | 0.0216 |
| | | 20.000 | 20.129 | 45.0 | 1.37 | 0.0196 |
| | Steel | 10.000 | 10.703 | 358 | 1.93 | 0.0892 |
| | | 15.000 | 15.152 | 113 | 1.58 | 0.0603 |
| | | 20.000 | 20.049 | 48.0 | 1.37 | 0.0544 |
| "STIFF" CASE | Fiberglass | 10.000 | 86.085 | 47792 | 61.1 | .005 |
| | | 15.000 | 86.099 | 46993 | 61.1 | .005 |
| | | 20.000 | 86.142 | 45897 | 61.1 | .005 |
| | | 23.000 | 86.189 | 45106 | 61.1 | .004 |
| | Aluminum | 10.000 | 53.734 | 24256 | 61.1 | .0098 |
| | | 15.000 | 53.800 | 23230 | 61.1 | .0093 |
| | | 20.000 | 53.974 | 21871 | 61.1 | .0089 |
| | | 23.000 | 54.164 | 20927 | 61.1 | .0085 |
| | Steel | 10.000 | 42.070 | 41078 | 61.1 | .0346 |
| | | 15.000 | 42.206 | 38284 | 61.1 | .0323 |
| | | 20.000 | 42.565 | 34728 | 61.1 | .0290 |
| | | 23.000 | 42.946 | 32361 | 61.1 | .0278 |

DATA FILE

ARMMODEL DATA - FILE: 2m22k9cm

INPUT DATA

Base Rotary Inertia: 55.87
Tube Inside Radius: 0.0382
Tube Outside Radius: 0.04445
X-sectional Inertia of Beam: 1.39362e-006
Payload Mass: 22.67
Mass/Length of Beam Material: 4.02558
Elastic Modulus of Beam: 7.5e+010
Length of Beam: 2
Beam Material Damping Coefficient: 2

INPUT PARAMETERS

DIAMETER — 9 CENTIMETERS

WEIGHT — 22 KILOGRAMS

LENGTH — 2 METERS

OUTPUT DATA FOR BETA = 1

Beta: 0.643195
CC1: -0.008135
CC2: 0.0161784
CC3: 0.0168967
CC4: -0.0161784
OMEGA (rads/sec): 66.6614
OMEGA P (hz): 10.6095
fip0: 0.00563545
fil: -0.0065375
f0p0: 0.0797364
f0l: 0.159473

OUTPUT PARAMETERS

MODE 1

OUTPUT DATA FOR BETA = 2

Beta: 1.98818
CC1: -4.58246e-005
CC2: 4.65435e-005
CC3: 4.66781e-005
CC4: -4.65435e-005
OMEGA (rads/sec): 636.94
OMEGA P (hz): 101.372
fip0: 1.69679e-006
fil: 5.43e-006
f0p0: 0.0797364
f0l: 0.159473

MODE 2

OUTPUT DATA FOR BETA = 3

Beta: 3.54733
CC1: -3.42374e-007
CC2: 3.43502e-007
CC3: 3.43483e-007
CC4: -3.43502e-007
OMEGA (rads/sec): 2027.65
OMEGA P (hz): 322.711
fip0: 3.93374e-009
fil: -2.37056e-008
f0p0: 0.0797364
f0l: 0.159473

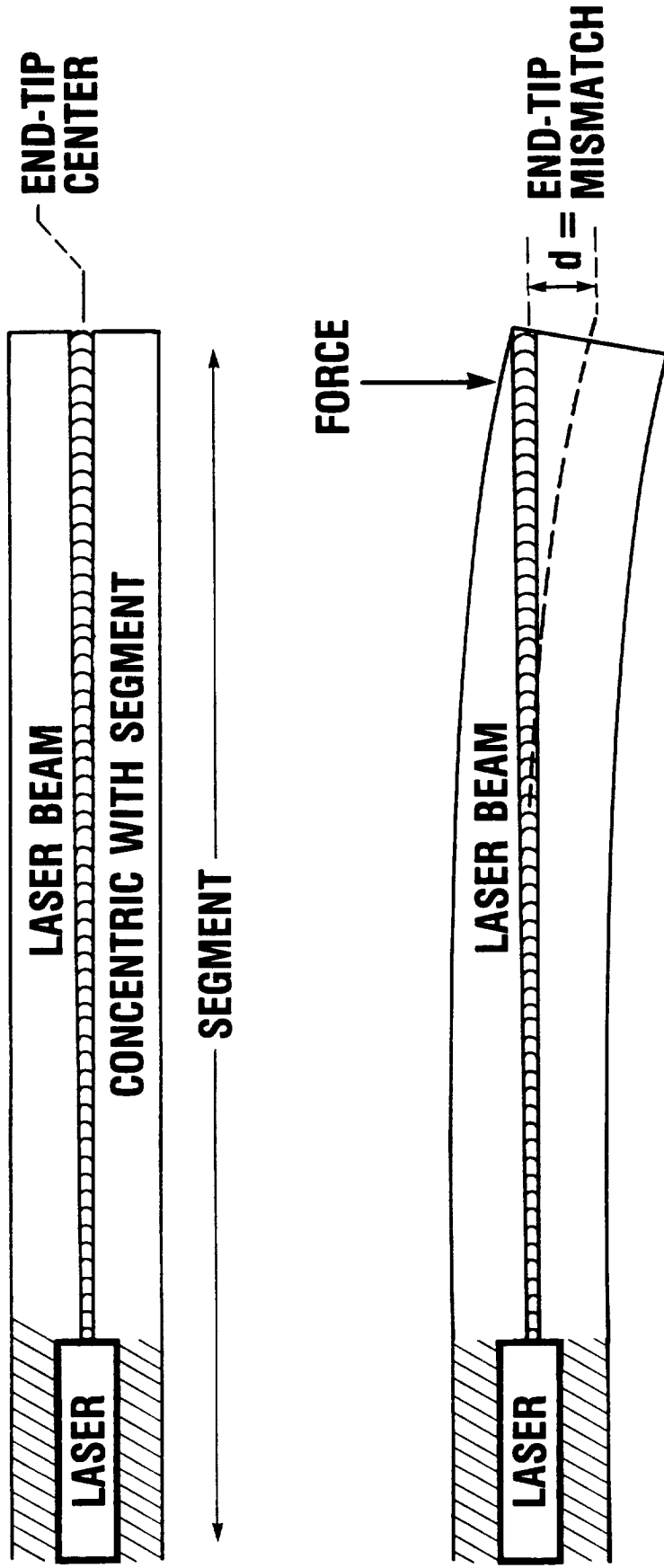
MODE 3

TABLE 5

Figure 1 End tip displacement

Assume a physical cantilever segment of length L . A force F perpendicular to the central axis of the segment will cause a displacement d . The magnitude of d is proportional to F and to the "stiffness" of the segment. Typically, robotic manipulators use short, stiff segments to minimize d , preferably to a point where it can be neglected during operation. A long segment can be defined as a segment which has a value of d that becomes significant during normal operation and, therefore, cannot be neglected. Since, in general, the prediction or calculation of d is difficult, accurate positioning of long, flexible segments in real time is difficult. Our concept utilizes the fact that a light beam is perfectly rigid. Thus, the light beam serves as an axis of absolute reference. The value d is the distance between the light beam and the segment's distal end-tip position. Since, by using our methods, we can measure this value in "real time", accurate positioning of long, flexible segments becomes feasible. (Real time is the sampling frequency required to observe the effects of induced modal contributions.)

LASER BEAM RIGID BODY POSITIONING CONCEPT



- LASER BEAM IS NORMALLY CONCENTRIC WITH SEGMENT
- APPLIED FORCE DISTORTS SEGMENT AND CAUSES END-TIP MISMATCH d

FIGURE 1

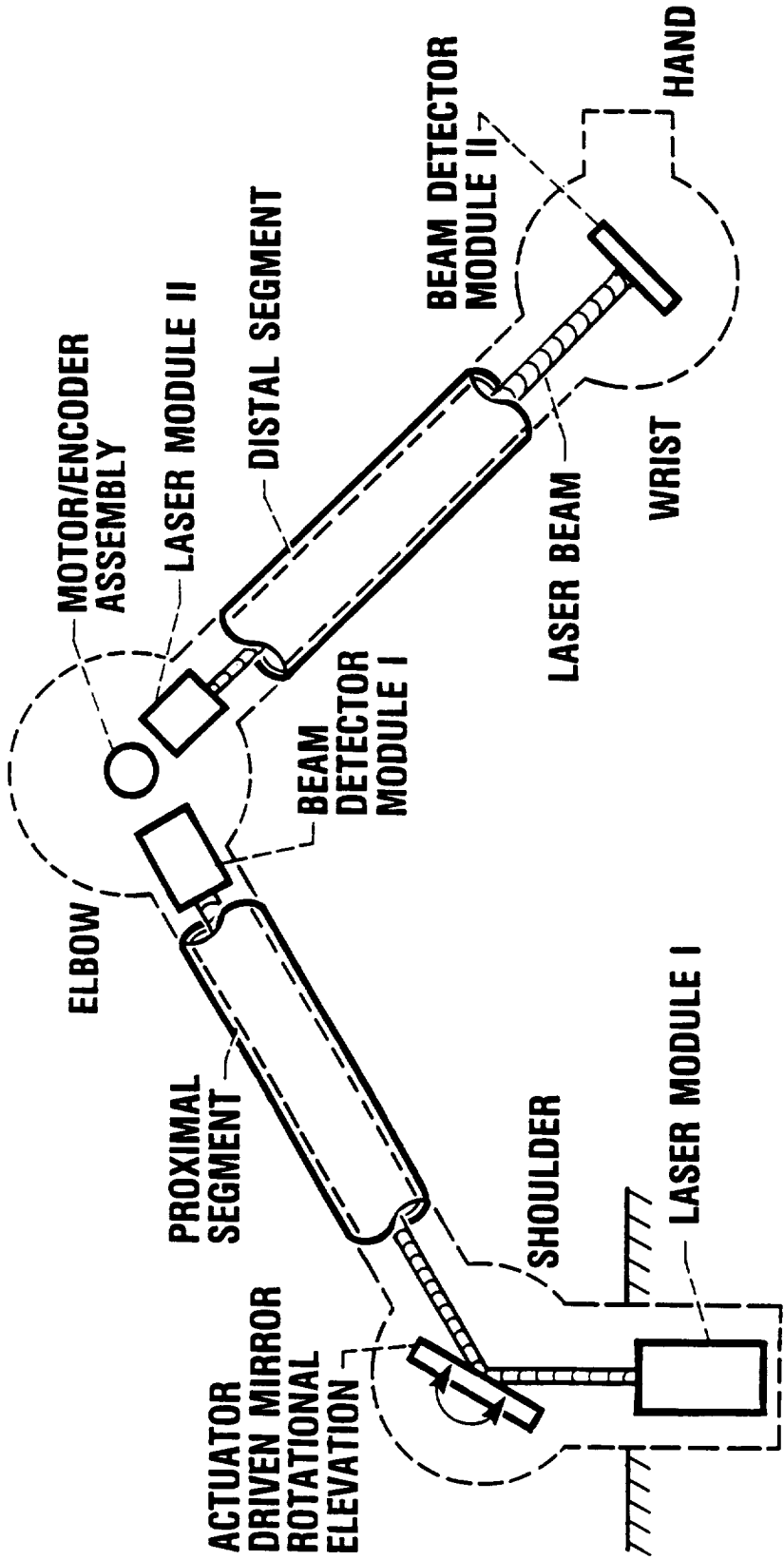
Figure 2 ARM configuration

We have designed a two-segment ARM. The shoulder articulation rotates and elevates. Concentric with the shoulder is a beam positioning unit which moves similarly. Both of these units are independently attached to the base reference point. The Beam Rider Module provides the vector position of the elbow with respect to the base reference point.

The rotation of the elbow articulation is monitored by a high-resolution encoder. This information is used to define the elbow laser reference point for the second segment. The second beam rider module provides the vector position of the wrist with respect to the elbow reference point.

A series of vector coordinate transformations is used to provide the position of the wrist end tip with respect to the base reference point. Thus, we can accurately specify the wrist end-tip position in real time.

ARM CONFIGURATION



FEATURES:

- LASER BEAM IS "INFINITE STIFFNESS" REFERENCE FOR FLEXIBLE STRUCTURE

- DETECTORS AND MIRROR DRIVES UNDER MICROPROCESSOR CONTROL TO TRACK ARM DEFLECTIONS

IMPACT:

- LOCATION OF END ARM IS KNOWN WITHIN 1 mm AT 10 m RADIUS
- POSITION, VELOCITY, ACCELERATION, AND FORCE OUTPUTS FOR ARM CONTROL AND REAL-TIME TRAJECTORY MANAGEMENT

FIGURE 2

Figure 3 Sensor configurations

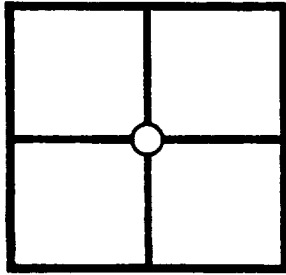
Four planar detectors were selected for evaluation. The first was the quadrant detector, with and without a central orifice. In operation, analog circuitry was used to detect beam movement; the beam was steered such that it was kept centered in the quadrant. This fast beam steering was necessary for the functioning of the DME and RME subsystems.

The second was the rectangular matrix detector. Digital circuitry was used to process the detector information and provide an X-Y coordinate of the beam spot. Significant amounts of digital signal processing was required; it was determined that this detector configuration would only be feasible at frequencies less than 30 hz.

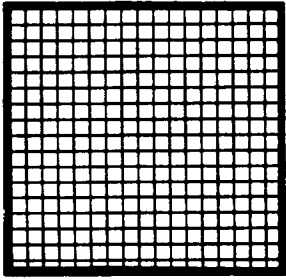
The third configuration was the annular matrix. This schema had the same limitations as the rectangular matrix. Additionally, it was not commercially available. Custom fabrication cost estimates were in the 30 to 50 thousand dollar range.

The fourth configuration was the lateral effects diode. This detector used analog circuitry to rapidly provide an X and Y value. It had sufficient resolution and linearity for our purposes.

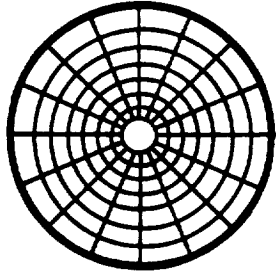
X-Y DETECTOR CONFIGURATIONS



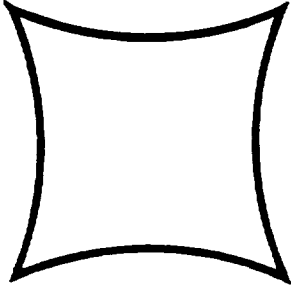
**QUADRANT
DETECTOR
ANALOG
2 × 2**



**RECTANGULAR
MATRIX
DIGITAL
500 × 500**



**ANNULAR
MATRIX
DIGITAL
200 × 200**



**LATERAL
EFFECTS
ANALOG
2000 × 2000**

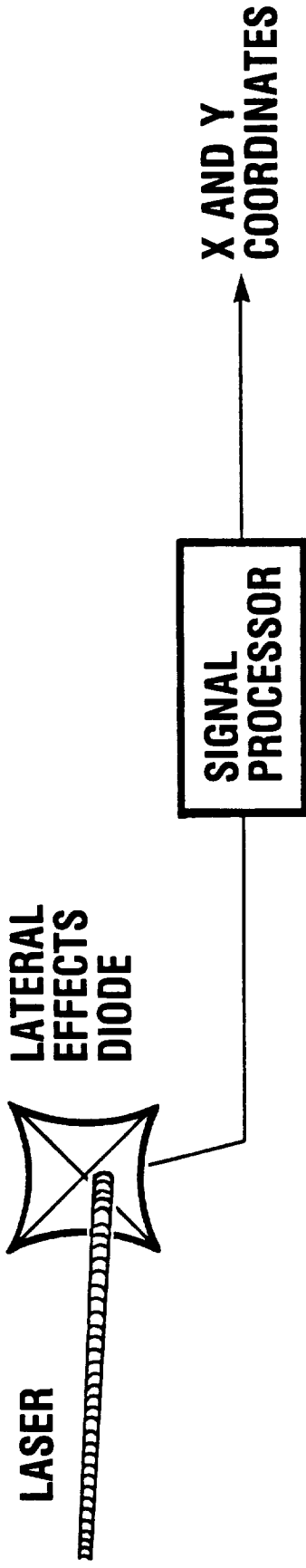
- DIFFERENT DETECTORS HAVE DIFFERENT RESOLUTIONS
- DETECTORS REQUIRE ANALOG OR DIGITAL PROCESSING

FIGURE 3

Figure 4 Detector circuitry output

The output of the lateral effects diodes and the quadrant diodes was passed through a multistage analog signal processor. The first stage isolated the diode from the processing stages. Ideally, the magnitude of the charge produced was sampled; any current drawn limited the resolution of the devices. The four outputs were added, subtracted, and divided in such a manner that the +/- X and +/- Y locations of the beam were represented by the output voltages. The frequency response of the system was limited by capacitance factors inherent to the diodes and required to stabilize the circuitry.

LATERAL EFFECTS DIODE



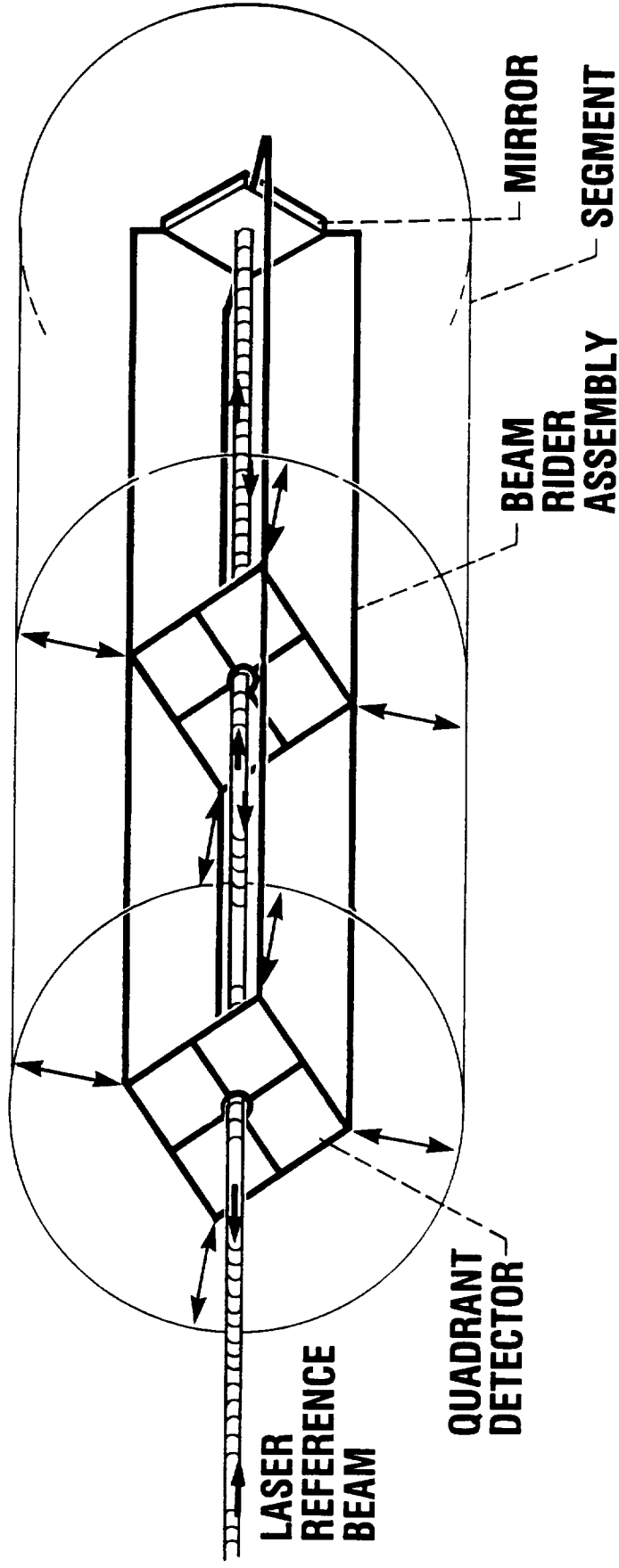
- SIGNAL FROM LATERAL EFFECTS DIODE CONVERTED TO X AND Y COORDINATES
- THIS INFORMATION USED BY INDIRECT ADAPTIVE CONTROLLER TO POSITION ARM

FIGURE 4

Figure 5 Original beam rider configuration

The original beam rider configuration was an active positioning system using a pair of quadrant detectors and a retroreflector. The BR would fit within the segment and translate in the X1, Y1 and X2 and Y2 directions. The beam was to be reflected back down the tube. A major problem with the concept was the lack of high frequency responsiveness. A second problem was the loss of beam intensity when passing through the central orifice of the detectors.

ACTIVE POSITIONING QUADRANT DETECTOR

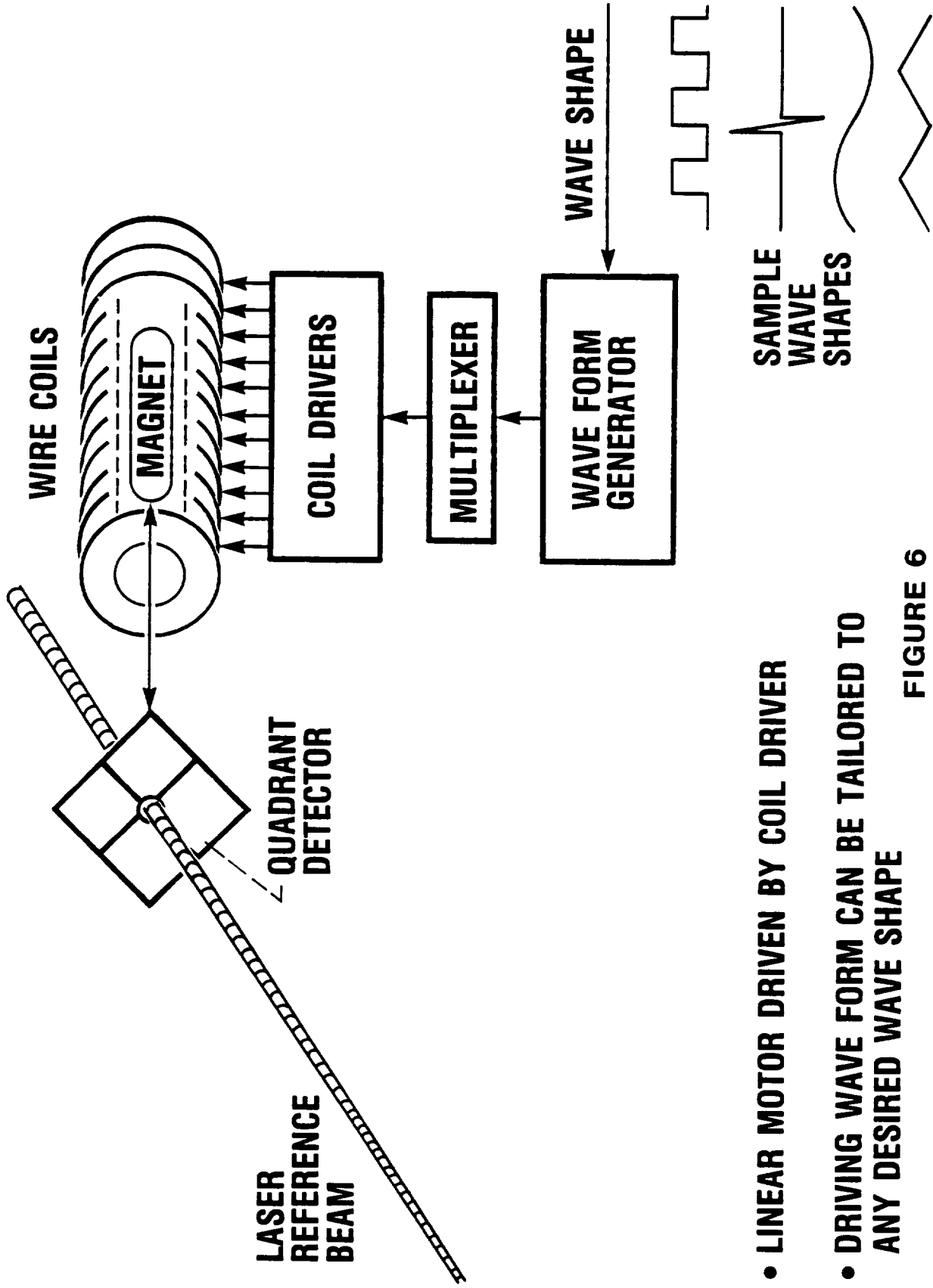


- BEAM RIDER ASSEMBLY FITS INSIDE SEGMENT
- ASSEMBLY HOLDS QUADRANT DETECTORS AND MIRRORS ASSEMBLY
- LINEAR MOTORS BETWEEN ASSEMBLY AND SEGMENT POSITION ASSEMBLY TO REMAIN COLINEAR WITH LASER REFERENCE BEAM

Figure 6 Linear voice coil motor

A linear voice coil actuator was designed as the actuator for the active positioning concept. The actuator had serial sets of coils. Sequential or simultaneous excitations of the coils provide the required linear travel and position resolution. The coil driver drove 256 coils with a positive or negative current. The value of the current in each coil was set by a multiplexing unit which addressed each coil uniquely by use of an 8-bit code. The drive value was stored until reset. The wave from a wave generator determined which value was placed on which address line. The wave form was generated by the computer and represented a standing wave. The most appropriate standing wave pattern was generated and sent to the linear actuator. The complexity of the circuitry and the computer requirements made this scheme unfeasible.

ACTIVE POSITIONING LINEAR MOTOR



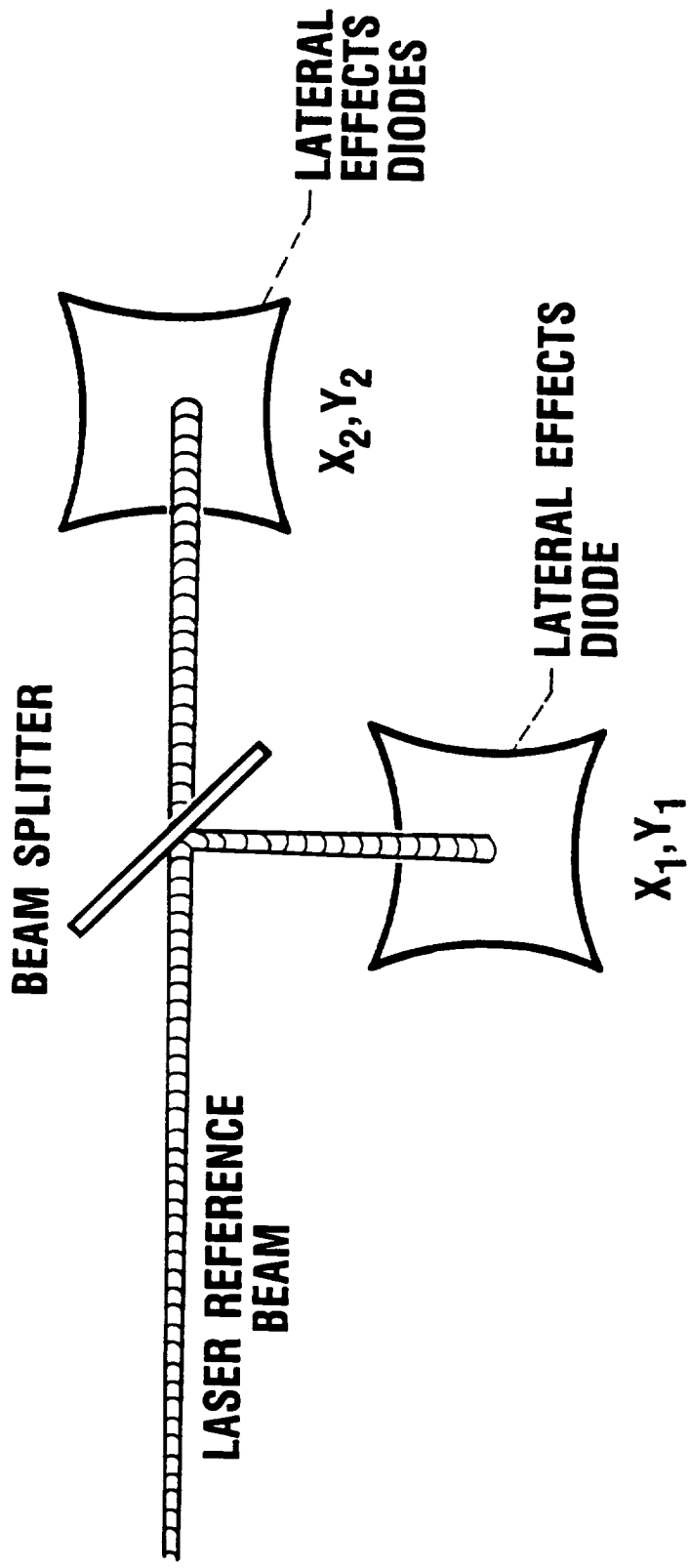
- LINEAR MOTOR DRIVEN BY COIL DRIVER
- DRIVING WAVE FORM CAN BE TAILORED TO ANY DESIRED WAVE SHAPE

FIGURE 6

Figure 7 Beam splitter beam rider configuration

A passive BR configuration was designed to provide the X and Y values. The final configuration used a variation of this design. A portion of the incident beam was reflected by the quarter wave plate placed in front of the fast steering retroreflector. The reflected split beam was incident upon the lateral effects diode which provided the lateral displacement value.

NONMOVING, FOUR-DEGREE-OF-FREEDOM DEFINING SCHEMA



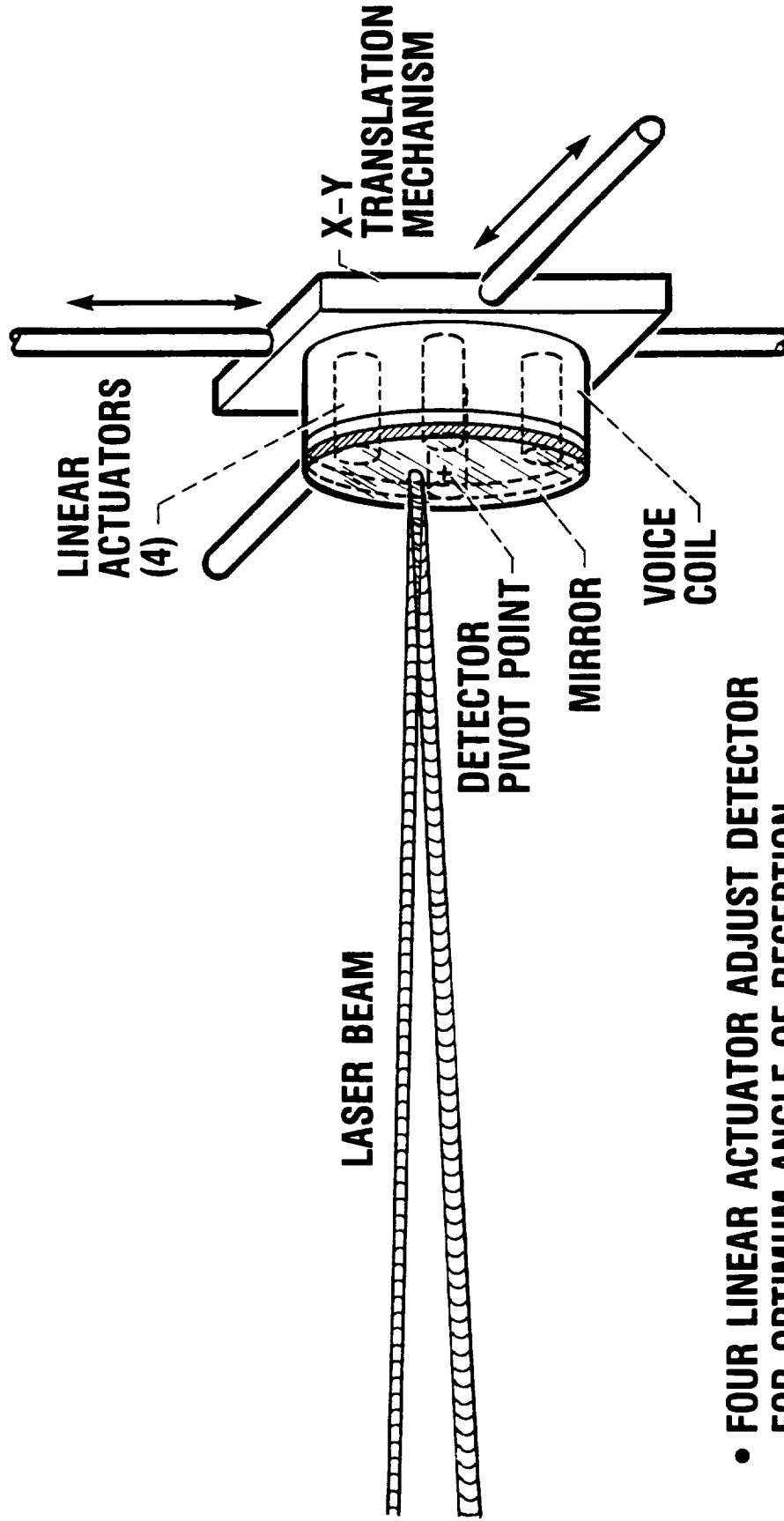
- DETECTOR ASSEMBLIES ATTACHED TO SEGMENT
- DEFLECTION OF SEGMENT CAUSES CHANGE IN POSITION OF LASER BEAM ON DIODE

FIGURE 7

Figure 8 Mirror positioner

An active mirror positioning device was required to keep the reflected laser beam centered on the DME interferometer. The output of a quadrant detector, driven by a portion of the return laser beam split from the main beam, was used to position the mirror. Electromechanical, electromagnetic, and piezoelectric mirror drivers were evaluated.

ACTIVE BEAM RETROREFLECTOR ASSEMBLY



- FOUR LINEAR ACTUATOR ADJUST DETECTOR FOR OPTIMUM ANGLE OF RECEPTION
- ENTIRE MIRROR POSITIONING MECHANISM MAY TRANSLATE IN X AND Y DIRECTIONS

FIGURE 8

Figure 9 BEI Fast steering mirror assembly

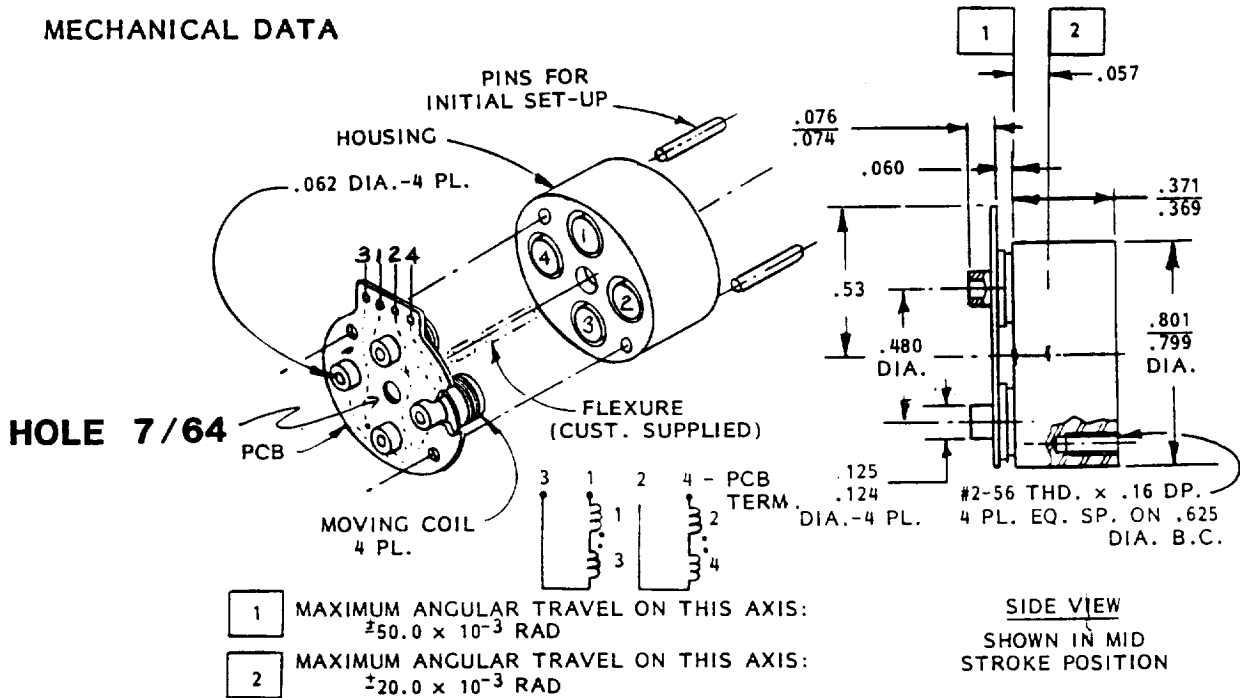
The BEI Fast steering mirror assembly was adopted for the final configuration. The mirror was positioned by a set of four voice coils arranged as mutually orthogonal pairs. Pairs of coils operated in push-pull configuration moved the mirror and kept the beam centered.

LINEAR ACTUATOR

-MOVING COIL-
-SmCo Magnet-

MODEL NO. LA08-05-

MECHANICAL DATA



PERFORMANCE DATA

- PEAK FORCE (F_p)
- FORCE CONSTANT (K_f)
- BACK EMF CONSTANT (K_B)
- MOTOR CONSTANT (K_M)
- CURRENT @ PEAK FORCE (I_p)
- POWER @ PEAK FORCE 25°C (P_p)
- RESISTANCE 25°C
- ELECTRICAL TIME CONSTANT
- THERMAL RESISTANCE OF COIL
- STROKE
- CLEARANCE EACH SIDE OF COIL
- MAX. ALLOWABLE COIL TEMP.
- WEIGHT MOVING MEMBER
- TOTAL WEIGHT

- OZ. PER COIL
- OZ./AMP PER COIL
- VOLTS/FT/SEC.
- OZ./ \sqrt{WATT}
- AMPS
- WATTS
- OHMS PER PAIR
- MICROSEC.
- °C/WATT
- IN. \pm
- IN.
- °C
- OZ.
- OZ.

| | WINDING | | | |
|--------------------|---------|---|---|---|
| | A | B | C | D |
| OZ. PER COIL | 0.6 | | | |
| OZ./AMP PER COIL | 1.0 | | | |
| VOLTS/FT/SEC. | .085 | | | |
| OZ./ \sqrt{WATT} | .63 | | | |
| AMPS | 0.6 | | | |
| WATTS | 0.9 | | | |
| OHMS PER PAIR | 4.6 | | | |
| MICROSEC. | 7.0 | | | |
| °C/WATT | --- | | | |
| IN. \pm | .01 | | | |
| IN. | .007 | | | |
| °C | 155 | | | |
| OZ. | .06 | | | |
| OZ. | .73 | | | |

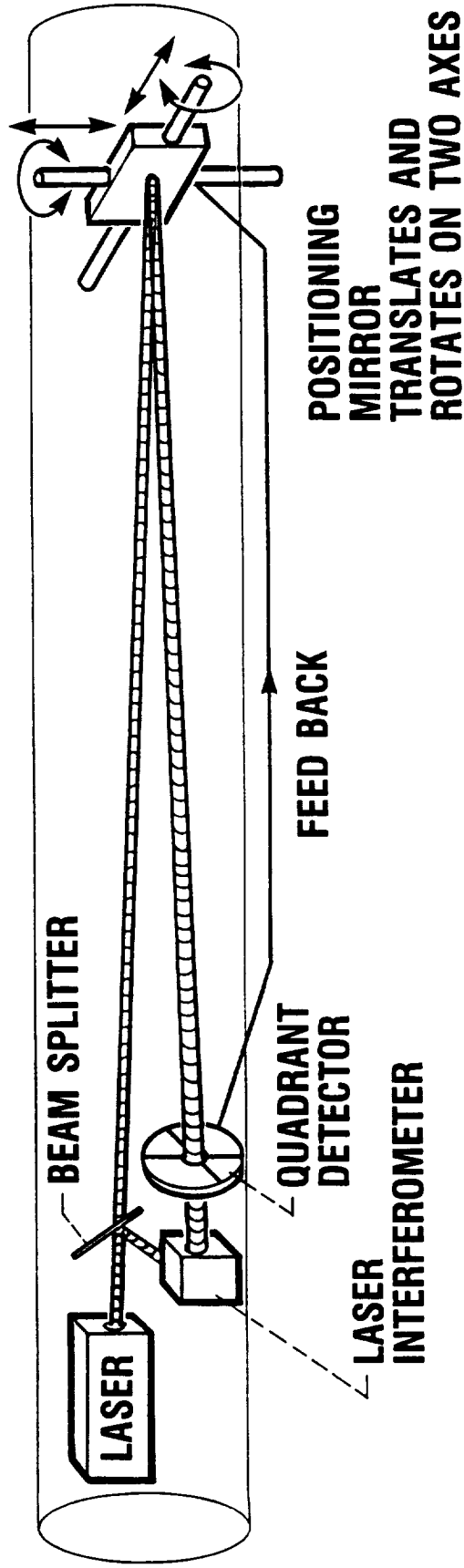
FIGURE 9

Figure 10 Original DME plane mirror configuration

A laser interferometer was used for distance measurement. During operation the incident reference beam and the return beam enter the interferometer. The interference fringes produced by changes in distance were counted and used to indicate changes in distance.

For operation a high degree of parallelism was required between the incident and the return beams. Initially, a pair of wedges was used in conjunction with the return beam to position it parallel to the incident beam. The sensitivity of the critical alignment of the wedges prevented the system from being a feasible final configuration.

DISTANCE MEASURING EQUIPMENT—LASER INTERFEROMETER



- QUADRANT DETECTOR SENDS FEEDBACK TO POSITIONING MIRROR TO ASSURE CORRECT POSITIONING OF BEAM ON INTERFEROMETER
- LASER INTERFEROMETER DETERMINES TOTAL DISTANCE TRAVELED BY LASER
- RESULT IS ACCURATE DETECTION OF ANY CHANGE IN LENGTH OF ARM DUE TO APPLIED LOAD OR OTHER EFFECTS

FIGURE 10

Figure 11 Laser reference system

The heart of the laser reference system was a lateral displacement prism. The function of the lateral displacement prism was to laterally displace the return from the incident beam by the 1 cm. required for operation of the interferometer. The prism was polarization sensitive, requiring rotation of the polarization of the laser beam by 90 degrees for operation. Since the interferometer was also polarization sensitive, the beam was required to be rotated 45 degrees after exiting and before entering the interferometer. Thus, during operation, the light beam experienced four sequential rotations of 45 degrees and, finally, was returned to its initial plane of polarization.

Secondary reflections split from the incident and return beams at the lateral displacement prisms were used as signal for the RME system. The ratio between the two intensity of the two beams was a function of the orientation of the quarter wave plate mounted to the distal segment end tip. Thus, the value of the ratio, was a function of the rotation of the distal end tip of the segment.

LASER POSITIONING SYSTEM

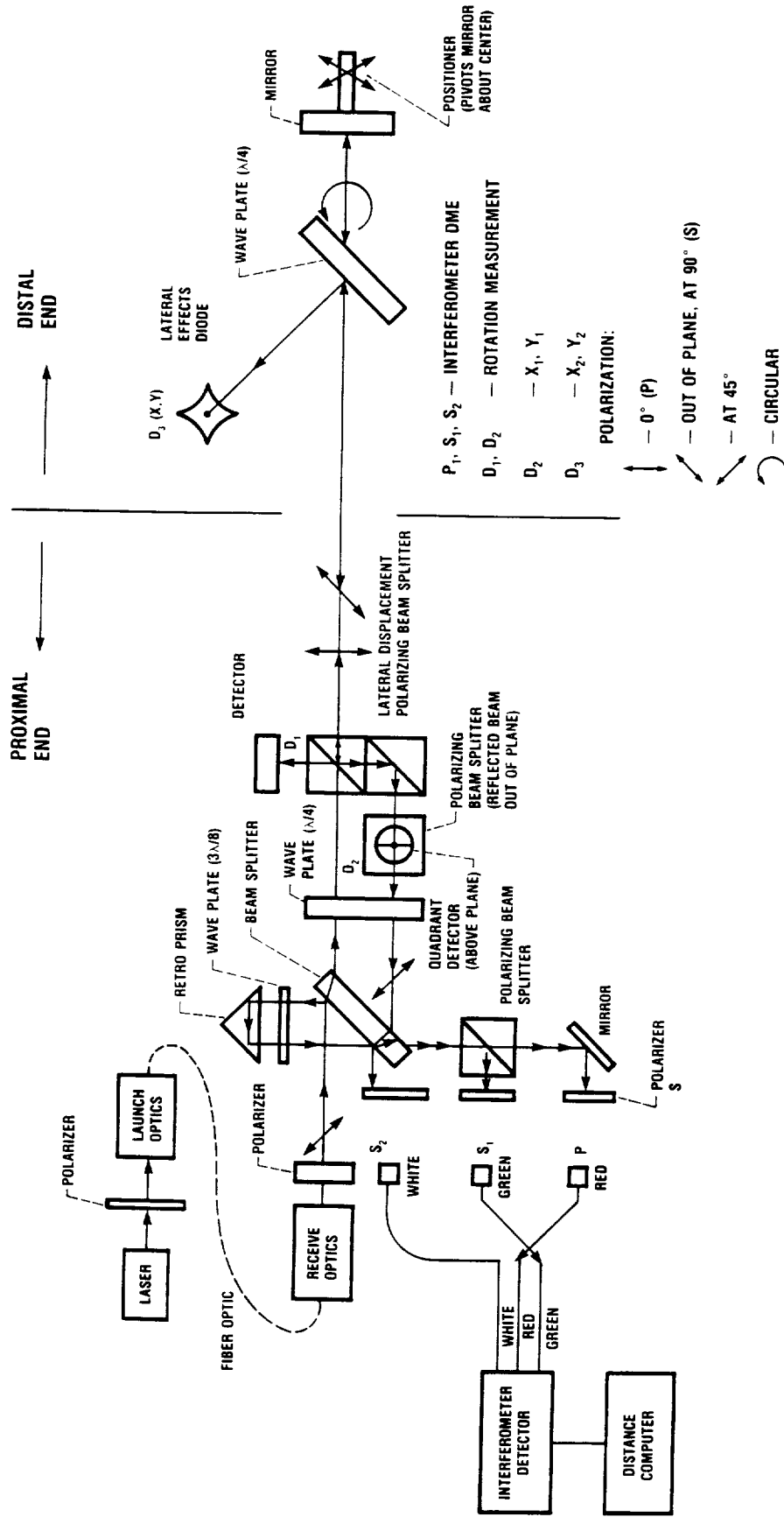
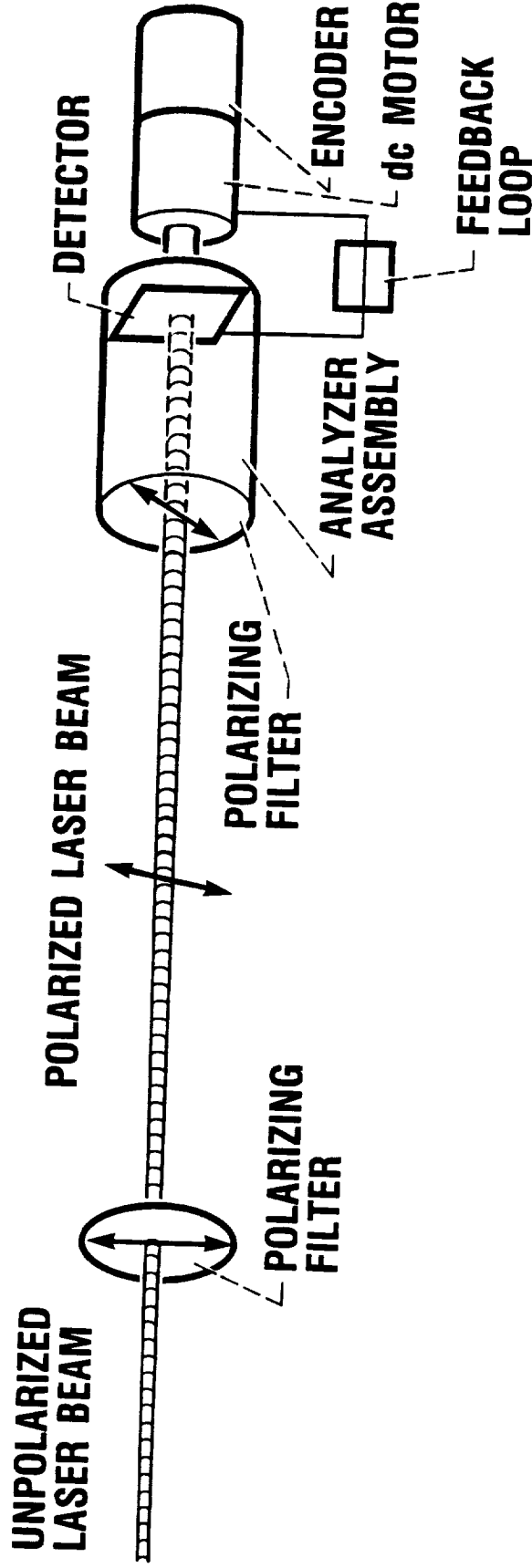


FIGURE 11

Figure 12 Original RME scheme

The rotational measurement equipment (RME) system made use of the polarized nature of the laser reference beam. The original concept incorporated an active analyzer which would keep the beam intensity constant. The analyzer would then rotate equally and opposite to the rotation of the distal portion of the segment.

ROTATIONAL MEASURING EQUIPMENT—BEAM POLARIZATION



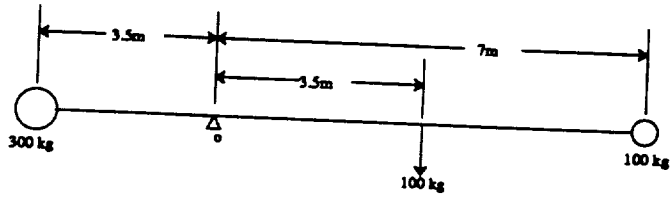
- ARM ROTATION DETECTED USING POLARIZING FILTERS
- dc MOTOR ROTATES ANALYZER ASSEMBLY UNTIL DETECTOR READS MAXIMUM INTENSITY

FIGURE 12

Figure 13 Preliminary ARM model configuration

The ARM model was based upon a counterbalanced configuration. The portion between the central pivot point and the distal end tip was assumed to be flexible. The opposite end of the assembly, between the central pivot point and the counterweight, was assumed to be rigid. Initially, a pair of seven meter segments were used to obtain a ten meter reach. Eventually, a pair of five meter segments were used. Segments were scaled such that the fundamental mode of vibration remained relatively constant.

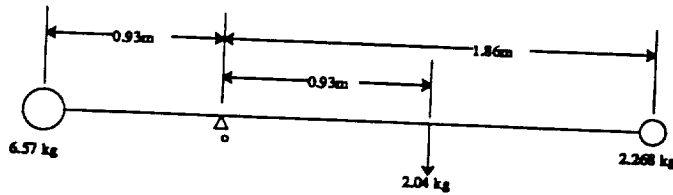
FULL SCALE SEGMENT



Inertia about point o
 full load : 8983.3 kg m ; no load and 100 kg counter weight : 1327.1 kg m

| rotational spd. to achieve tip spd of 5 m/sec | full load start torq max accel = 10 g | no load start torq max accel = 1g max accel = 1.5g |
|---|---|---|
| 6.82 rpm | $12.6 \times 10^{-3} \text{ Nm}$ | 1860 Nm 2790 Nm |

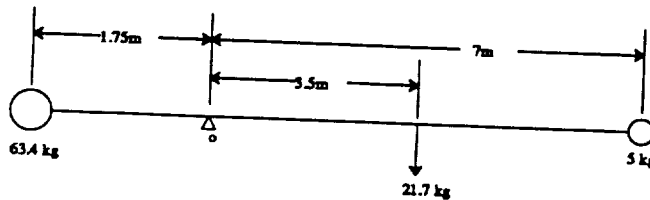
ARM II TEST BED WITH FIBERGLASS SEGMENT



Inertia about point o
 full load : 17.32 kg m no load and 2.04 kg counter weight : 5.26 kg m

| rotational spd. to achieve tip spd of 5 m/sec | full load start torq max accel = 10 g max accel = 1.5g | no load start torq max accel = 1g max accel = 1.5g |
|---|---|---|
| 25.7 rpm | $91.3 \times 10^{-6} \text{ Nm}$ 137 Nm | 27.7 Nm 41.6 Nm |

ARM II TEST BED WITH 7m Al SEGMENT $r_c=5\text{cm}$, $r_t=5.34\text{cm}$



Inertia about point o
 full load : 531 kg m ; no load and 43.3 kg counter weight : 224.7 kg m

| rotational spd. to achieve tip spd of 5 m/sec | full load start torq max accel = 10 g max accel = 1.5g | no load start torq max accel = 1g max accel = 1.5g |
|---|---|---|
| 6.82 rpm | $744 \times 10^{-6} \text{ Nm}$ 1116 Nm | 315 Nm 472 Nm |

ORIGINAL PAGE IS
 OF POOR QUALITY

FIGURE 13

Figure 14 Mode contribution graph 1

The first three fundamental modes of vibration and the magnitude of their contributions were plotted for the typical configuration. The fundamental mode had the most significant impact upon performance.

$$\mu_p = 10.16$$

0.04 First 3 Modes: 5.52 Hz., 39.2 Hz. and 124 Hz.

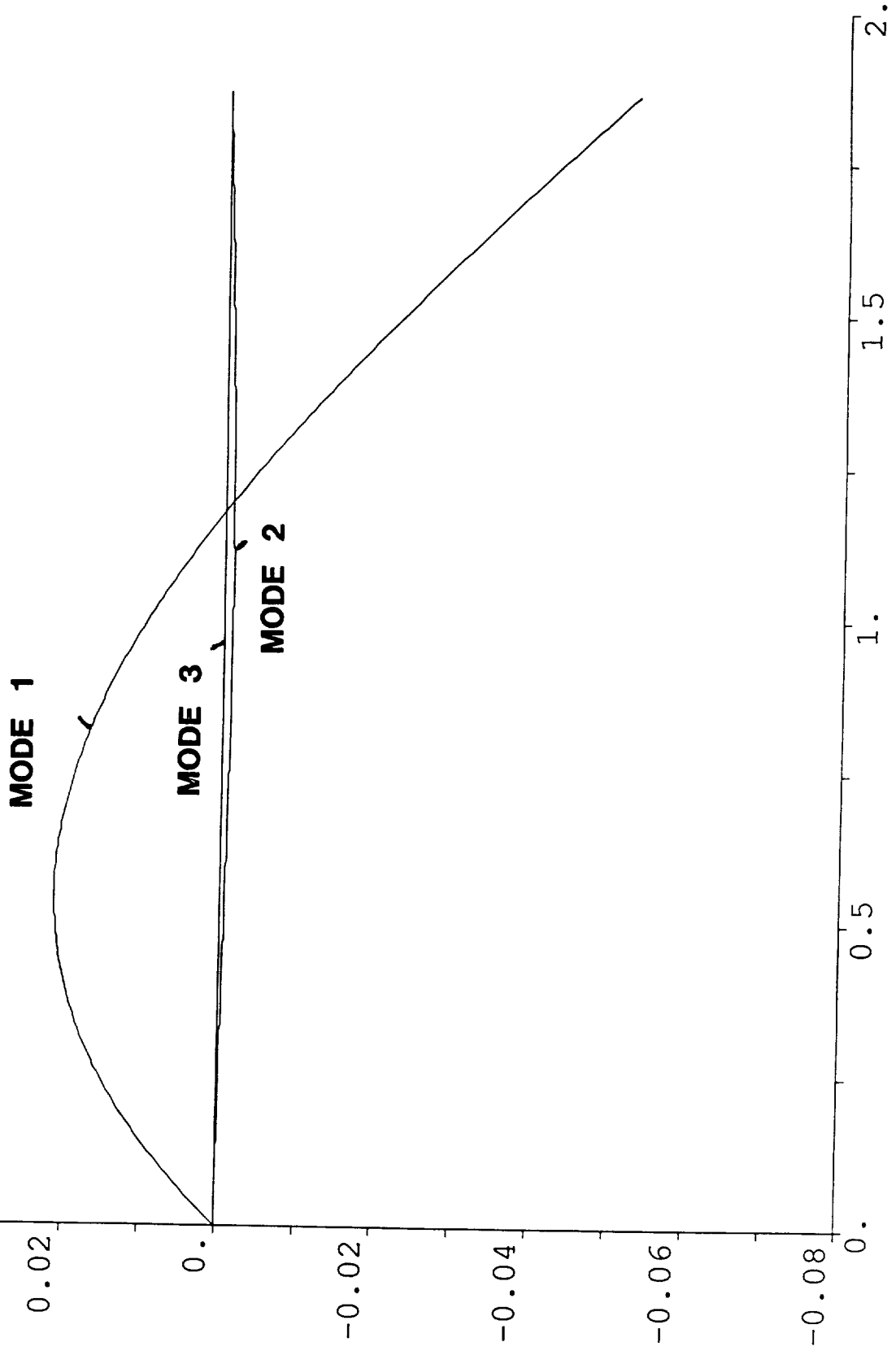


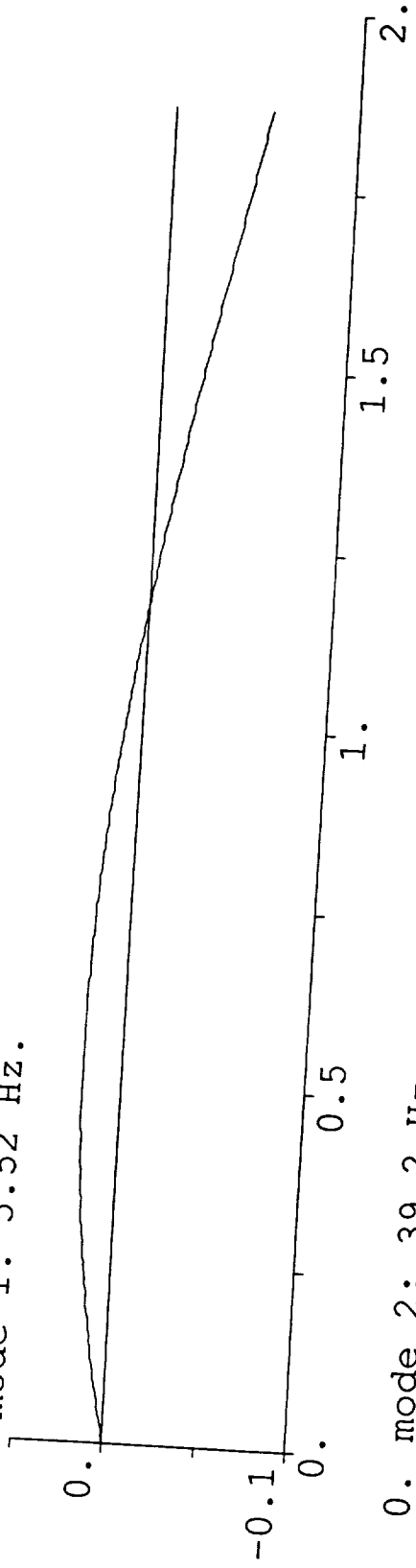
FIGURE 14

Figure 15 Mode contribution graph 2

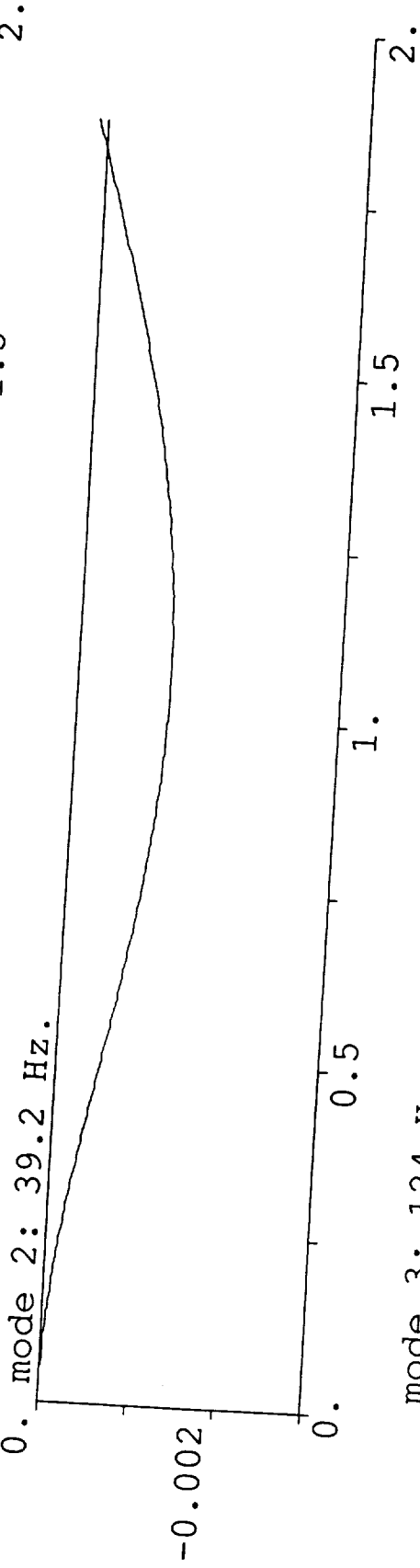
The first three fundamental modes were plotted at different magnitudes to produce normalized output.

$m_p = 10.06$.

mode 1: 5.52 Hz.



mode 2: 39.2 Hz.



mode 3: 124 Hz.

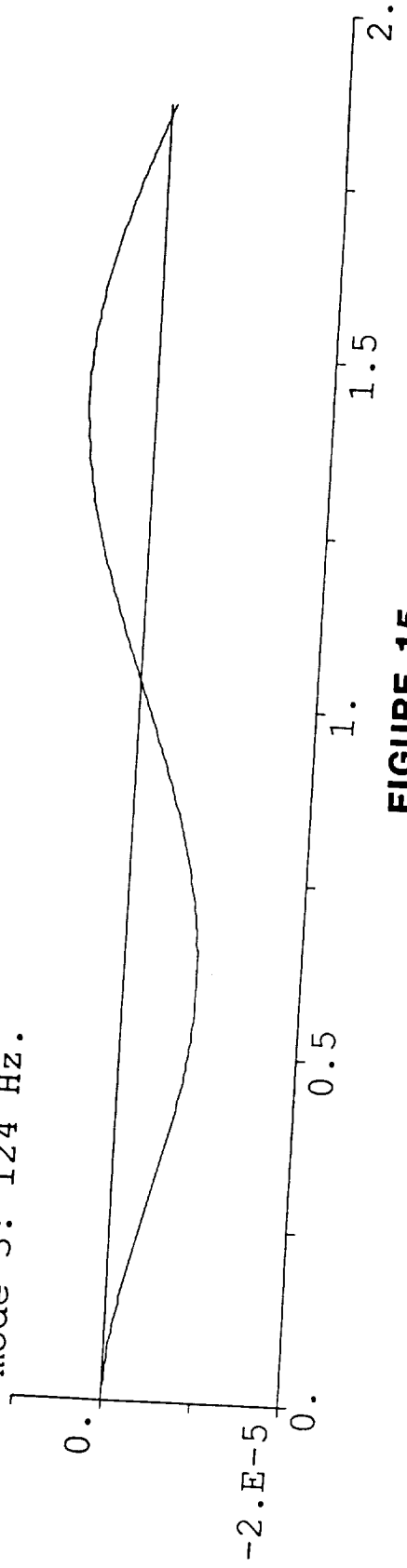


FIGURE 15

ORIGINAL PAGE
BLACK AND WHITE PHOTOGRAPH

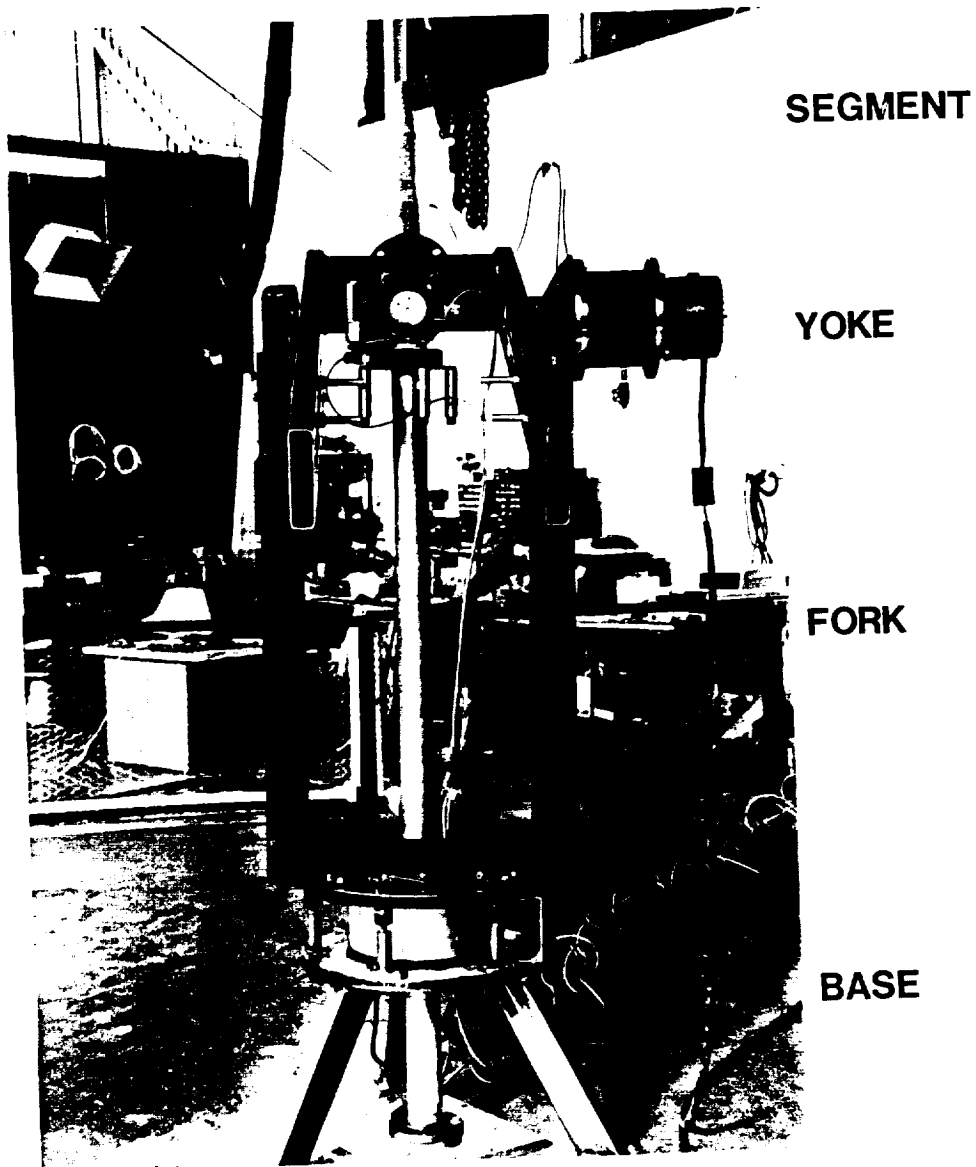


Figure 16 A Base and Shoulder Assembly Photograph

The shoulder was a two axis articulation. The direct drive azimuthal motor rested upon the tripod supported base plate. The fork bolted to the mounting plate resting upon the azimuthal drive and outrigger bearing posts. The yoke mounted on the top of the fork; the elevation motor and gearbox assembly was mounted on the right fork. The counterweighted yoke assembly contained attachment points for the segment. The split yoke configuration was necessary to allow the Beam Positioning Module to be centered at the azimuthal and elevation axes. Concentric with the shoulder articulation was the post that supported the Beam Positioning Module.

ORIGINAL PAGE
BLACK AND WHITE PHOTOGRAPH

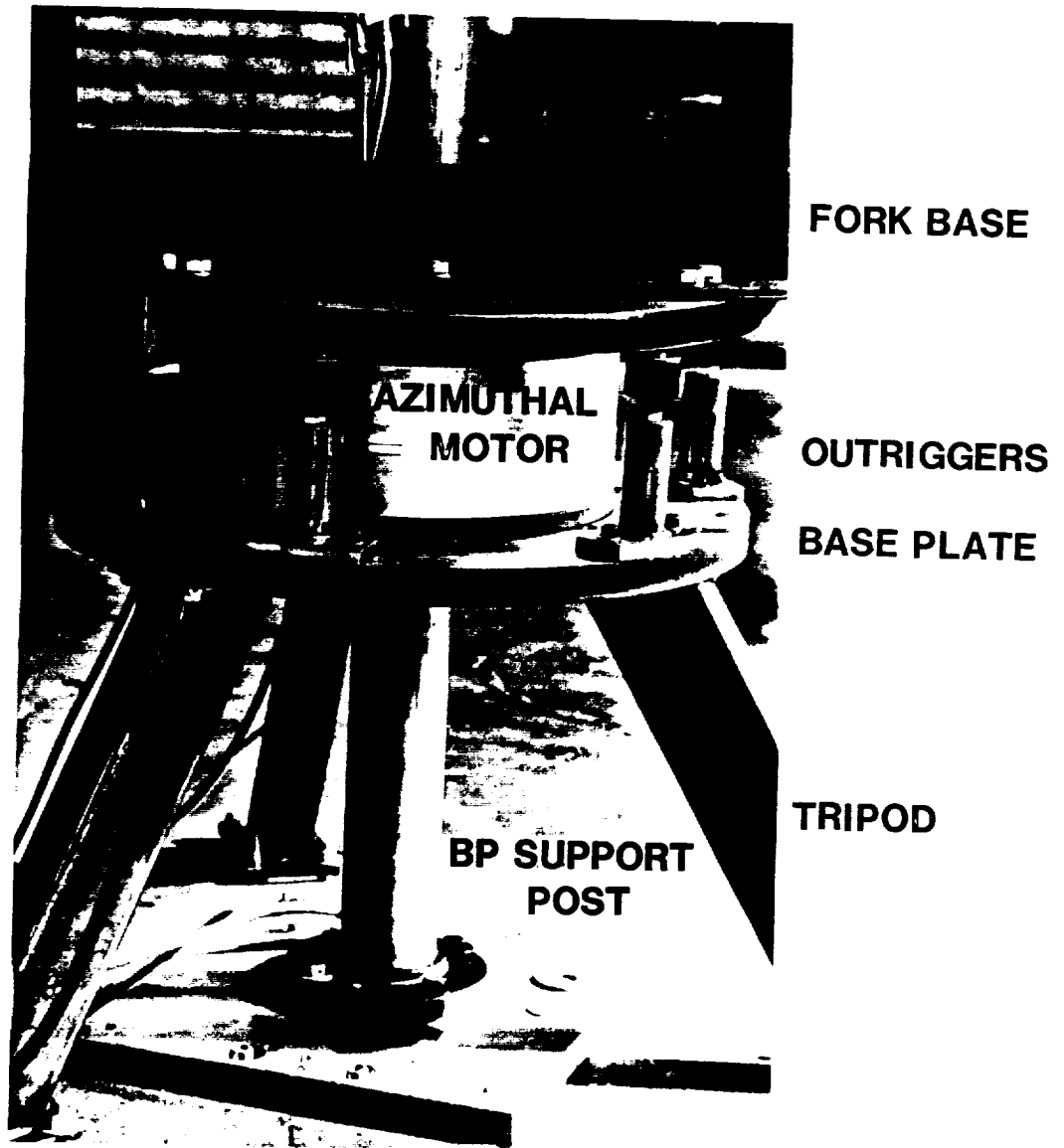


Figure 16 B. Base and Azimuthal Motor Assembly Photograph

The base plate rested upon a tripod which bolted to the floor. The direct drive azimuthal motor mounted upon the base plate. Six outrigger bearing support pillars were mounted around the motor assembly to provide additional lateral stability to the fork mounting plate. This arrangement protected the azimuthal motor bearings during full torque application by the elevation motor. The fork attached to the motor plate and supported the elevation drive and the yoke. The Beam Positioning Module support post mounted to the floor and was concentric with the azimuthal motor and assembly.

ORIGINAL PAGE
BLACK AND WHITE PHOTOGRAPH

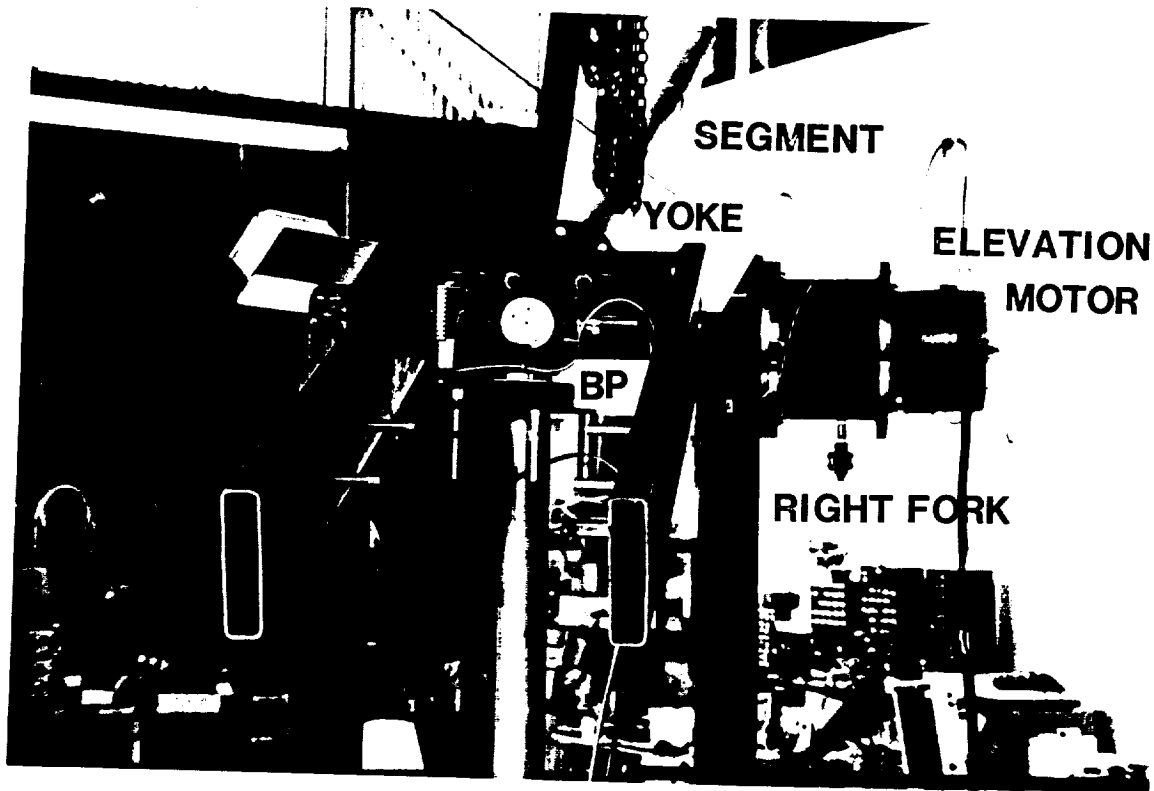
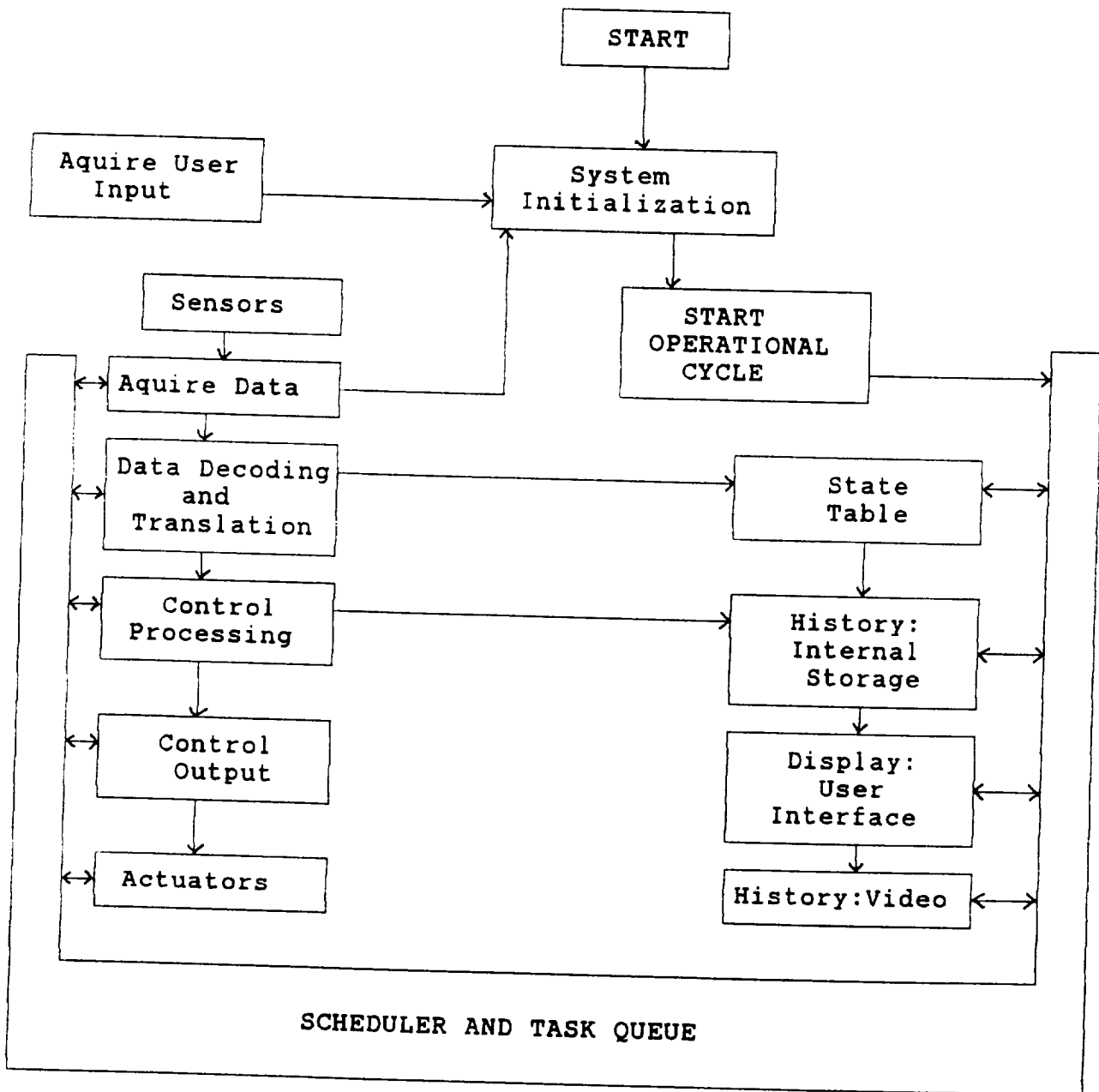


Figure 16 C Shoulder Elevation Articulation Photograph

The yoke mounted to the top of the fork. The DC motor and torque amplification zero backlash gearbox bolt to the fork. The output shaft served as a pivot point for one side of the yoke assembly. The opposite side of the yoke and second pivot point was supported by a bearing assembly and shaft. The yoke had provisions for mounting of the segment on one end and the counter weights on the other. Two segment mounts were provided. One, closest to the axis of rotation, accepted the smaller diameter segments and provided maximum segment length proportional to reach. This position was used for single segment experimental configurations. The second, approximately 25 cm. more distal, accepted the larger diameter segments required for the support of the added weight of the elbow articulation and distal segment.

Figure 17 Software control system scheme

At the start of operation the system was initialized and user input provided. The computer polled the sensors to determine the initial operating conditions and component status. Based upon the state of the indirect adaptive controller, the scheduler organized the requisite tasks to accommodate the user input commands. Once the required sequence of events had been prioritized and coordinated with the user, commands were outputted to the controller and, thence, to the actuators. The motion was tracked and revised as required.

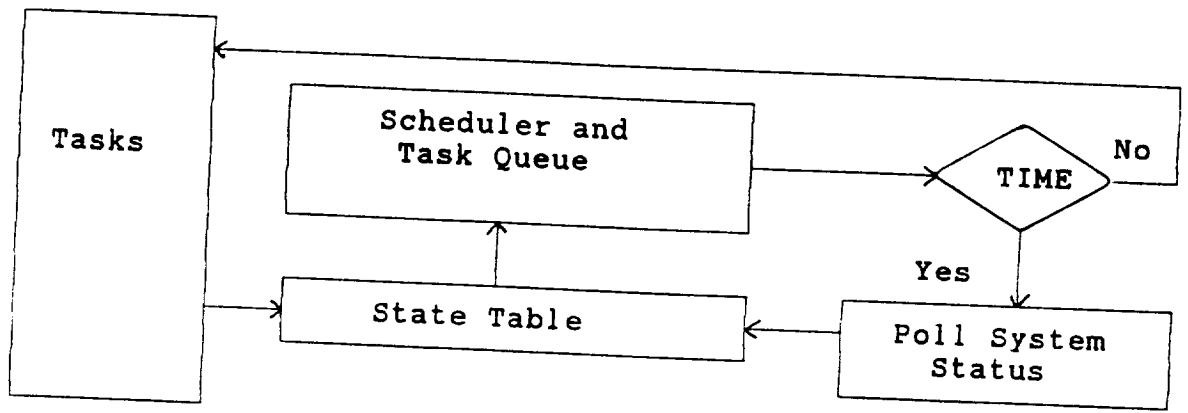


Software control system schematic

FIGURE 17

Figure 18 Task scheduling scheme

It was determined that the use of the state machine was the preferred design on the macro level. This was a non-interrupt driven cyclic system driven from the state table. The program flow at the macro level was constant and, therefore, no critical events were allowed to be missed. This condition held true as long as the timing of the system was of the appropriate resolution. The system timing resolution was set by a hardware timing generator. The scheduler was the package of modules which consisted of the collection of tasks that directed traffic within the system.

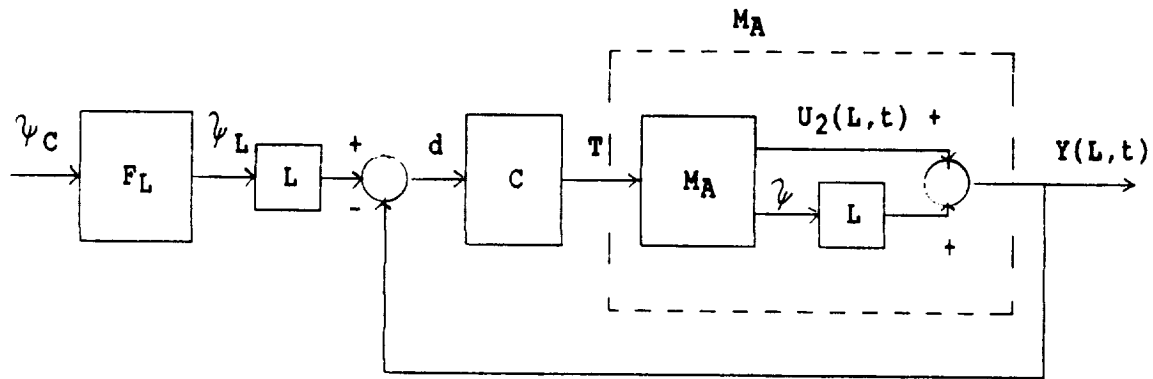


Software task scheduling schemetic

FIGURE 18

Figure 19 Robust control

The idea behind robust control design was to account for all system uncertainties within a single fixed controller. Therefore, all parameter variations and any possible combination of variables and unknowns must be incorporated into the initial controller. Such universal applicability led to an overly conservative design.



F_L : Transfer Function: Desired Angular Position, ψ_C , to actual Laser Angular Position, ψ_L .

C : Transfer Function of Controller:

Input; Measured Laser End Tip, Arm Segment Position Mismatch, d .
Output; Torque applied at the base of ARM Segment, T .

M_A : Model of Arm Segment:

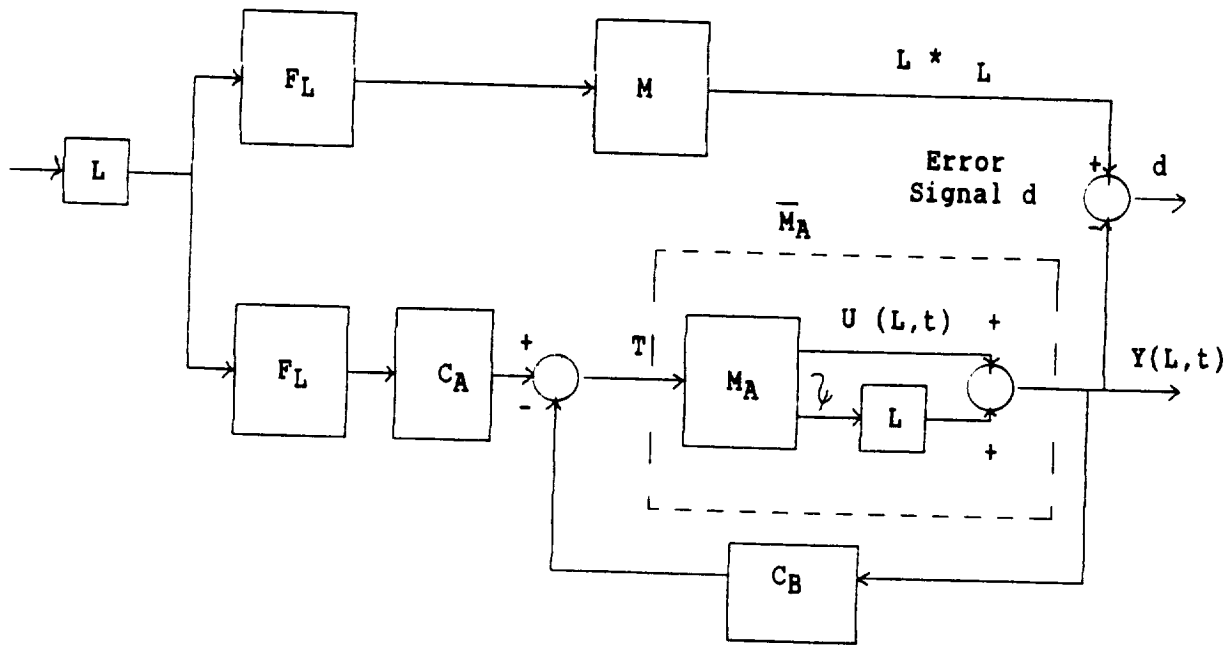
Input; Torque applied at the base of Arm Segment, T .
Output; Position of lArm Segment End Tip, $Y(L,t)$

Robust Controller Block Diagram

FIGURE 19

Figure 20 Adaptive control

Adaptive control was nonlinear and time varying. The desired system response model was chosen. Pre-filtering of the input and feedback of the output were used to force the resultant input/output properties of the controller plus the real system to equal the input/output properties of the chosen model. Such a scheme performed well when parameters were constantly varying. Continual re-adaptation under a static condition significantly increased processing overhead.



F_L : Transfer Function of Mirror Movement Dynamics

\bar{F}_L : Approximation of F_L

C_A : Prefiltering Component of Adaptive Controller

C_B : Feedback Component of Adaptive Controller

Note: Parameters in C_A and C_B are functions of d , the Measured Position Mismatch between Laser and Arm Segment End Tip Position.

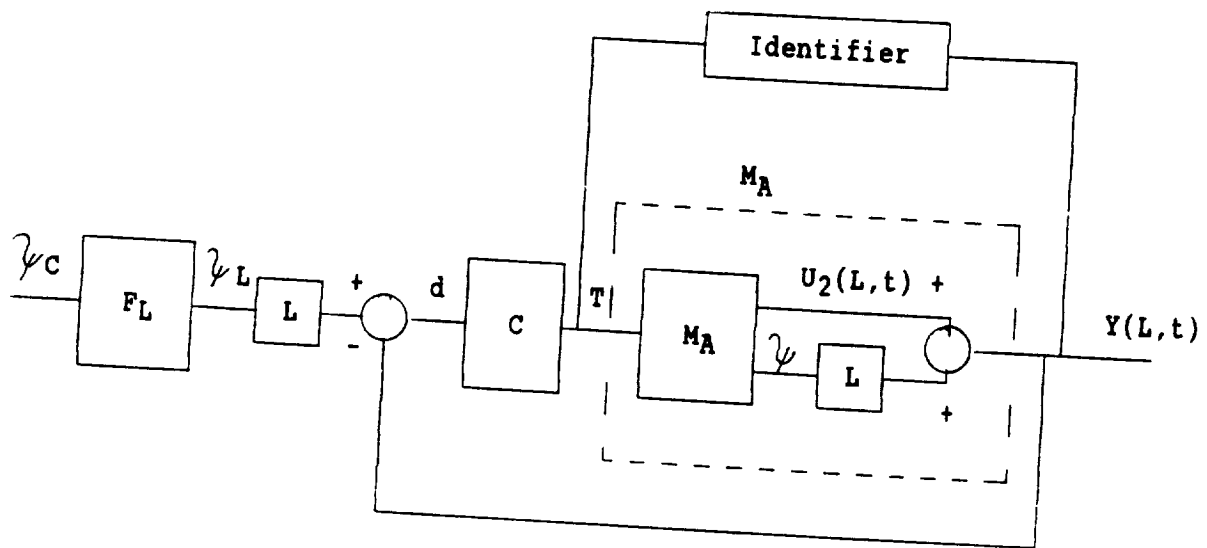
M_A : Model of Arm Segment

Direct Adaptive Control Block Diagram

FIGURE 20

Figure 21 Identification/control

The use of identification techniques in conjunction with periodic control parameter updates streamlined the control process. The controller needed only to consider the variables and parameters of import in a certain situation. The system only required re-tuning, or adaptation, when the parameters varied. Thus, it became an indirect adaptive controller.



F_L : Transfer Function: Desired Angular Position, φ_c , to actual Laser Angular Position, φ_L .

C : Transfer Function of Controller:

Input; Measured Laser End Tip, Arm Segment Position Mismatch, d .
Output; Torque applied at the base of ARM Segment, T .

M_A : Model of Arm Segment:

Input; Torque applied at the base of Arm Segment, T .
Output; Position of lArm Segment End Tip, $Y(L,t)$

Identification/Control Block Diagram

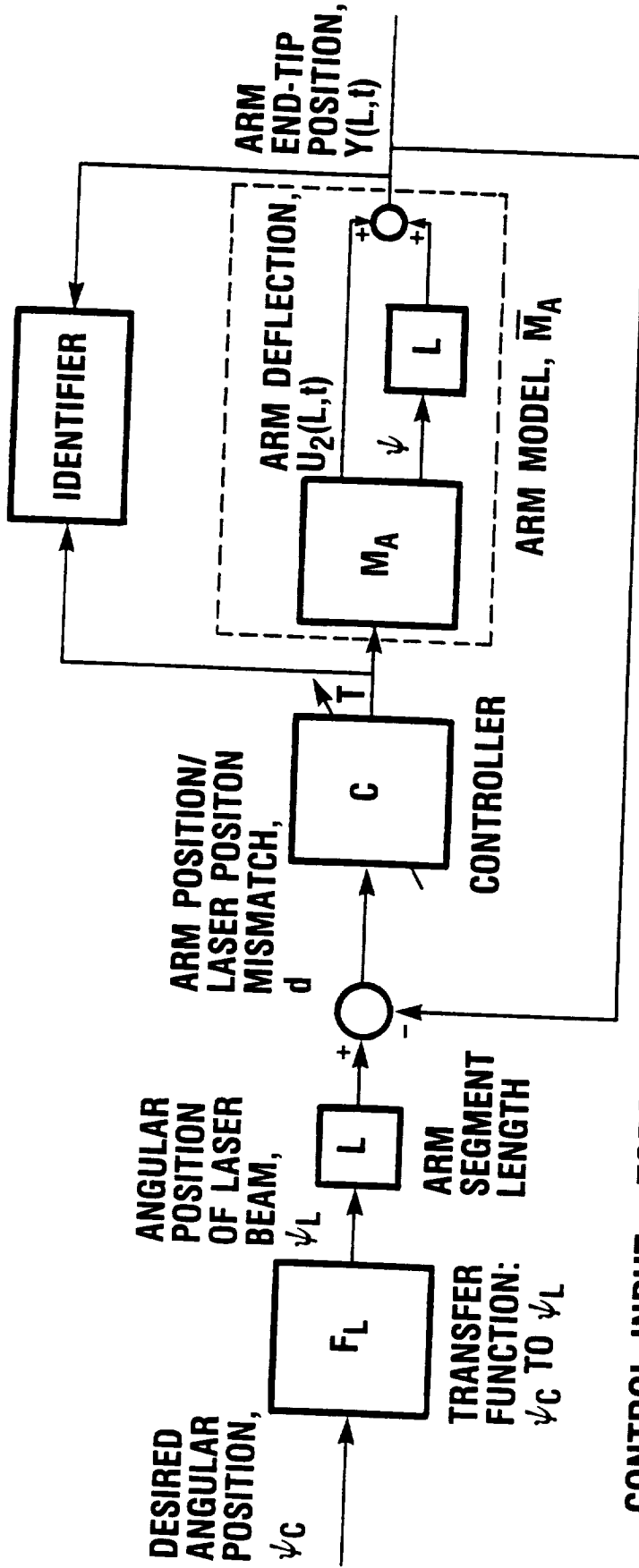
FIGURE 21

Figure 22 Indirect adaptive control

In order to design a controller for a system, one must have an accurate model of the system. In the case of the ARM, we assumed that its model consisted of a finite number of linear, ordinary differential equations. The driving term, or input, to this model was torque applied to the base of the ARM, and the response, or output, was the end-tip position of the ARM. We employed an identifier to determine the number of modes which must be included in the model and the model parameters (e.g., damping coefficients) required. The identifier took input and output measurements and used those to estimate the values of the coefficients in the differential equations which composed the model.

From the model the actual controller was constructed. The controller variables became functions of the identifier's ARM parameter estimates; as the identifier obtained better estimates of the ARM's parameters, the controller became more finely tuned to the ARM. Any changes in the ARM's characteristics, e.g., a change in arm segment material compliance due to heating or cooling, would be sensed by the identifier. The identifier then changed the corresponding variables in the in-line controller. This provided continuous smooth operation of the overall system. An identifier linked to an in-line controller was referred to as an indirect adaptive control scheme.

INDIRECT ADAPTIVE CONTROL SCHEME



CONTROL INPUT: TORQUE T APPLIED TO BASE OF ARM
 OUTPUTS TO BE CONTROLLED: 1. POSITION OF ARM END TIP

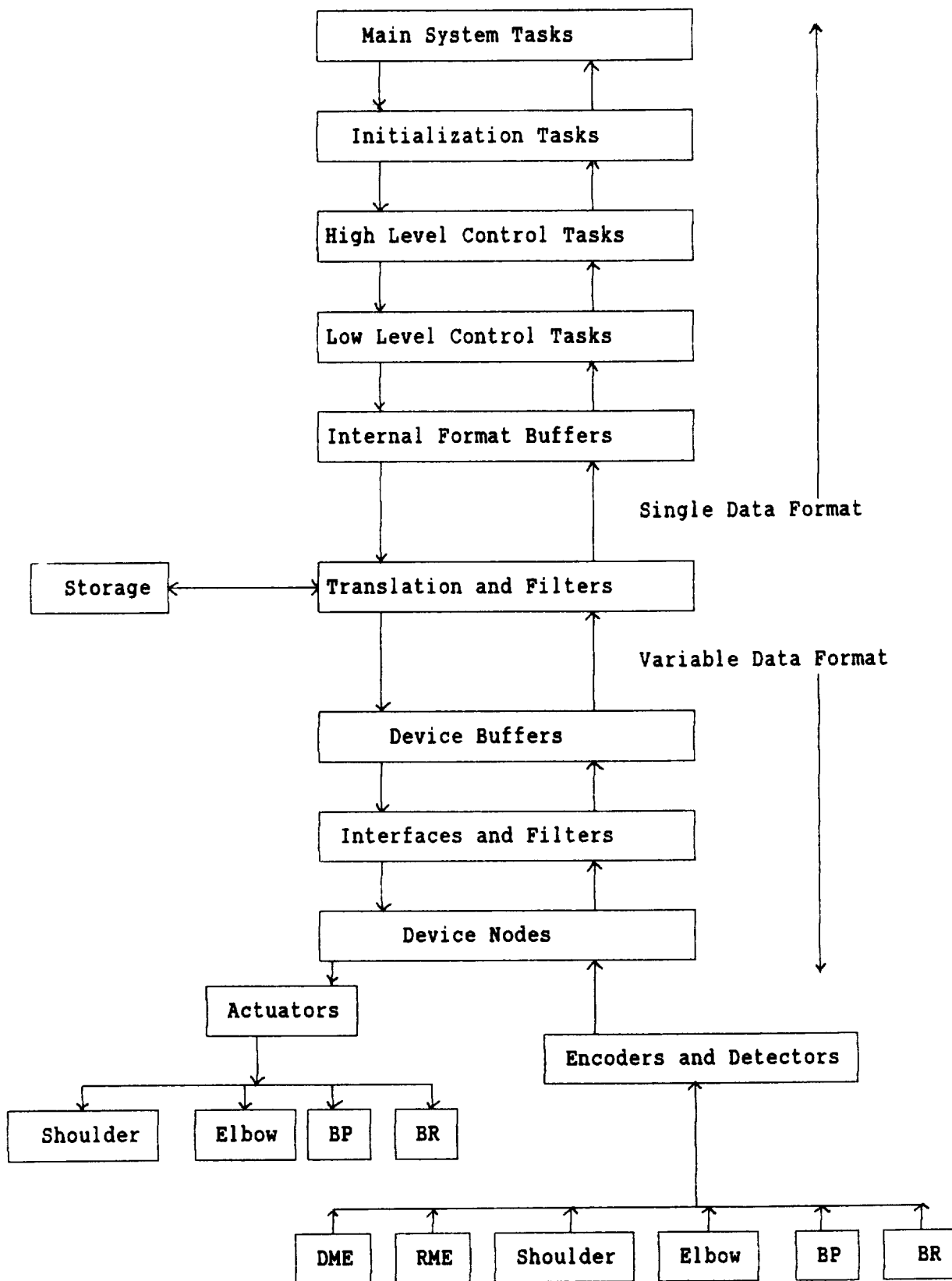
- 2. DEFLECTION OF ARM END TIP
- LASER MEASURES ARM DEFLECTION AT END TIP
- TORQUE MEASURED (KNOWN) AT ARM BASE
- THESE TWO MEASUREMENTS USED TO FINE TUNE ARM MODEL WHICH IS USED TO FINE TUNE ARM CONTROLLER

LST '88

FIGURE 22

Figure 23 ARM III System configuration

The ARM used a 32 bit VME based Intel 80386 processor for overall control and coordination. This 32 bit wide bus format was the single data format used by the high end of the system found at the top of the diagram. This format was selected because it was wide enough to encompass all of the possible variable data formats used by the system. Local encoders, detectors, processors, and actuators were mixtures of variable resolution (number of data bits required) analog and digital technology. For the low end of the system, bottom of the figure, the resolution and technology were selected as required to perform the requisite function.

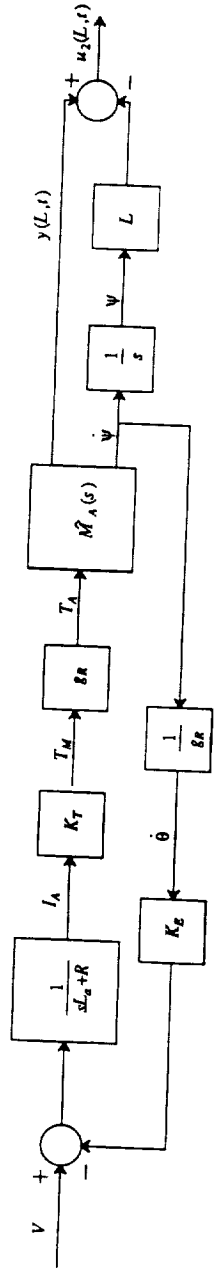


ARM III System Configuration

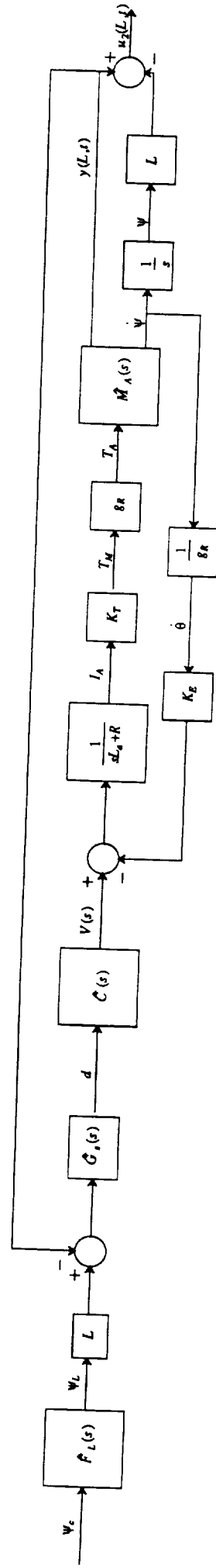
FIGURE 23

Figure 24a and 24b MOTGER model configuration

Both open loop and closed loop systems were considered for the ARM. Figure 24 a is a block diagram of an open loop system consisting of the DC motor, gear box, and the flexible segment. Figure 24 b is the block diagram of the closed loop system which consisted of the DC motor, gear box, flexible segment, controller, and the end tip position sensor. From the closed loop block diagram the actual model system was constructed. The matrix algebraic model was constructed from the families of differential equations describing the segment assembly's modal behavior. (See page 94 for symbol explanations)



Block diagram of open loop system: DC Motor, Gear Box and Single Segment Flexible Arm.



Block diagram of closed loop system: DC Motor, Gear Box, Single Segment Flexible Arm, Controller and end tip position sensor.

FIGURE 24

Figure 25 ARM behavior with DC input

After substituting the actual system parameters in the model, the model was run under various simulated conditions. This figure demonstrates the behavior of the endtip given an initial step start to a constant drive torque to the system. The model predicts the classic damped harmonic response expected to be exhibited by such a system. The dotted line is the drive voltage and the dashed line the end tip response.

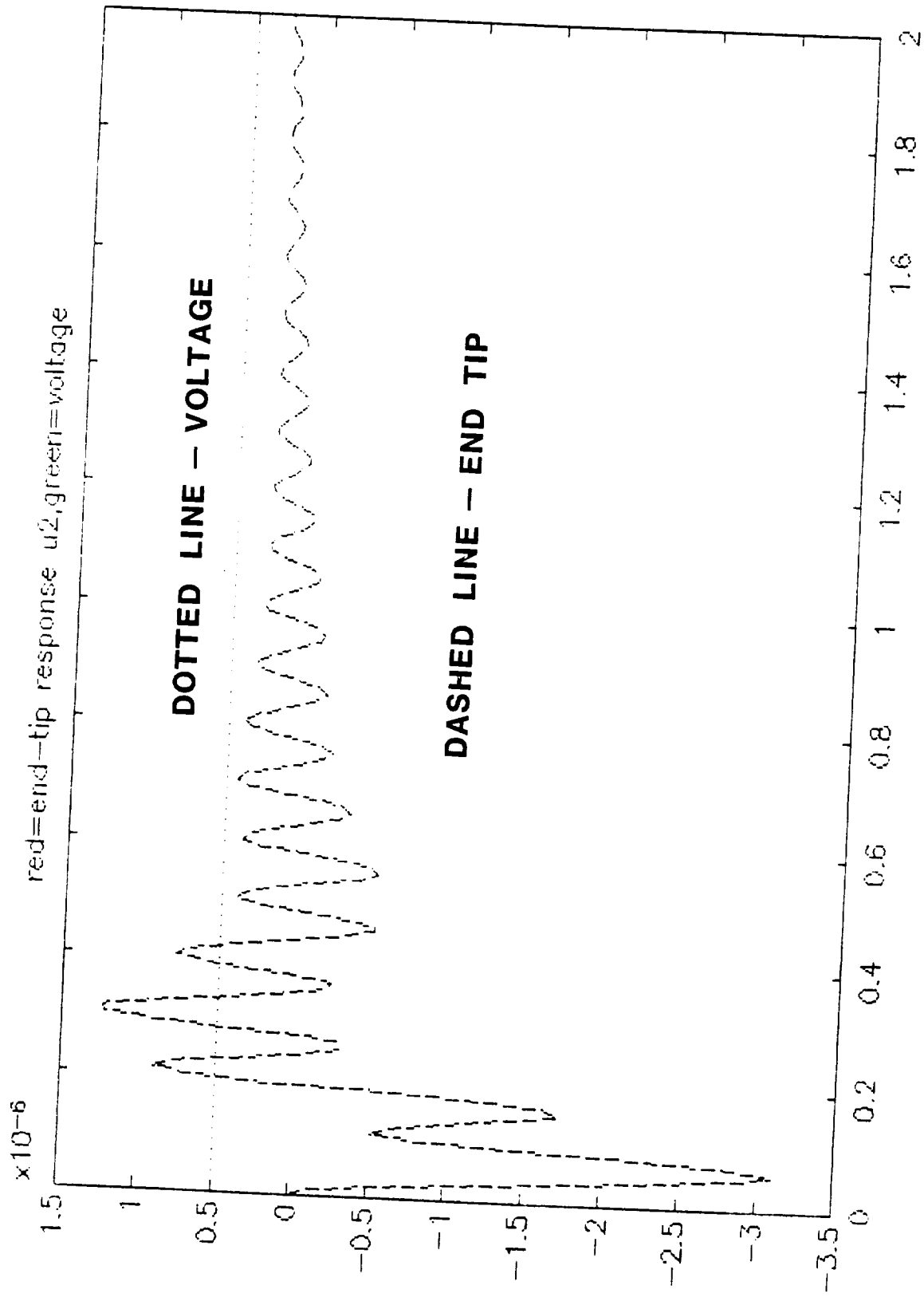


FIGURE 25

Figure 26 ARM behavior step DC input with decay

After substituting the actual system parameters in the model, the model was run under various simulated conditions. This figure demonstrates the behavior of the endtip given an initial step start and subsequently exponentially decreasing to zero. The system exhibits the expected initial harmonic oscillation which damps out with time. The dotted line is the drive voltage and the dashed line the end tip response.

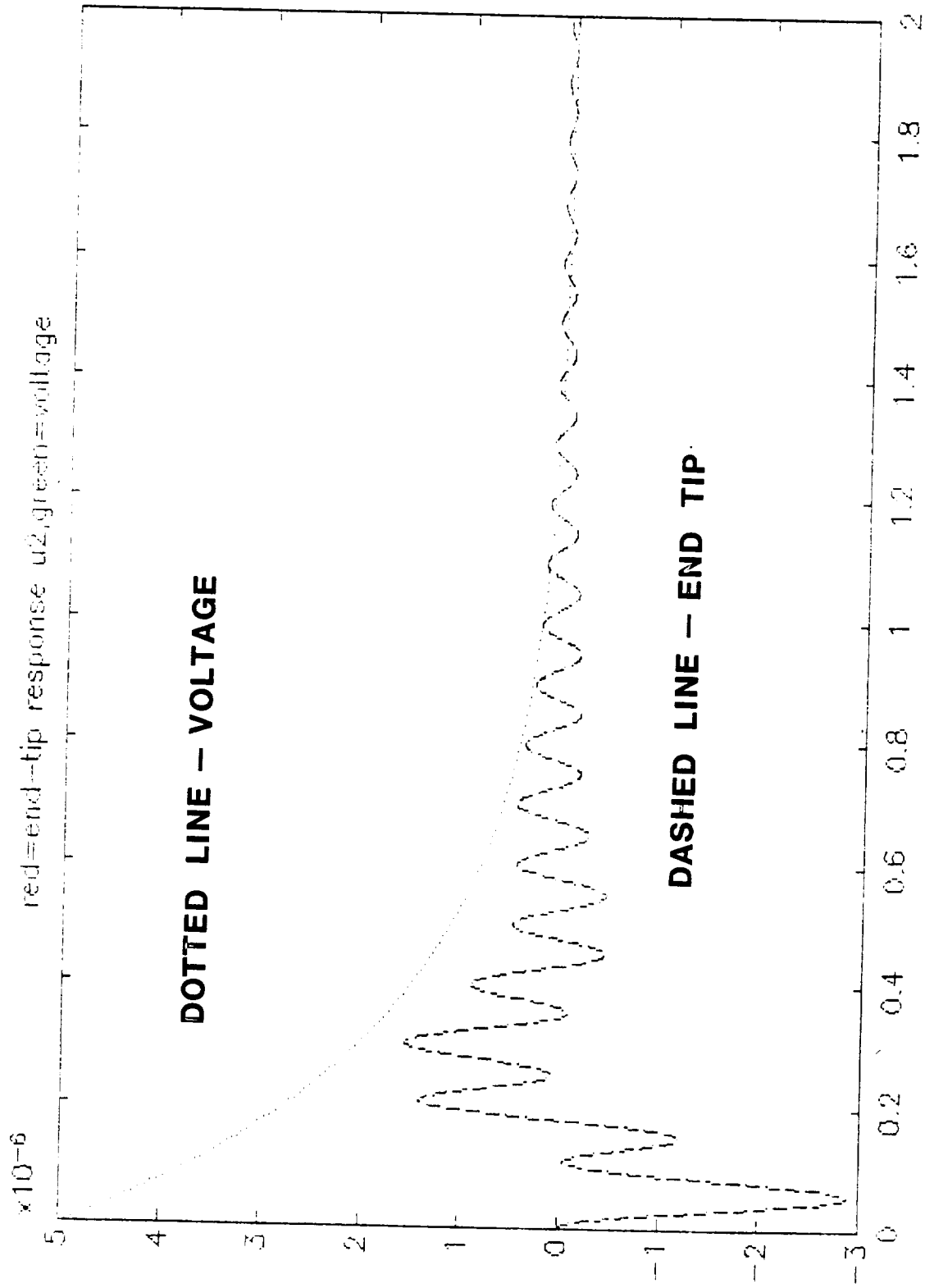


FIGURE 26

Figure 27 ARM behavior with ramp-up DC input

After substituting the actual system parameters in the model, the model was run under various simulated conditions. This figure demonstrates the behavior of the endtip given an initial step start to the system and the subsequent decay of the drive torque to zero. The dotted line is the drive voltage and the dashed line the end tip response.

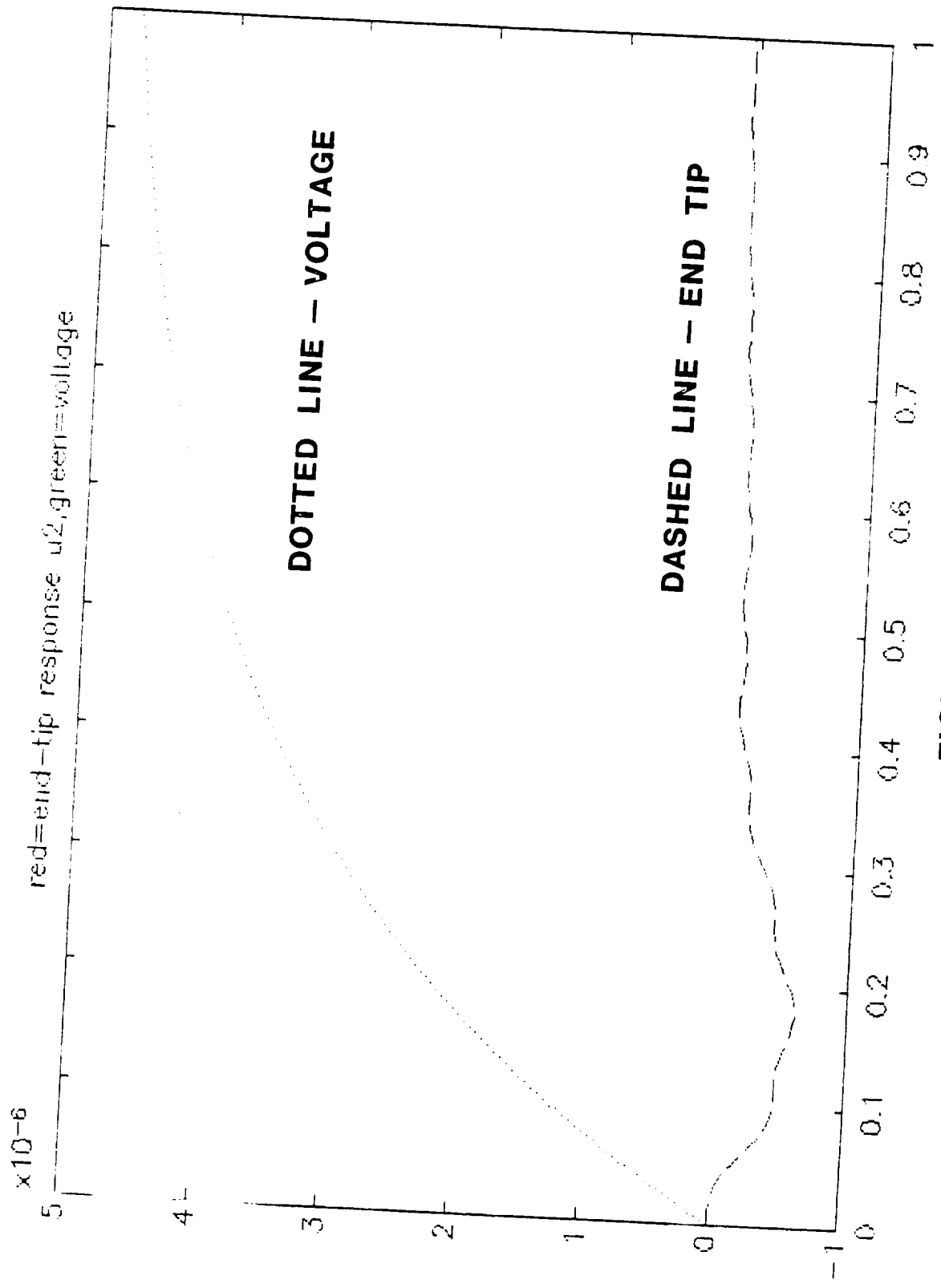


FIGURE 27

Figure 28 ARM behavior with AC and ramp up DC input

After substituting the actual system parameters in the model, the model was run under various simulated conditions. This figure demonstrates the behavior of the endtip given a ramp up of the drive voltage, and, thus, torque, to the same value as in figures 25, 26, and 27. Additionally, an AC input at a frequency close to the harmonic frequency and of a polarity opposite to the induce vibrations was applied. The displacement scale was an order of magnitude less than that of the previous figures. The induced vibrations have been significantly reduced. The end tip returned to close to its starting position. This was the same stimulus/response modeled in figure 29. The dotted line was the drive voltage and the dashed line the end tip response.

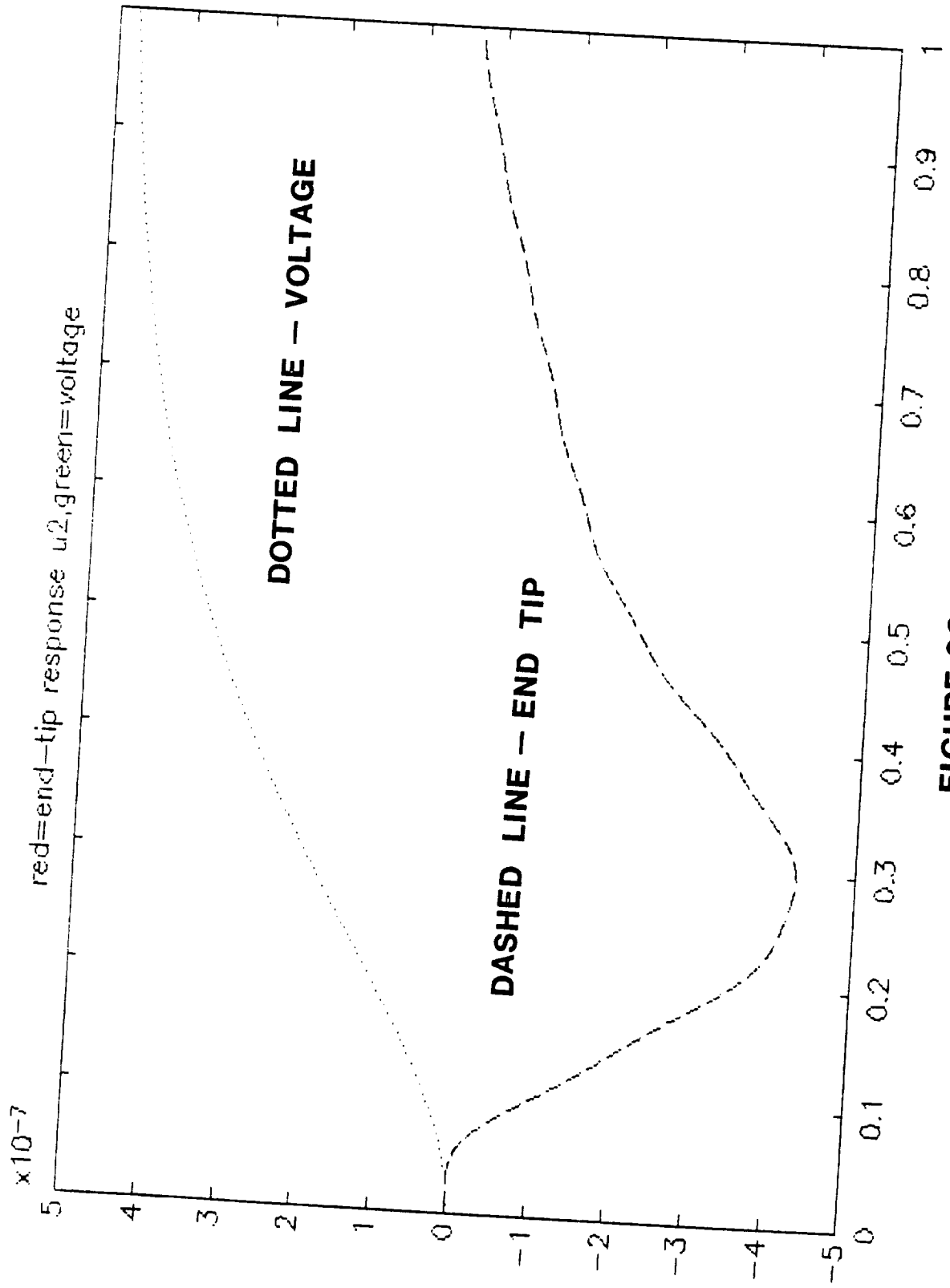
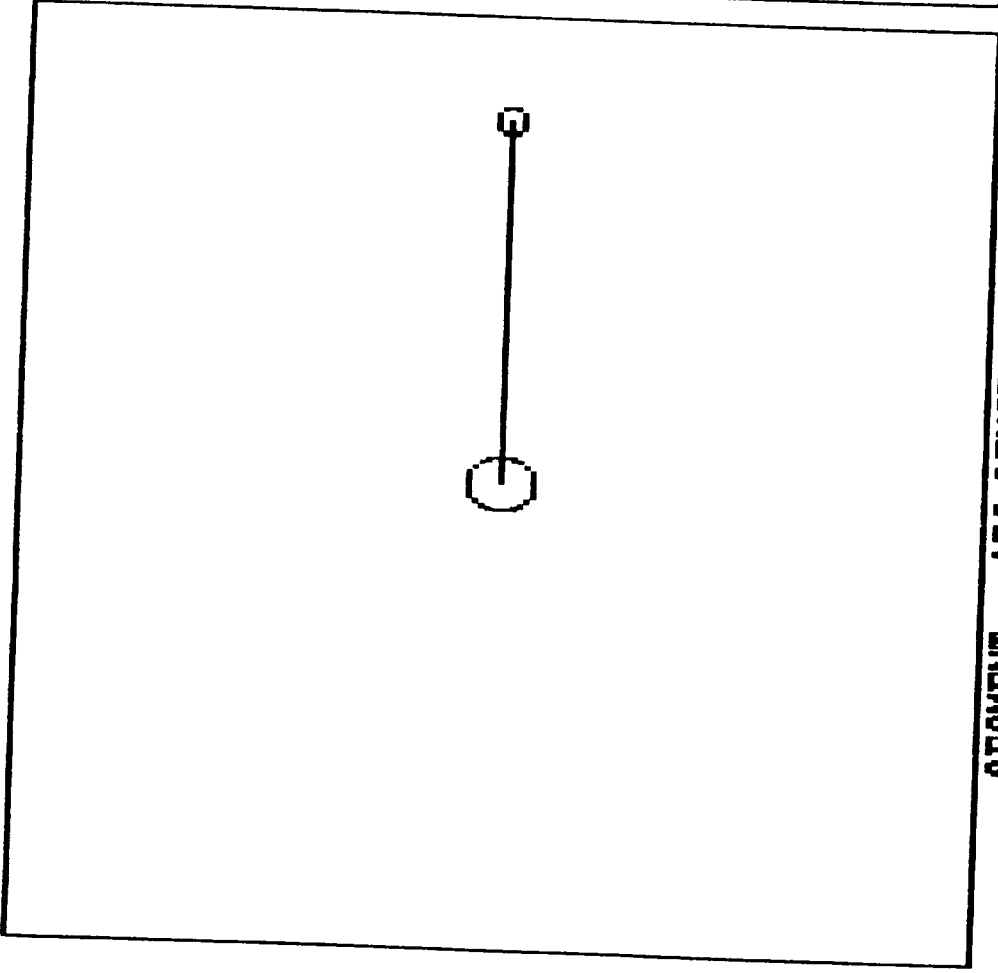


FIGURE 28

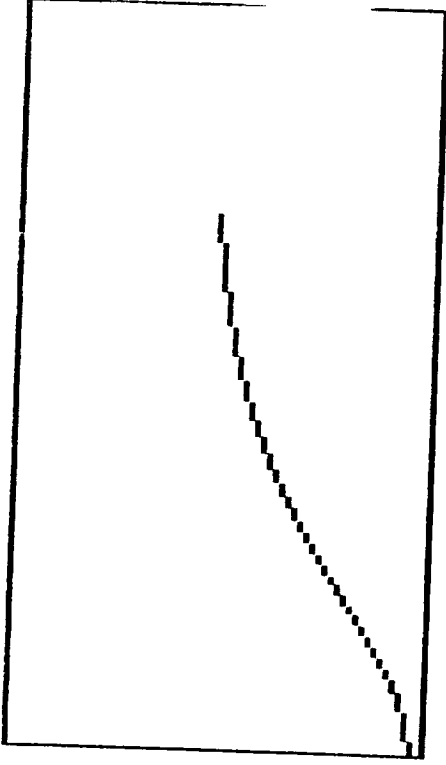
Figure 29 SIMIAC display for ramp up DC input

SIMIAC provided an on line, on screen simulation of the several parameters of the model as it was executed. The box on the left represented the movement of the ARM around the central pivot point. The ARC LENGTH was updated at each time interval. The display was stopped and frozen at 0.9950 seconds. The box in the upper right provided a graphic history of the drive voltage and its value at termination. The box in the lower right provided a history of the end tip displacement. The magnification of the displacement was of the same order of magnitude used in Figure 28. The primary modes of oscillation were just evident; these were essentially damped to zero after several seconds.

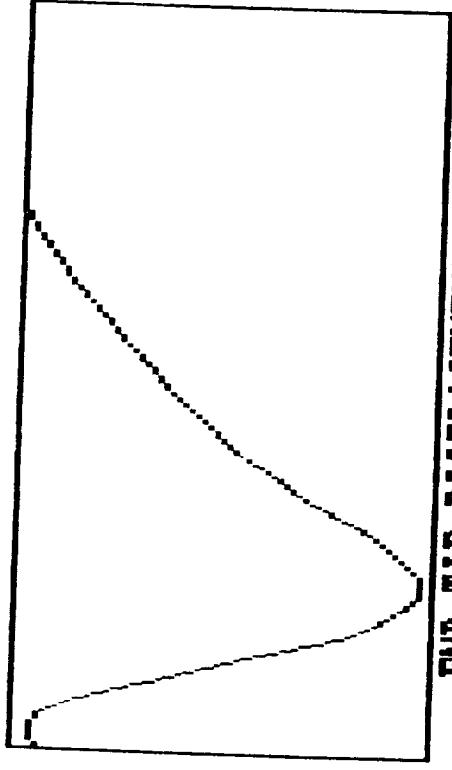


SEGMENT - ARC LENGTH : 0.02560

TIME : 0.9950



VOLTAGE : 4.73192



END-TIP DISPLACEMENT : 0.00000

END-TIP VELOCITY : 0.00000

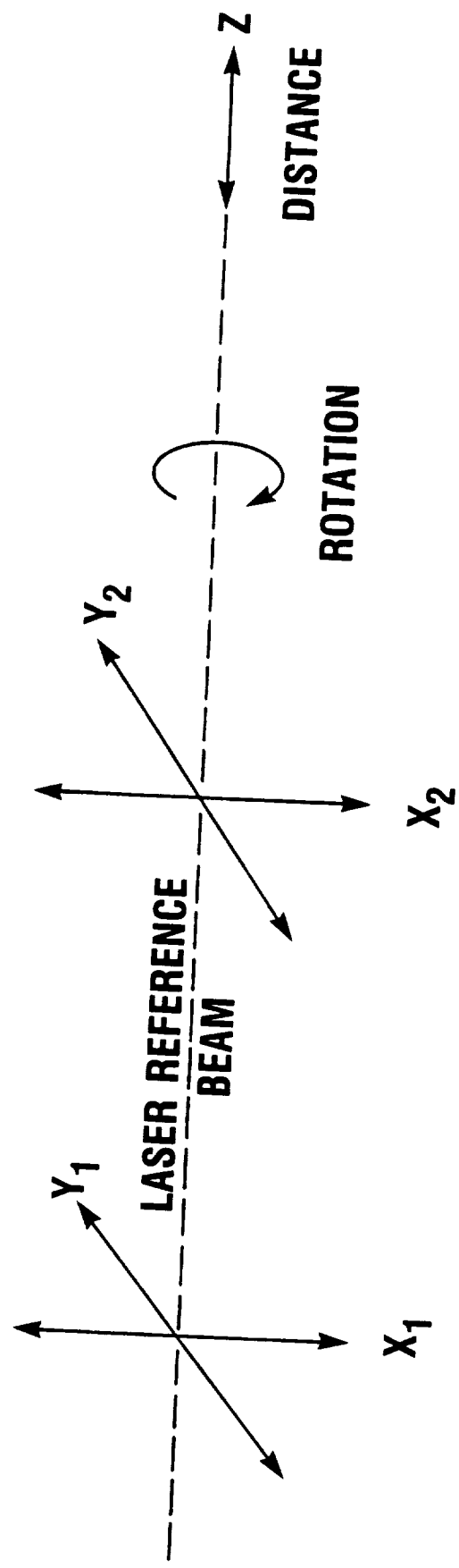
END-TIP ACCELERATION : -0.0001

FIGURE 29

Figure 30 Six degrees of freedom

A two-segment ARM configuration maximized the work space envelope. To accurately position the wrist end-tip platform of such an ARM in space required the definition of six degrees of freedom. Although a variety of coordinate systems would have met this criterion, we choose the one most suitable for integration with the laser reference beam. The first point was determined by the values X_1 , Y_1 , and Z . A second point along the beam, an angular offset due to the bend of the segment, was defined by X_2 and Y_2 . The angular value of rotation, about the Z-axis, defined the sixth degree of freedom. Together these values were used to uniquely specify the positions of the beam rider module (BRM) on the laser reference beam. It was the purpose of the BRM to determine the mismatch between the laser reference beam and the segment end tip, the vector d . This value was used to accurately determine the position of the ARM.

BEAM RIDER MODULE DEFINES SIX DEGREES OF FREEDOM



- FIVE LINEAR DEGREES OF FREEDOM
- ONE ROTATIONAL DEGREE OF FREEDOM

FIGURE 30



National Aeronautics and Space Administration

Report Documentation Page

| | | | | | |
|--|--|--|--|---|-------------------|
| 1. Report No. NASA CR-185151 | | 2. Government Accession No. | | 3. Recipient's Catalog No. | |
| 4. Title and Subtitle Beam Rider for an Articulated Robot Manipulator (ARM) Accurate Positioning of Long Flexible Manipulators | | | | 5. Report Date April 1990 | |
| | | | | 6. Performing Organization Code | |
| 7. Author(s) M. J. Malachowski, Ph.D. | | | | 8. Performing Organization Report No. None | |
| | | | | 10. Work Unit No. | |
| 9. Performing Organization Name and Address CCE Robotics/Electronic Photography P. O. Box 9315 Berkeley, CA 94709 | | | | 11. Contract or Grant No. NAS 3-25917 | |
| | | | | 13. Type of Report and Period Covered Contractor Report Final | |
| 12. Sponsoring Agency Name and Address National Aeronautics and Space Administration Lewis Research Center Cleveland, Ohio 44135-3191 | | | | 14. Sponsoring Agency Code | |
| | | | | 15. Supplementary Notes | |
| 16. Abstract <p>Laser beam positioning and beam rider modules were incorporated into the long hollow flexible segment of an articulated robot manipulator (ARM). Using a single laser beam, the system determined the position of the distal ARM endtip, with millimetric precision, in six degrees of freedom, at distances of up to 10 meters. Preliminary designs, using space rated technology for the critical systems, of a two segmented physical ARM, with a single and a dual degree of freedom articulation, were developed, prototyped, and tested. To control the positioning of the physical ARM, an indirect adaptive controller, which used the the mismatch between the position of the laser beam under static and dynamic conditions, was devised. To predict the behavior of the system and test the concept, a computer simulation model was constructed. A hierarchical artificially intelligent real-time ADA operating system program structure was created. The software was designed for implementation on a dedicated VME bus based Intel 80386 administered parallel processing multi-tasking computer system.</p> | | | | | |
| 17. Key Words (Suggested by Author(s)) Robotics, Manipulators, Flexible Bodies Adaptive Control, Real Time Operation Laser Ranger/Tracker, Position Control Simulation, Controllers | | | | 18. Distribution Statement Unclassified - Unlimited Subject Category 63 | |
| 19. Security Classif. (of this report) Unclassified | | 20. Security Classif. (of this page) Unclassified | | 21. No of pages 180 | 22. Price* A09 |